ABSTRACT

Title of Document: EMPLOYING MODERATE RESOLUTION SENSORS IN HUMAN RIGHTS AND INTERNATIONAL HUMANITARIAN LAW MONITORING

Andrew J. Marx, Doctor of Philosophy, 2013

Dissertation directed by: Professor Samuel N. Goward
Department of Geographical Sciences

Organizations concerned with human rights are increasingly using remote sensing as a tool to improve their detection of human rights and international humanitarian law violations. However, as these organizations have transitioned to human rights monitoring campaigns conducted over large regions and extended periods of time, current methods of using fine-resolution sensors and manpower-intensive analyses have become cost-prohibitive. To support the continued growth of remote sensing in human rights and international humanitarian law monitoring campaigns, this study researches how moderate resolution land observatories can provide complementary data to operational human rights monitoring efforts.

This study demonstrates the capacity of moderate resolutions to provide data to monitoring efforts by developing an approach that uses Landsat Enhanced Thematic Mapper Plus (ETM+) as part of a system for the detection of village destruction in Darfur, Sudan. Village destruction is an indicator of a human rights or international humanitarian law violations in Darfur during the 2004 study period. This analysis approach capitalizes on Landsat's historical archive and systematic observations by constructing a historic spectral baseline for each village in the study area that supports automated detection of a potentially destroyed village with each new overpass of the sensor. Using Landsat's near-infrared band, the approach demonstrates high levels of accuracy when compared with a U.S. government database documenting destroyed villages.

This approach is then applied to the Darfur conflict from 2002 to 2008, providing new data on when and where villages were destroyed in this widespread and long-lasting conflict. This application to the duration of a real-world conflict illustrates the abilities and shortcomings of moderate resolution sensors in human rights monitoring efforts.

This study demonstrates that moderate resolution satellites have the capacity to contribute complementary data to operational human rights monitoring efforts. While this study validates this capacity for the burning

of villages in arid environments, this approach can be generalized to detect other human rights violations if an observable signal that represents the violation is identified.

EMPLOYING MODERATE RESOLUTION SENSORS IN HUMAN RIGHTS AND INTERNATIONAL HUMANITARIAN LAW MONITORING

by

Andrew J. Marx

Dissertation submitted to the Faculty of the Graduate School of the
University of Maryland, College Park in partial fulfillment
of the requirements for the degree of
Doctor of Philosophy
2013

Advisory Committee:

Professor Samuel N. Goward, Chair
Professor Shunlin Liang
Professor Tatiana V. Loboda
Professor William L. Reed
Dr. Lee R. Schwartz

Acknowledgements

It was only through the consistent and patient support from my friends and family that I was able to complete this dissertation. To my advisor, Dr. Sam Goward, I'm very grateful for what could best be called an excellent apprenticeship over the past few years. The progression from teaching me about remote sensing, to working for you as a researcher, to the advice and guidance you provided me as an independent researcher will never be forgotten.

I would also like to thank the rest of my committee, Dr. Liang, Dr. Loboda, Dr. Reed, and Dr. Schwartz for sharing their time, experience an expertise as my dissertation has progressed. This dissertation would not have been possible without the support of the U.S. Department of State and my Office Director, Dr. Schwartz, as I pursued this research first through the Pat Roberts Intelligence Scholar's Program and later as a Research Fellow at the U.S. Holocaust Memorial Museum's Center for the Prevention of Genocide.

Table of Contents

List of Figures

List of Tables

Chapter 1. Introduction

The crimes committed against humanity during World War II shocked the global community into action. As the world continued to uncover the full extent of the Holocaust, international leaders in the newly formed United Nations (U.N.) drafted the Universal Declaration of Human Rights and established a mandate to protect human rights and prevent atrocities (United Nations, 1948). However, certain situations increase the likelihood of human rights violations and therefore the need for human rights monitoring of conflicts (Edwards & Koettl, 2011):

- The conflict is in a remote area.
- There are multiple armed groups.
- There are few external observers.
- It is a regime where information flow to the outside is limited.

Because of ongoing abuses, the U.N., along with other governmental and nongovernmental organizations (NGOs), conducts widespread and intensive human rights monitoring campaigns. Broadly described by the Office of the High Commission for Human Rights as the "active collection, verification and immediate use of information to address human rights problems" (Office of the High Commissioner for Human Rights, 2001),

human rights monitoring documents any violations that include governmental and non-state transgressions of human rights and the failures of the state to protect those rights.

1.1. The Basis of Human Rights and International Humanitarian Law

Human rights are those rights that protect individuals and groups from governmental actions that interfere with fundamental freedoms and human dignity (Office of the High Commissioner for Human Rights, 2001). Established through the Universal Declaration of Human Rights in 1948, international humanitarian law is the body of law applicable in situations of armed conflict and is designed to protect humanity and diminish the evils of war (United Nations, 1948). This declaration was expanded through the four Geneva Conventions of 1949 and the two 1977 Protocol Additions to those conventions to provide important protections for persons taking no active part in hostilities, including detainees and those places hors de combat (outside of combat) (United Nations, 1949, 1977a, b). All parties to a conflict, including non-state actors, are obliged to comply with international humanitarian law.

A human rights violation occurs any time a state or non-state actor breaches any part of human rights. Remote sensing has successfully

provided evidence for several violations that the International Criminal Court (ICC) prosecutes, defined in Article 5 as "the most serious crimes of concern to the international community as a whole" (United Nations, 1998) (Table 1-1), and which include violations of human rights and international humanitarian law.

Table 1-1: Jurisdiction of the ICC (United Nations, 1998)

Genocide: Any of the following acts committed with intent to destroy, in whole or in part, a national, ethnical, racial, or religious group
-Killing members of the group
-Causing serious bodily or mental harm to members of the group
-Deliberately inflicting on the group conditions of life calculated to bring about its physical destruction in whole or in part
-Imposing measures intended to prevent births within the group
-Forcibly transferring children of the group to another group
Crimes Against Humanity: Any of the following acts when committed as part of a widespread or systematic attack directed against any civilian population
-Murder
-Extermination
-Enslavement
-Deportation or forcible transfer of population
-Imprisonment or other severe deprivation of physical liberty in violation of fundamental rules of international law
-Torture
-Rape, sexual slavery, enforced prostitution, forced pregnancy, enforced sterilization, or any other form of sexual violence of comparable gravity
-Persecution against any identifiable group or collectivity on political, racial, national, ethnic, cultural, religious, gender
-Enforced disappearance of persons
-The crime of apartheid
-Other inhumane acts of a similar character intentionally causing great suffering, or serious injury to body or to mental or physical health
War Crimes: Grave breaches of the Geneva Conventions of 1949
-Willful killing
-Torture or inhuman treatment, including biological experiments
-Willfully causing great suffering, or serious injury to body or health
-Extensive destruction and appropriation of property, not justified by military necessity and carried out unlawfully and wantonly
-Compelling a prisoner of war or other protected person to serve in the forces of a hostile power
-Willfully depriving a prisoner of war or other protected person of the rights of fair and regular trial
-Unlawful deportation or transfer or unlawful confinement
-Taking of hostages

1.2. Using Remote Sensing to Detect International Law Violations

Remote sensing is a tool that improves detection of and potentially provides a deterrent to human rights and international humanitarian law violations. Remote sensing platforms include helicopters and fixed-wing or unmanned aerial vehicles. However, these platforms are limited in several aspects, including limited range and the need for basing facilities near conflict areas, which are often in very remote locations. These platforms also require overflight permission from the host government, which is often the alleged transgressor. For these reasons, organizations that monitor human rights have increasingly turned to space-based imagery to identify and document conflict.

The process of using remote sensing to detect human rights and international humanitarian law violations involves many different factors. However, organizations tend to follow a standard sequence of steps: 1) they identify the violation they are attempting to detect; 2) they select a remotely-sensed, observable event, or phenomenon, that is associated with this violation; and then 3) they choose a sensor and a type of analysis that will permit detection of this phenomenon's signal from the noise.

These phenomena include anything the sensor can detect that may represent a violation of human rights or international humanitarian law.

Satellites can directly detect some phenomena, such as extensive destruction of civilian property, which is a violation if not justified by military necessity. For example, investigators will use satellite images and analysis to look for widespread destruction of houses. Satellites can also indirectly detect violations, such as the forcible transfer of a people. An example of this is detection of abandoned agricultural fields or greening pastoral areas (Table 1-2) (UNOSAT, 2009).

Table 1-2: Select Human Rights Violations with Identification Requirements

Violation (Location)	**Phenomena**	**Signal Analysis**	**Sensor / Revisit Used**	**Source**
Artillery Targeted Near Civilians (Sri Lanka)	Artillery, bomb craters	Identification of craters near civilians	WorldView 1 (0.5m) 2 Weeks	(UNOSAT 2009)
Mass Executions (Bosnia)	Creation of mass graves	Disturbed earth, earthmovers	U-2 (unk) n/a	(New York Times, 1995)
Ethnic House Destruction (Georgia)	Individuals houses destroyed	Destroyed roof change detection	DigitalGlobe (2m) 6 months	(AAAS, 2008)
Targeting of Civilian Infrastructure (Georgia)	Damage to public buildings	Identification of destroyed buildings	WorldView 1 (0.5m) n/a	(UNOSAT 2008)
Political Prison Camps (North Korea)	Expansions of prisons	Prison size change detection	DigitalGlobe (2m) 10 years	(Amnesty International, 2011)
Targeting of Civilian Infrastructure (Turkey)	Destroying forests, fields, and villages	Change in land cover classification	Landsat 5 (30m) 4 years	(De Vos et al., 2008)
Civilian Population Removed (Sudan)	Disruption of agricultural land	NDVI change near population areas	MODIS (250m) Annual	(Schimmer, 2008)
Civilian Population Removed (Bosnia)	Abandonment of agricultural land	Agricultural field change detection	Landsat 5 (30m) 4 years	(Witmer, 2008)
Attacking Village (Sudan)	Burning of arid villages	MODIS fire detection	MODIS (250m) Annual	(Bromley, 2010)
Attacking Village (Sudan)	Burning of arid villages	Drop in village's reflectance	Landsat 5 / 7 (30m) Annual	(Prins, 2008)

The detection of different phenomena requires specific sensor characteristics. Although some monitoring capacity has been shown using moderate resolution (MODRES) (10-100 spatial resolution) sensors (Bromley, 2010; Prins, 2008), most phenomena currently being used in human rights monitoring require a fine (1 to 10m spatial resolution), or very-fine resolution (under 10m) sensor (Table 1-3).

Table 1-3: Image Spatial Resolution Categories (Warner et al., 2009)

Pixel Size (m)	**Spatial Resolution**	**Example Satellite-borne sensors**
< 1	Very fine	WorldView
1 - 10	Fine	IKONOS
10 - 100	Moderate	ASTER, AWIFS, ETM+, MSS, SPOT
100 - 1000	Coarse	MODIS, MERIS
> 1000	Very coarse	AVHRR, GOES, METEOSAT

The sensor's temporal resolution, or how often a satellite passes over a target area, is also critical in the detection of violations. Some phenomena, such as the deployment of tanks to protests, can require an image that day, while other phenomena, such as the abandonment of agriculture fields, may take several months to manifest themselves.

The importance of temporal resolution is demonstrated in a report by AAAS and Amnesty International on the Russian occupation of Tskhinvali, the capital of the disputed region of South Ossetia (AAAS, 2011; Amnesty International, 2008). In response to Amnesty's eyewitness reporting on the destruction of ethnic Georgian homes, AAAS purchased imagery for August 10, two days after major hostilities ceased and the beginning of Russian occupation of the area. AAAS also purchased imagery for August 19. By imaging on these specific dates, AAAS was able to show that several hundred Georgian homes were destroyed after major hostilities concluded and during the time of Russian occupation (Edwards & Koettl, 2011). This report corroborated eyewitness reports of widespread human rights violations occurring while under Russian occupation.

Certain crimes, such as genocide, are by definition systematic, and evidence of them requires a time-series analysis. The necessity of systematically detecting phenomena associated with some violations has led organizations to conduct human rights monitoring campaigns. In these monitoring campaigns there is typically a standing request to collect all images over a certain region. Later analysts look through the images to see if there is a systematic nature to the violations; both when and where the crimes occurred. One of the first examples of this was when the U.S.

Department of State's Humanitarian Information Unit (HIU) posted on-line a database and map based on hundreds of fine (under 10m spatial resolution) satellite images that linked eyewitness accounts with imagery-derived evidence of widespread destruction of villages in Darfur, Sudan (HIU, 2004).

1.3. Development of "Landsat Class" Observatories and Archive

Civilian, moderate resolution, satellite-based imaging systems were developed from the recognition that military land observatories, such as CORONA, could provide valuable observations of the Earth's land areas (Goward et al., 2009; National Research Council, 1969). From that recognition, the concept of 30m to 100m multispectral, or "Landsat class", observatories was developed through the convergence of conflicting views held by the National Aeronautics and Space Administration (NASA), the Department of Interior, the U.S. Intelligence Community, and the U.S. Academic Community (Goward et al., 2011).

From this conceptualization, in 1972 the Earth Resources Technology Satellite (ERTS-1, later named Landsat-1) was launched. Its sensors included the Return Bean Vidicon (RBV) and the Multispectral Scanner System (MSS). The successes of the MSS, coupled with the failure of the

RBV shortly after launch, resulted in the MSS becoming the primary sensor on ERTS-1 and later Landsat missions (Goward et al., 2011). The MSS six-band design was improved on later missions, and renamed the Thematic Mapper (TM) and Enhanced Thematic Mapper Plus (ETM+).

In 2004, the Landsat program was declared a "national asset" by the U.S. President's Science Advisor (Marburger, 2005) due to it's unique provision of a continuous record of earth observation since 1972. The observations produced by its spatial, spectral, and temporal resolutions have proven valuable in a wide variety of ecological and anthropological applications (Leimgruber et al., 2005; Townshend & Justice, 1988). More recently, advanced computing power has introduced new methods of analyzing Landsat's historic database. Such analysis is possible due to the public and free availability of Landsat's archives (Woodcock et al., 2008), its commitment to systematic global coverage (Goward et al., 2006), and its rigorous calibration and quality assurance (Markham et al., 2004).

In 1992 the Land Remote Sensing Policy Act provided for the creation of the National Satellite Land Remote Sensing Data Archive (NSLRSDA) to preserve and make accessible the collection of satellite observations (U.S. Congress, 1992). This act also mandated continued systematic monitoring of Earth land areas. Today the U.S. Geological

Services' Earth Resources Observation System (EROS) Data Center provides for the reception, processing, archiving, and hosting of Landsat data.

Because Landsat-7 can only process about 400 per day (Wulder et al., 2008), a long-term acquisition plan is used to prioritize scene selection (Arvidson et al., 2006). The result of this acquisition plan is dense temporal coverage in some areas, and relatively poor coverage in other areas (Goward et al., 2006). This discrepancy is magnified by the fact that not all Landsat observations are held in the NSLRSDA holdings. Goward (2006) identifies gaps of varying magnitudes in the holdings which reflect administrative or technical gaps throughout Landsat's history.

While Roy (2010) notes that there is a mean of 6.9 acquisitions per path/row per year with cloud cover ≤ 40% across Africa for 2000 to 2008, temporal coverage for western Sudan improved significantly in 2004 when daily scene collection increased from 250 to 300 starting on 11 May 2004 (Arvidson et al., 2006). Landsat TM was not available because the study area is not within a ground receiving antenna and the transmitter failed in 1987.

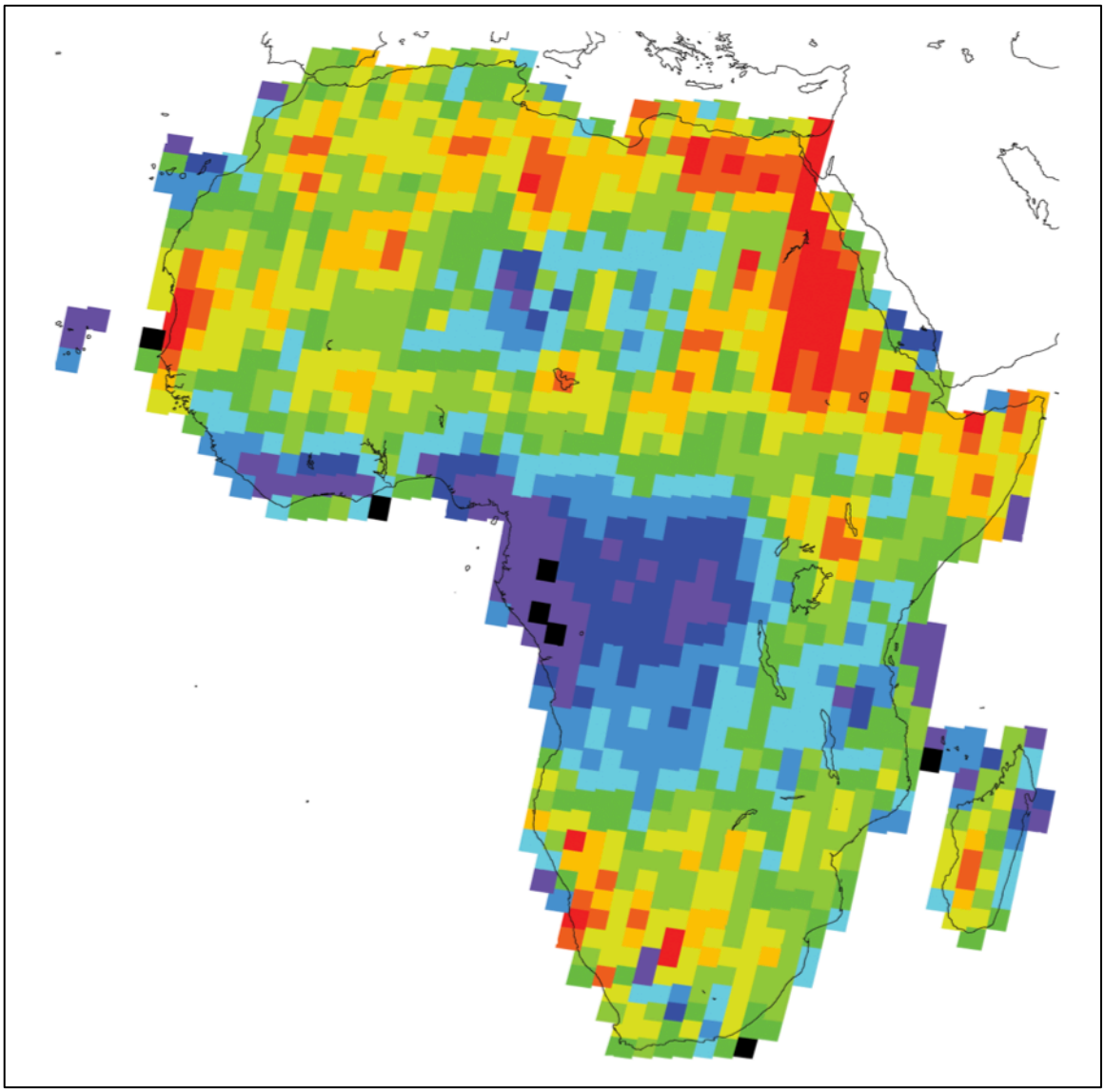

Figure 1-1: The annual mean number of African ETM+ acquisitions, 2000–2008, with cloud cover ≤ 40%, stored in the US Landsat archive. Colors show the mean number of acquisitions available at a given Landsat path/row: 0 to 1 (black), 1 to 2 (purple), 3 to 4 (royal blue), 4 to 5 (blue), 5 to 6 (aqua), 6 to 7 (dark green), 7 to 8 (green), 8 to 9 (light green), 9 to 10 (orange), 10 to 11 (light red), 11 to 12 (orange), 12 to 13 (dark red).

1.4 Development of MODRES Change Detection Applications

Digital change techniques for use with Landsat and other satellites, typically only analyze one image pair at a time (Lu et al., 2005; Singh, 1989). Some algorithms have been developed to analyze three or more images at a time, though these suffer from the same shortcomings as bi-temporal techniques (Coppin et al., 2004; Lunetta et al., 2006). More recently, temporal trajectory, or temporal profile analysis uses high temporal frequency in data acquisitions to characterize spectral profiles through time. This has been most often used to successfully documenting forest disturbance and regrowth (Huang et al., 2008; Jin & Sader, 2005; Kennedy et al., 2007).

Much of the work developed in this dissertation is inspired and made possible from principles developed in the North American Forest Dynamics (NAFD) project. This work evaluated forest disturbance and regrowth for the conterminous U.S. by combining Landsat observations and field measurements (Goward et al., 2008; Huang et al., 2008). This project pioneered the use of dense Landsat Time Series Stacks (LTSS), defined as a temporal sequence of Landsat images acquired at specific temporal intervals, usually every year, or every two years (Huang et al., 2009).

The image pre-processing system developed in the NAFD project, called the Landsat Ecosystem Disturbance Adaptive Processing System (LEDAPS) (Masek et al., 2006; Wolfe et al., 2004) was used in this study. This system is a more appropriate pre-processing system for the study than image-to-image normalization procedures (Chavez, 1996; Moran et al., 1992) which are designed for pairs of images. While LEDAPS was designed for time-series analysis of North American forest disturbance, it is effective for application by converting images from digital numbers to TOA reflectance and then accounting for water vapor and aerosol atmospheric attenuation, which permits conversion of the images to surface reflectance. The LEDAPS system consists of four steps:

- Extracts metadata, creates header files and masks for scanline gaps
- Converts to top-of-atmosphere (TOA) reflectance and TOA brightness temperature for band 6
- Generates cloud mask from the Automated Cloud Cover Assessment (Irish et al., 2006)
- Converts to Surface Reflectance using concurrent MODIS information (Vermote et al., 2002) and dark vegetation differencing for aerosols (Kaufman et al., 1997)

Analysis of the LTSS is done through an algorithm developed for reconstructing forest disturbance history, called the Vegetation Change Tracker (VCT) (Huang et al., 2010). The VCT first samples forest values to build an integrated forest z-score (IFZ). This score is used to further equalize forest pixels in the LTSS and is also used as a metric to create

temporal profiles of different land cover and forest change processes (Fig. 1-2). Decision rules are the applied to these profiles to identify persisting land cover types or disturbances. The result is an accurate, trajectory-based analysis that detects forest disturbance and regeneration, with little to no fine-tuning for each LTSS.

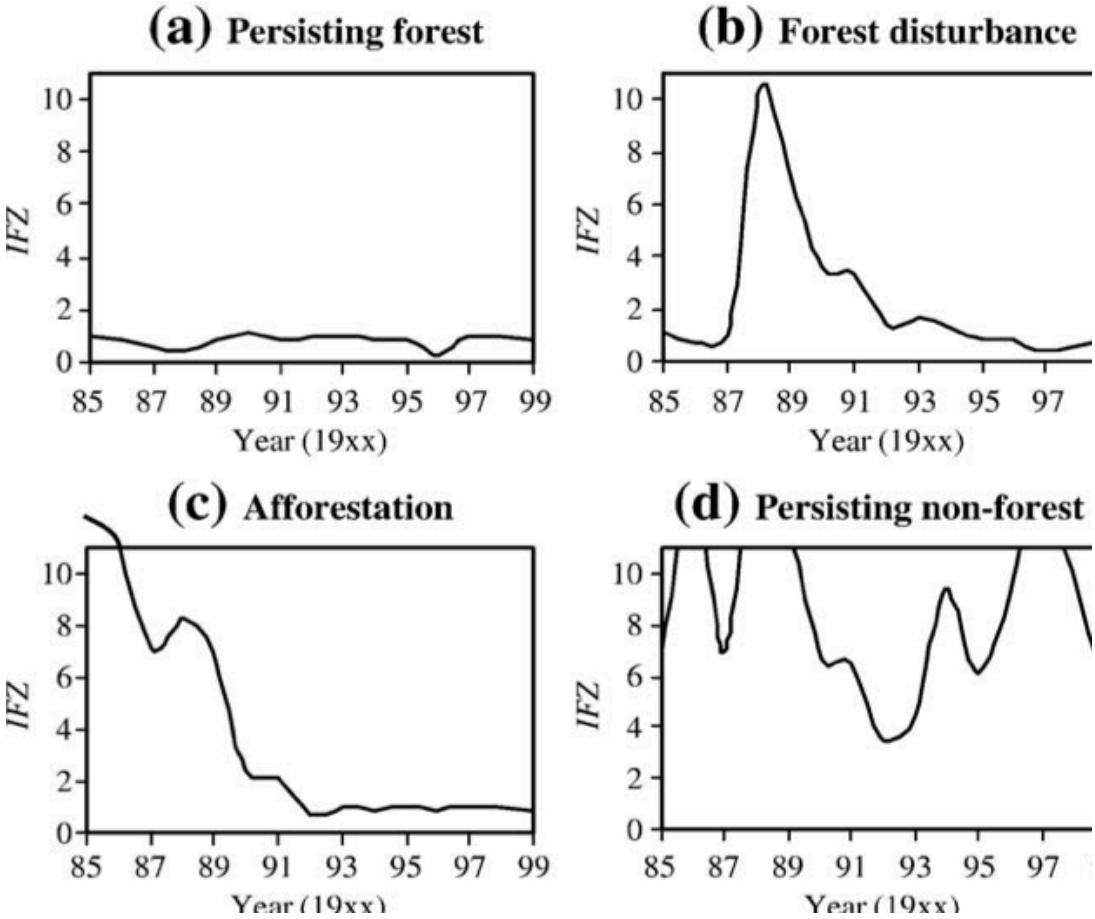

Figure 1-2: Typical temporal profiles of major forest cover change processes (a-c) and non-forest (d) (Huang et. al, 2010).

1.5 Drylands Fire Detection

Research into the remote sensing of burn scars has predominantly focused on forest fires, showing that bands 4 and 7 perform the best in discriminating burned areas (Koutsias & Karteris, 2000). The Normalized Burn Ratio (NBR) is well documented in its ability to detect fire scars $NBR = \frac{(Band\ 4 - Band\ 7)}{(Band\ 4 + Band\ 7)}$ (Garcia & Caselles, 1991) and has been shown to out-perform other time-series analysis techniques, such as image

differencing and ratioing (Lyon et al., 1998). The time-series use of NBR, called NBR differencing (dNBR) subtracts the pre-fire NBR from the post-fire NBR (Key & Benson, 2002). For intra-seasonal fire detection, previous studies include the registering of reduced NDVI within a growing year (Kasischke & French, 1995) and a frequency based approach considering dNBR values for a biome (Loboda et al., 2007).

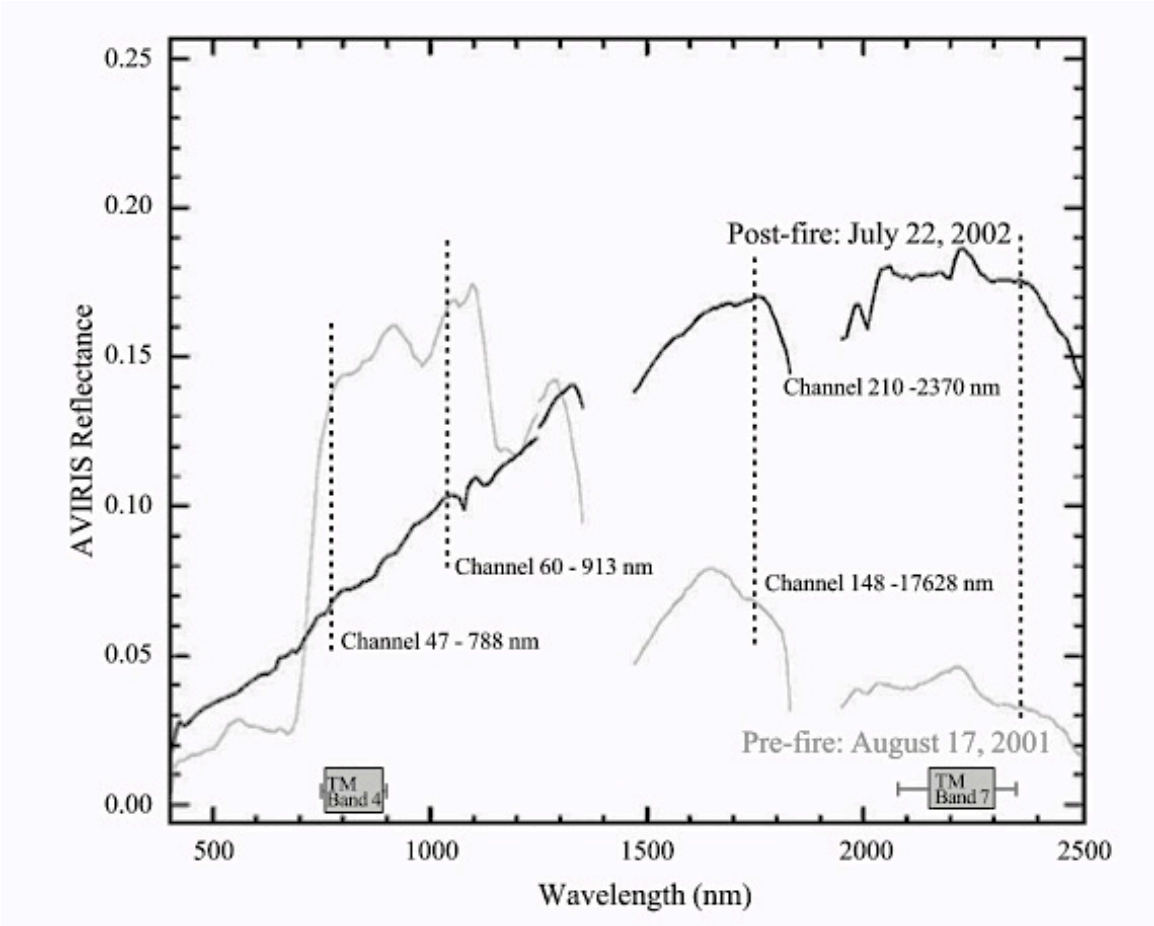

Figure 1-3: Garcia (1991) demonstrated how the normalizing of Landsat bands 4 and 7 capture pre- and post-fire reflectance differences.

There is considerably less research for burn scars in drylands. Principal Components Analysis (PCA) was shown to out-perform raw data and Kauth-Thomas transformations in using Landsat to detect fires in African savannas (Hudak & Brockett, 2004), however results however were poor. Of the validation points in Hudak's study, only 26 of 34 (76%) burned pixels were correctly identified.

The performance of Landsat in drylands fire detection is much more difficult because band 7 (wavelengths 2.08-2.35μm) is not as useful as in forest fires. In forest fires, band 7 is used to distinguish the low reflectivity of moist forest canopy with the high reflectivity of charred soil (Jia et al., 2006). In a drylands fire, reflectance from bands 4 and 5 drop as the ground transitions from pre-burn materials (soil, deadwood, dead twigs and dead litter) to post-burn materials (soil, charwood, charred soil and ash) (Fig. 1-4) (U.S. Geological Society, 2011). Roy's (2006) studies of grasslands or shrub areas have shown more sensitivity in the near infrared than mid-wavelength infrared (3–8 μm) in pre- and post-fire situations (Fig. 1-5).

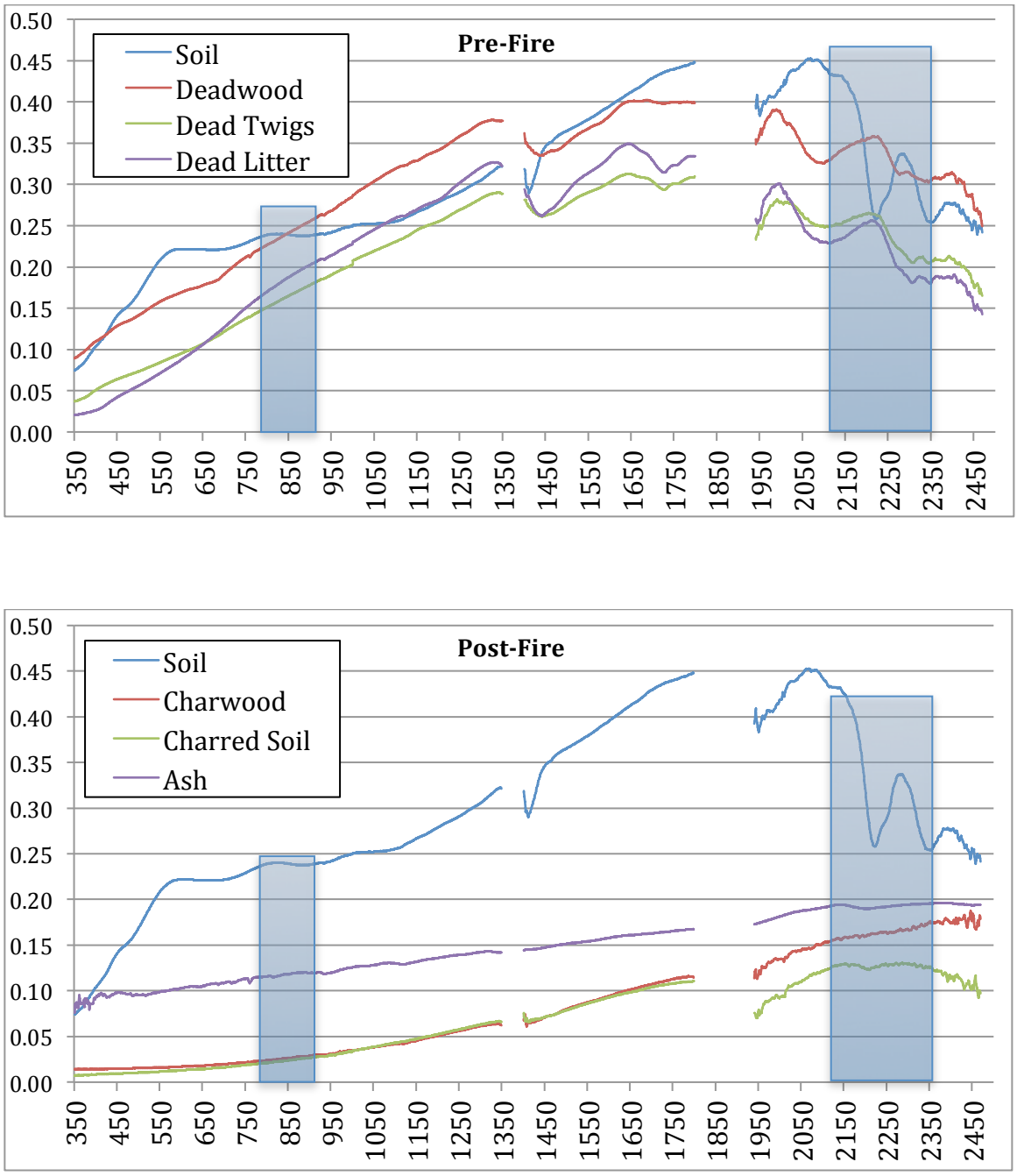

Figure 1-4: Pre- and Post-Fire Spectral Properties of soil and litter with ETM+ bands 4 and 7 (U.S. Geological Society, 2011). The water absorption bands from 1350um to 1400um and 1800um to 1900um are omitted.

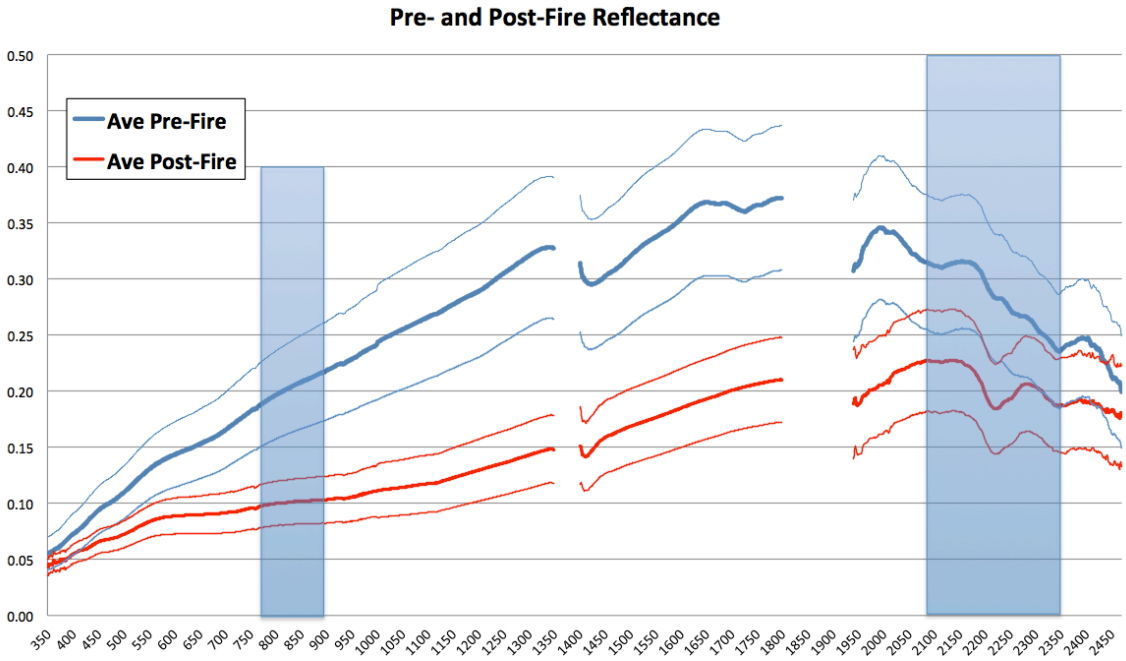

Figure 1-5: Pre- and Post-Fire Average Spectral Profiles of a arid village ETM+ bands 4 and 7 (U.S. Geological Society, 2011). +1 and -1 standard deviations are shown for both profiles. Theater absorption bands from 1350um to 1400um and 1800um to 1900um are omitted.

1.6. Research Goals

To date remote sensing research studies have largely failed to create new methods for the human rights community to assist in the timely and accurate detection of human rights violations. This has been acknowledged; for example, "no large scale remote sensing monitoring of villages or a comprehensive map of burnt villages in Darfur is available" (Prins, 2008) and "there is a clear need for a rapid data collection and analysis methods with minimal cost for human rights groups" (Sulik & Edwards, 2010). New remote sensing methods for human rights practitioners need to be developed

because constraints posed by the current methodology are already limiting the growth of remote sensing in the human rights community.

Within this study, prior research and practices of remote sensing in human rights was examined to identify areas where moderate resolution satellites could provide complementary data to monitoring campaigns. The study identified an approach where moderate resolution could be employed, validated its performance, and demonstrated advantages that can be gained by implementation of such a system. To accomplish this goal, the following specific research questions were addressed:

1. What are the concepts and principles of human rights and international humanitarian law? (Chapter 1).
2. What are the concepts and principles of remote sensing in human rights and international humanitarian law? (Chapter 1).
3. How can data from moderate resolution sensors be employed to address shortfalls in current remote sensing monitoring? (Chapter 2).
4. Focusing on arid regions that with a history of human rights transgressions, can an observable signal associated with human rights be identified and used in an early-warning system? (Chapter 3).

Basic Approach:

a. Identify a signal that is associated with a human rights violation.
b. Develop an approach to detect this signal considering the time profile and separability of the signal.
c. Test the approach on different Landsat bands and indices.
d. Evaluate the approach's success based on a U.S. government database of destroyed villages.

5. What are the benefits that this complementary data provides when implemented in an actual conflict? (Chapter 4).
6. Results of this thesis are summarized in the final chapter (Chapter 5) along with the significance and future applications of this work.

Parts of this thesis have been combined into a manuscript titled 'Remote Sensing in Human Rights and International Humanitarian Law Monitoring' published in the *Geographical Review* (Marx & Goward, 2013) and 'Landsat-based early warning system to detect the destruction of villages in Darfur, Sudan', which has been accepted for publication by *Remote Sensing of Environment* (Marx & Loboda).

Chapter 2.
Methods of Remote Sensing in International Humanitarian Law

There are two broad categories of remote sensing in international humanitarian law. "Human rights mapping" consists of quickly ordering images of specific locations to verify an alleged human rights violation, while "human rights monitoring" systematically collects images over a large region to document any suspected violations. Information gathered using remote sensing products such as DigitalGlobe or Geoeye imagery helps the U.N. and NGOs provide evidence of international law violations to fact-finding bodies and criminal courts and supports U.N. peacekeeping missions (Pisano, 2011). In the future, these organizations expect to conduct larger human rights monitoring campaigns (UNOSAT, 2011).

2.1. HIRES Mapping

High-resolution (HIRES) (under 10m spatial resolution) mapping images a specific area and time that is either at risk of human rights violations or as verification of an alleged human rights violation. This high-resolution, often panchromatic image can produce compelling, corroborating evidence to complement eyewitness reporting and is the most commonly

used application of remote sensing in human rights. Images can be overlaid with facts from geographic information systems (GIS), such as borders, ethnic neighborhoods, or locations of eyewitness reporting, to help analysts document the events.

The U.S. government began to routinely used HIRES mapping to monitor human rights violations in the mid-1990s. In 1995 then Secretary of State Madeleine Albright presented high-altitude, aircraft reconnaissance images to the U.N. Security Council depicting an excavator digging a mass grave and oblong objects, reputedly human bodies, awaiting burial (Bjørn, 2000). These HIRES photographs, combined with U.S. national satellite photographs and eyewitness reporting of mass executions of 7,000 Muslim men in the Bosnian town of Srebrenica, were effective in significantly increasing U.N. and international pressure on the leadership of the Bosnian Serbs (Figure 2-1) (New York Times, 1995). These images were also used as evidence in the successful genocide prosecutions by the International Criminal Tribunal for the former Yugoslavia of several individuals involved in the massacre, most notably Slobodan Milosevic, the former president of Serbia and Yugoslavia (Keeley & Huebert, 2004).

Figure 2-1: Possible mass graves in the Kasaba / Konjevic Polje area of Bosnia, July 1995. The arrows indicate recently disturbed earth or vehicle revetments. Source: New York Times, 29 October 1995.

HIRES mapping is an excellent tool for organizations with human rights programs, for it can detect very small phenomena associated with human rights violations, such as the destruction of a single house. In addition, it enables organizations that monitor human rights to decrease the amount of time between receipt of eyewitness reports of a violation and distribution of the images to the international community. Well-funded human rights campaigns such as the Satellite Sentinel Project (SatSentinel) purchase imagery from a constellation of HIRES sensors and can publicize

imagery from a location with a reported human rights violation in as little as twenty-four hours (SatSentinel, 2011).

HIRES mapping is most limited, in that it must receive eyewitness reports, either from victims or international observers, before an organization can order satellite images to gather evidence of suspected violations. In armed conflict, observers may be denied access, and reports by victims may be delayed for weeks or months if they leave the conflict area. Because HIRES sensors are on demand, unlike some MODRES observatories like Landsat, these sensors may miss time-sensitive phenomena because human rights organizations may not yet have a reason to direct them to the violation.

2.2. HIRES Monitoring

HIRES monitoring differs from HIRES mapping in that many digital images are recorded over a large region in a long-term, systematic effort. Images are not ordered in response to reports of specific incidents but are continually taken over time, either to provide a deterrent in an area with a population at risk of suffering from human rights violations or to document crimes over time.

Most operational work in human rights monitoring employs trained imagery analysts, who use at least two images from different times to determine whether there is a change in the image, known as "change detection". As with HIRES mapping, the images are often overlaid with GIS layers and the locations of eyewitness reports that provide context and guide analysis. Some organizations also overlay these images with data from other satellites, such as sensors that detect fire (Bromley, 2010; Wolfinbarger & Drake, 2012).

SatSentinel, established in 2010 to serve as a deterrent to human rights violations in southern Sudan, is a well-publicized example of a HIRES monitoring campaign. Sudan's government-sponsored violence against civilians in southern Sudan has been feared following South Sudan's 2011 vote for independence. In this campaign SatSentinel regularly acquires HIRES imagery, conducts analysis, and publishes the reports online. Villages, barracks, and transportation nodes are frequently imaged to record any suspicious activity (SatSentinel, 2011) (Figure 2-2). It is disputed whether the SatSentinel program, as well as other campaigns that document human rights violations for later use in court, successfully deters perpetrators (Brown, 2011). Matthew Levinger questions the effectiveness of GIS-based surveillance as an instrument for preventing genocide, noting that "projects

such as Crisis in Darfur and Eyes on Darfur are likely to be effective only if they can motivate external actors such as the U.S. government to take action against genocidal regimes" (Levinger, 2009).

Figure 2-2: Apparent intentional destruction of the village of Tajalei, in the Abyei region of Sudan, 6 March 2011. The black marks indicate recently burned huts and surrounding fields. Source: SatSentinel 2011.

HIRES monitoring is also used in U.S. public diplomacy efforts to promote the safety of civilians in areas of conflict. Imagery from either commercial or U.S. military satellites is used in multilateral (U.N.), bilateral (nation to nation), and media campaigns. In 2009 the U.S. State Department

used images acquired from HIRES sensors to support ongoing efforts to encourage international intervention in Sri Lanka (British Broadcasting Corporation, 2009). The imagery demonstrated the rapid concentration of internally displaced persons (IDPs) trapped between warring Sri Lankan military and Tamil Tiger forces, promoted an end to hostilities, encouraged relief efforts for IDPs in the safe zone, and provided evidence of a humanitarian crisis (Figure 2-3).

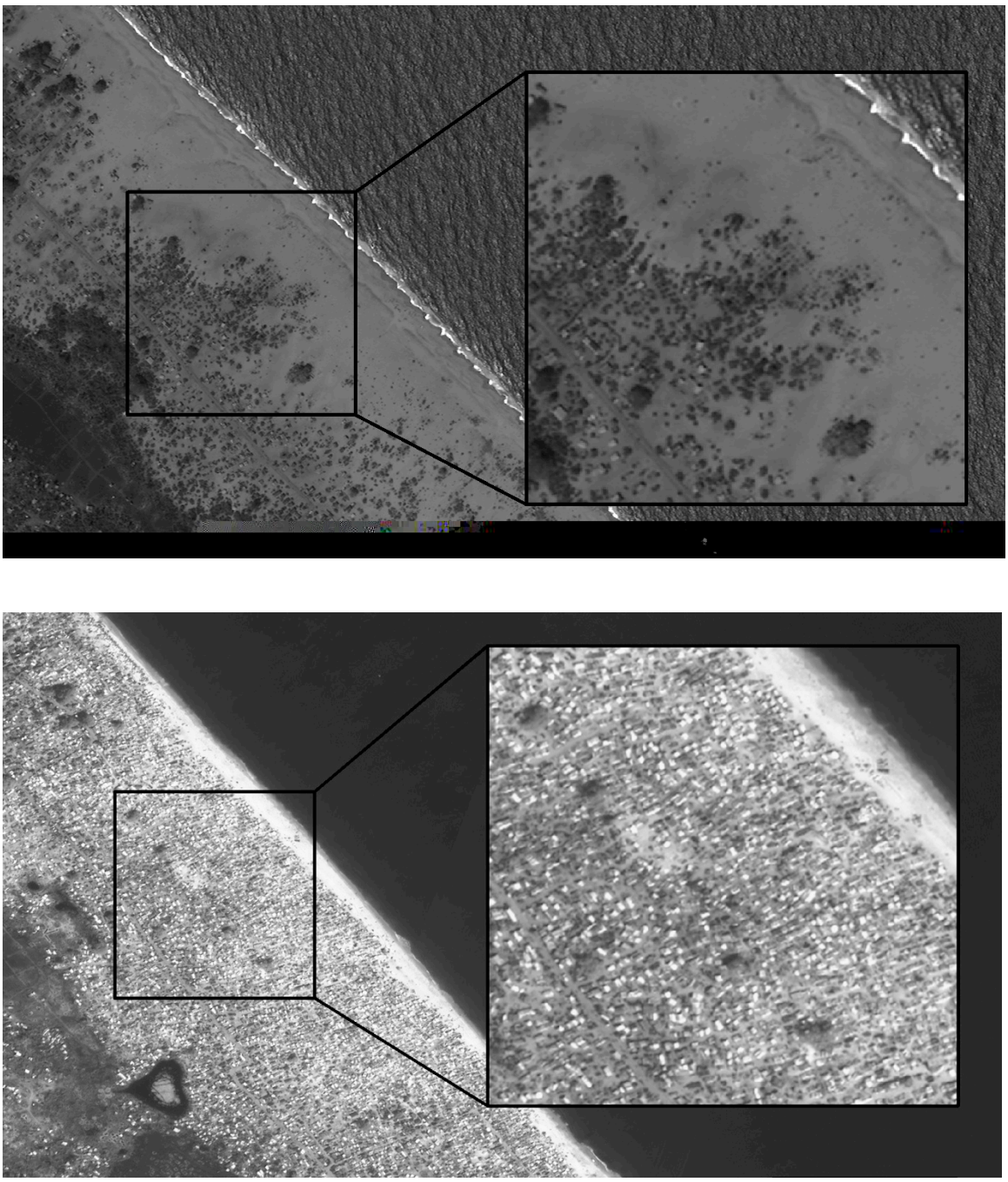

Figure 2-3: A section of a civilian safe zone in northeastern Sri Lanka. Few tents speckle the beach in the top image, taken in February 2008 but just two months later, in April, the bottom image shows the same beach packed with displaced persons' tents (BBC, 2009).

Although HIRES monitoring suffers from few methodological weaknesses, it is limited by the expense and manpower required to carry out a monitoring campaign. Depending on the satellite and the contract, images can several thousands of dollars per image, incurring prohibitive costs on the part of monitoring campaigns that require tens or hundred of images. The manual analysis of many images requires trained analysts and many hours of their time, additional factors that also contribute to the expense.

2.3. Direct MODRES Monitoring

Because MODRES sensors are continually imaging over land, organizations concerned with human rights violations can look for phenomena even if eyewitness reports come in weeks or months after the occurrence. Because of their coarser spatial resolution, human rights work and research with MODRES monitoring has focused on detecting changes to entire villages (Table 1-2). Even then, detectable changes associated with the destruction of a village can be slight, so they require careful calibration and consideration of environmental and seasonal issues such as precipitation or soil moisture. Therefore MODRES observations are most effective on large villages that experience a significant amount of destruction.

Prins (2008) provides an example of MODRES remote sensing in human rights monitoring demonstrating that Landsat ETM+ could detect the

destruction of medium to large villages in Darfur on an annual basis. In a more recent study, Bromley (2010) links the Moderate Resolution Imaging Spectroradiometer (MODIS) sensor, which detects fire, with eyewitness reports of violence in Darfur.

Although these studies have demonstrated that MODRES sensors are successful in identifying phenomena that can be linked to human rights violations, such as a change in a village's reflectivity or a fire in an area, they are still limited in several respects. Successful monitoring has been demonstrated only on spatially large phenomena, and it requires a significant change to the village that causes a physical modification of the landscape, such as burning across a large section of a village. And, unlike HIRES monitoring and mapping, MODRES sensors do not always produce compelling graphics, which limits their use in public-advocacy campaigns.

2.4. Indirect MODRES Monitoring

MODRES sensors can also be used to indirectly monitor an area for human rights violations. Sensors can look for phenomena such as abandonment of agricultural fields or removal of livestock herds, both of which indicate the departure of a civilian population. To detect these phenomena, researchers use methods that have proved effective for

measuring environmental change. This was first demonstrated in using a variety of sensors to identify war-induced agricultural abandonment in Kosovo over a two-year period (Terres et al., 1999). Other studies have followed, demonstrating the ability of MODRES sensors to detect agricultural abandonment in Croatia and Bosnia (Landsberg et al., 2006; Witmer, 2008). Schimmer (2008) used MODRES sensors to track an increase in vegetation cover and vigor in Darfur, which he linked to the displacement of people and their livestock. He noted that the spatial and temporal tracking of population displacement could provide important evidence of the scale and systematic nature of the violence, evidence that is essential in genocide trials.

These studies suffer from some methodological weaknesses, however. For example, the phenological changes that the sensor detects in the environment may be due not to conflict-related causes but to other factors. Abandoned fields may be only lying fallow (Terres et al., 1999), Schimmer (2008) acknowledges that he did not control for interannual environmental differences such as rainfall or earlier green-up periods. It may be possible to control for environmental factors, but this requires detailed weather data that are less likely to be available in locations experiencing conflict (Nicholson & Farrar, 1994). Moreover, using MODRES sensors to detect phenomena

indirectly associated with human rights violations works best when preconflict and postconflict remote sensing data are available (Witmer, 2008). Preconflict data, gathered either through ground sampling or HIRES imagery, may not exist, and postconflict ground sampling may not be possible due to persistent security threats, such as land mines.

2.5. New Methods Needed

The international human rights community continues to use remote sensing for human rights mapping or to corroborate eyewitness reporting of a violation at a specific time and location. This work has improved with decreased time lapses between reports of violations and the ordering, acquisition, processing, analysis, and dissemination of images. International human rights and humanitarian organizations are also increasingly using remote sensing for human rights monitoring or to observe regions where populations are at risk of suffering from human rights violations. However, few organizations are able to conduct monitoring campaigns because of the expense of HIRES imagery and trained imagery analysts.

Operational methods have changed little since 2003, when the Humanitarian Information Unit (HIU) demonstrated the ability to use a collection of information, including HIRES sensors, to depict village

destruction in Darfur. Since then only a few organizations have incorporated advanced remote sensing techniques such as time-coincident MODIS fire detection (Sulik & Edwards, 2010).

Chapter 3.
Landsat-based early warning system to detect the burning of villages in Arid Environments

Although previous studies have shown promising results, these methods are more suitable to scientific research than operational monitoring due to the considerable lag in time between the impact of the armed conflict on population and its identification in satellite imagery. In *Preventing Genocide: A Blueprint for U.S. Policymakers*, former U.S. Secretary of State Madeleine Albright writes that "at its most basic level, early warning means getting critical information to policymakers in time for them to take effective preventive action" (Albright & Cohen, 2008).

The strategic data acquisition plan for Landsat missions provides a suitable data source to serve as a prototype for development of such a warning system (Goward et al., 2006). The 16-day repeat cycle from Landsat 7 allowed us to collect an archive of images over Darfur between 2000 and 2008. In May 2003 the scan line corrector (SLC) malfunctioned on Landsat 7 that left only 75% of each acquired scene usable (http://landsat.gsfc.nasa.gov/about/landsat7.html). While a combination of

two Landsat satellites would have provided a better return frequency of 8 days, and thus greater opportunities for monitoring, this was not possible over Darfur region, as Landsat 5 was functioning in a very limited capacity during this time period and has since been decommissioned.

Subsequently, this project uses ETM+ as a prototype to develop such a warning system and to test its abilities. The proposed approach may then be operationally deployed using Landsat 8 (LDCM or Landsat Data Continuity Mission) that was successfully launched on February 11, 2013.

Methods applied within an early warning system require an economically viable combination of frequent observations of the affected area, as well as an appropriate spatial resolution and spectral range for detecting the footprint of the phenomena associated with human rights violations. The price of individual fine of very fine images (Table 1-2), and the limitations of some platforms in the spectral range of their observations, makes an operational application from these sensors economically unfeasible. However, only fine or very fine imagery allows for definitive identification of individual households and their condition in the Darfur region. Therefore, an early warning system for monitoring impacts of an armed conflict on population in Darfur requires a coordinated effort of fine

or very fine data acquisition strategy, guided by the early-stage impact identification from the MODRES data.

This chapter introduces a methodology for an early warning system using ETM+ that is designed to provide automated detection of the destruction of villages in arid environments. This remote sensing algorithm capitalizes on Landsat program's historical archive, radiometric stability (Markham et al., 2004), consistent calibration, and systematic observations by constructing a historic spectral baseline for each village in the study area. The application of the algorithm to the archived or operationally acquired Landsat and Landsat-like imagery identifies areas of high likelihood for village destruction in space-time and provides specifications for fine or very fine image acquisition and analysis to verify impact and quantify the extent of damage at the individual household level.

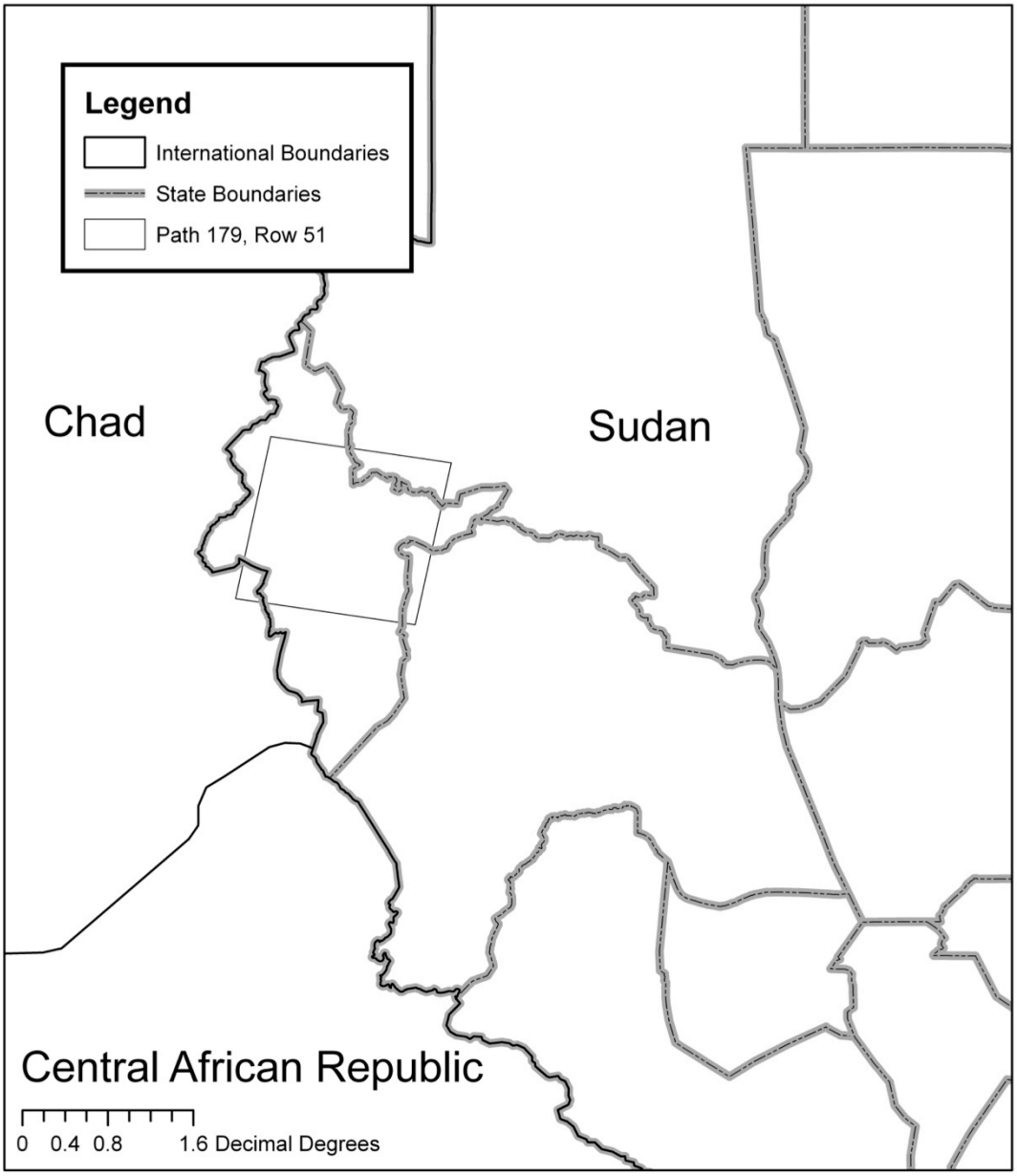

Figure 3-1: The study area in covers portions of West, North and South Darfur in western Sudan.

3.1. Study area

In the late 1980s and 1990s, the Sudanese state of Darfur experienced clashes from both inter-tribal conflicts and armed insurrection by rebel

groups. Beginning in 2003, the violence significantly escalated as government-supported militia groups, and later Sudanese military forces, attacked and destroyed thousands of villages (Flint & De Waal, 2008). By September 2005 over 2 million people had fled the rural areas of Darfur to camps and the larger towns, and another 200,000 had sought refuge in neighboring Chad (Petersen & Tullin, 2006). Refugees reported a similar pattern of attack: 1) their village was bombed, 2) soldiers and militia surrounded and entered the village, and 3) villages were looted and frequently burned.

The proposed algorithm detects a remotely sensed phenomenon associated with a human rights violation. Specifically it detects a dramatic change in surface reflectance, which is associated with the burning destruction of a village. This approach provides a high degree of accuracy because, at the time in Darfur, such destruction was almost always due to an armed group violently removing a population and preventing their return by destroying the village (Flint & De Waal, 2008).

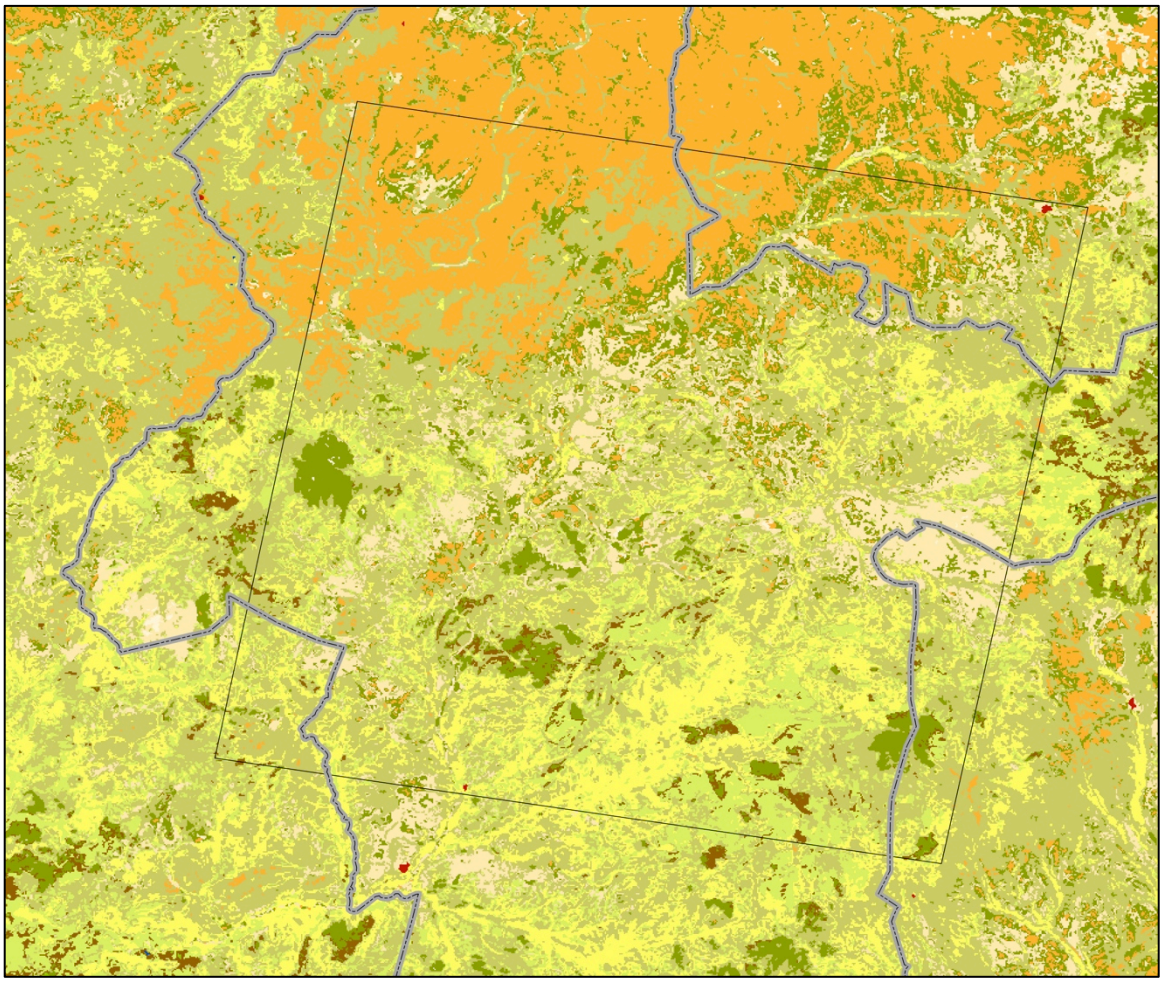

Figure 3-2: The study area consists primarily of closed to open grassland (140) in the north, to rainfed croplands (14) and mosaic vegetation/croplands in the south (30) (Defourny et al., 2006). Path/row 179/51 is indicated in black.

The study area consists of Landsat ETM+ path/row 179/51 in western Darfur, Sudan. The land cover consists primarily of open grassland in the north, increasing to rainfed croplands and mosaic vegetation/croplands in the south in the south (Fig. 3-2) (Defourny et al., 2006). It experiences heavy rain from the beginning of July to the end of September, with little rainfall in other months (Fig. 3-3) (Huffman et al., 2009). While the widespread conflict in Darfur was distributed across 8 Landsat path/rows, this location was chosen because it contains the greatest concentration of destroyed villages in a one-year period (HIU, 2010).

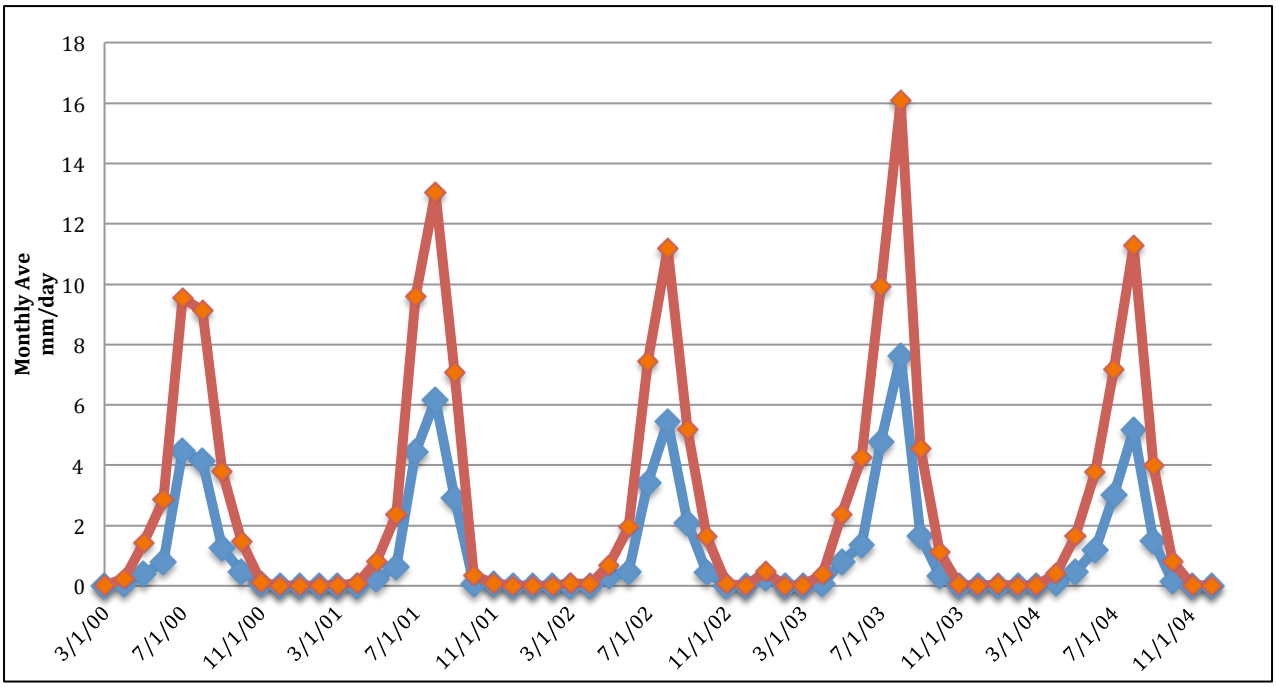

Figure 3-3: Mean Precipitation for latitude 12-13 North, 22-24 East (red) and 13-14 North, 22-24 East (blue) (Huffman, 2009).

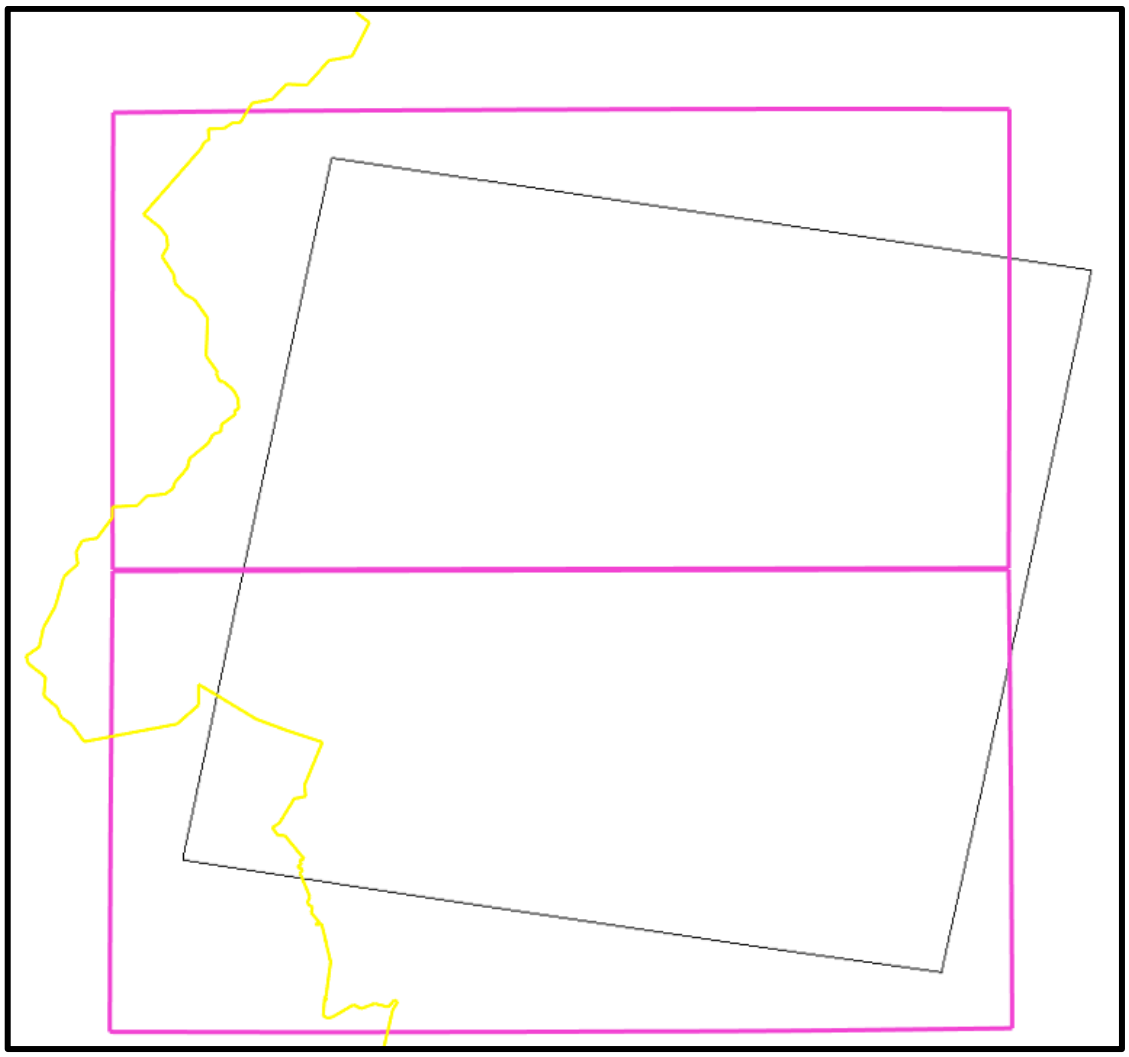

Figure 3-4: Huffman (2009) precipitation grids 12-13 North, 22-24 East and 13-14 North, 22-24 East (pink). Sudanese international boundary (yellow). Landsat ETM+ path/row 179/51 (grey).

3.2. Methodology

The input data for the algorithm includes Landsat surface reflectance data and the Humanitarian Information Unit's database of villages in Darfur (HIU, 2010). The methodology is presented in three parts: 1) image

processing and village delineation; 2) algorithm flow; and 3) evaluation of 16 bands/indices derived from ETM+.

3.3. Image processing

The analysis of the change in surface reflectance caused by village destruction was performed using Landsat 7 ETM+ images. Images were collected from four baseline years, ranging from 15 October 2000 to 26 December 2003 and the entire test year in 2004 (Table 3-2). There was a total of 21 SLC-on and 3 SLC-off images available (http://earthexplorer.usgs.org) for the baseline period, and 25

Table 3-1: Images Used in Study.

USGS ID	Date
LE71790512000289EDC00	15-Oct-00
LE71790512000353SGS00	18-Dec-00
LE71790512001035SGS00	4-Feb-01
LE71790512001099EDC00	8-Apr-01
LE71790512001131SGS00	10-May-01
LE71790512001179EDC00	27-Jun-01
LE71790512001291SGS00	17-Oct-01
LE71790512001355SGS00	20-Dec-01
LE71790512002070EDC00	10-Mar-02
LE71790512002294SGS00	20-Oct-02
LE71790512002310SGS00	5-Nov-02
LE71790512002342SGS00	7-Dec-02
LE71790512003009SGS00	9-Jan-03
LE71790512003057SGS00	26-Feb-03
LE71790512003089EDC00	29-Mar-03
LE71790512003313ASN01	8-Nov-03
LE71790512003361ASN01	26-Dec-03
LE71790512004028ASN01	28-Jan-04
LE71790512004044ASN01	13-Feb-04
LE71790512004076ASN01	16-Mar-04
LE71790512004092ASN01	1-Apr-04
LE71790512004108ASN01	17-Apr-04
LE71790512004124ASN01	3-May-04
LE71790512004140ASN01	19-May-04
LE71790512004156ASN01	4-Jun-04
LE71790512004316ASN00	11-Nov-04
LE71790512004332ASN00	27-Nov-04
LE71790512004348ASN00	13-Dec-04

SLC-off for 2004. Of these, 17 images were not significantly impacted by clouds and were used for the baseline, and eleven images in 2004 were used to test the algorithm. The SLC corrector issues of ETM+ imagery that began in May 2003 affect 25% percent of the footprint (Fig. 3-6). Landsat 5 TM imagery is unavailable for this location because of the 1987 failure of the Tracking and Data Relay Satellite System (TDRSS) transmitter and because this path/row is not within range of a downlink station (Goward et al., 2006).

All Landsat terrain corrected (L1T) imagery were converted to surface reflectance using the Landsat Ecosystem Disturbance Adaptive Processing System (LEDAPS) (Wolfe et al., 2004). LEDAPS includes the Automated Cloud Cover Assessment (ACCA) algorithm, which creates an automatic cloud and cloud shadow mask based on Landsat bands 2 through 6 (Irish et al., 2006); however, ACCA does not perform well on semi-transparent clouds or cloud edges. Two baseline images (4/28/02 and 6/15/02) were not used due to cloud contamination that was not successfully masked with the ACCA (Fig. 3-5).

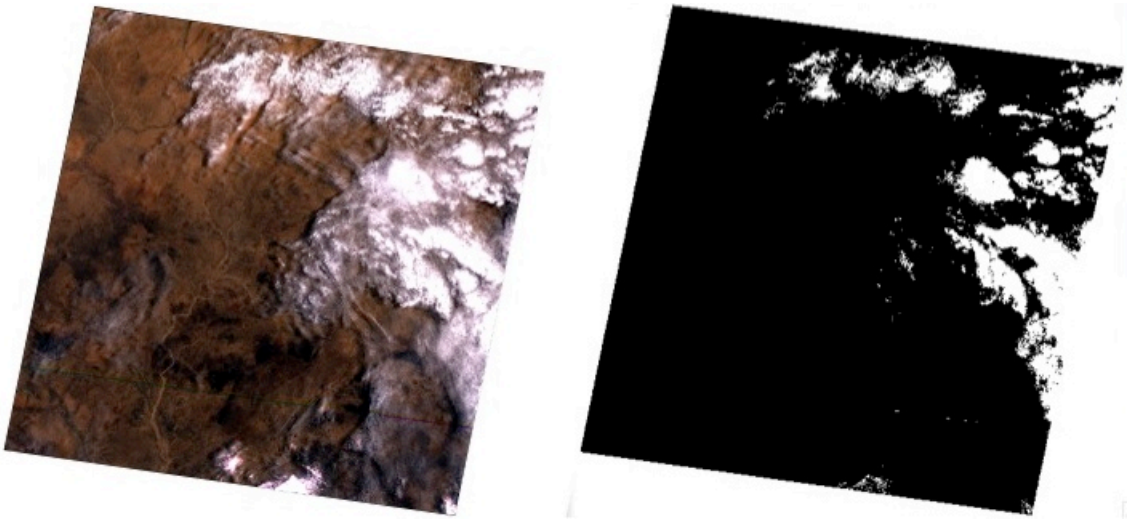

Figure 3-5: Landsat 7 image from 4/28/2002 (path 179 row 51) (RGB – left) (ACCA mask – right). Cloud edges and semi-transparent cloud were not successfully masked.

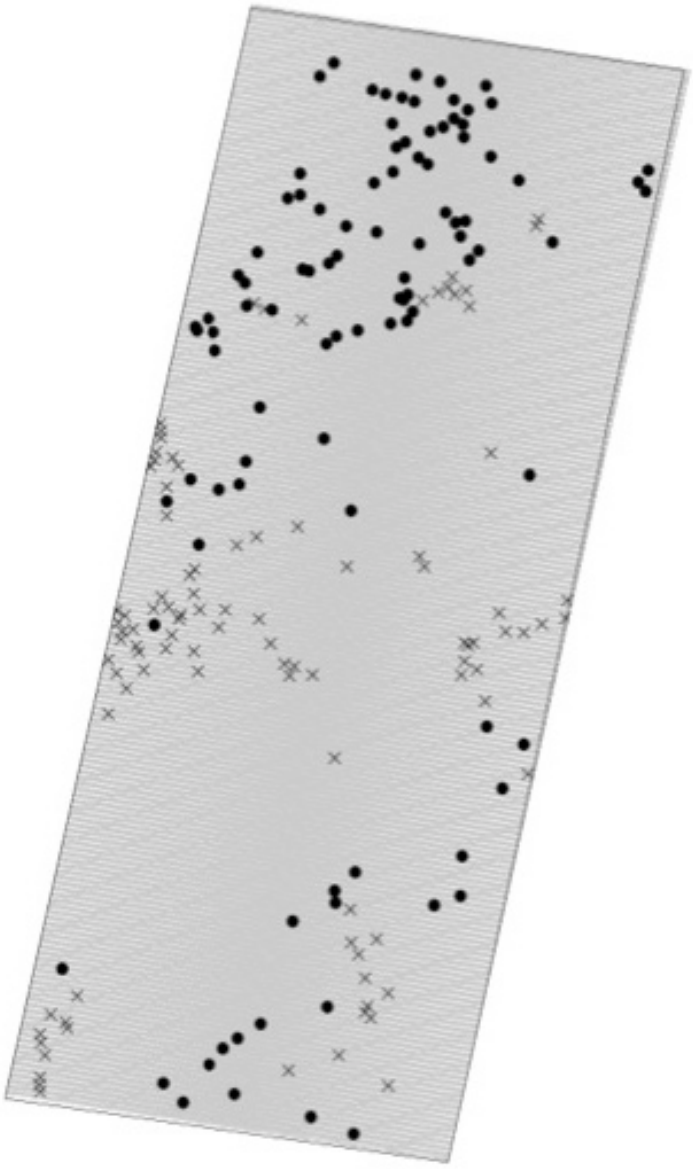

Figure 3-6: Study area path/row 179/51 showing a) scan line error areas in white, b) study area polygon, c) destroyed villages X, and d) control villages O. Villages in the study were chosen from the middle of the Landsat scene to minimize a lack of coverage due to scan lines.

Villages used in the case study were selected from the HIU's database of villages in Darfur (HIU, 2010). This database provides a center point (latitude and longitude) of all villages in Darfur and, where possible, its

status by year (damaged, destroyed, or no damage). The extent of each village's structures was delineated manually from VHR imagery available in Google Earth and villages that are in areas significantly impacted by the SLC errors were omitted from the study. All villages in the study area that were listed as destroyed in 2004 and not significantly impacted by SLC errors were selected to test the algorithm—a total of 92 villages. These villages ranged in size from 25 to 262 Landsat pixels, or 750 to 7,860m^2. Another 92 villages were randomly selected from villages that were not in SLC error areas and were never listed as damaged or destroyed (Fig. 3-6). Five of these villages were smaller than 20 Landsat pixels or 600m^2 and were removed from the control dataset, bringing the number to 87 villages.

While control villages were selected randomly, they tended to be smaller on average (2,659m^2) than villages that were identified as destroyed (3,634m^2). This is likely due to the fact that large destroyed villages have more eyewitnesses reporting attacks and are easier to identify through imagery. Control villages also tended to have larger baseline NIR observations (NIR= 0.32) than destroyed villages (0.28), indicating a greater density of built structures that are made of dried plant material.

3.4. Band/Index Selection

Sixteen different bands/indices derived from ETM+ were evaluated for use in the proposed analysis approach. The band/index must produce a stable signal for each village throughout the baseline years. This creates a stable baseline with which to compare future observations and identify possible village destruction. This also prevents the incorrect identification of a destroyed village during the test year (i.e. commission error). However, the signal must be sensitive enough to identify the destruction of even small villages with sparsely built structures during the test year. This analysis focused on testing a combination of surface reflectance and derived indices on two major components: 1) signal stability and 2) signal sensitivity.

3.4.1. Signal Stability

Seventeen ETM+ images from 15 October 2000 to 27 December 2003 created a population of observations for 179 different villages to evaluate 16 different bands/indices in their ability to produce a stable population of observations throughout the baseline years (Table 3-1). These metrics were chosen because they are the bands and indices most commonly researched in burn scar detection. The bands/indices includes Landsat ETM+ bands 1

through 8, the normalized burn ratio (NBR) (Key & Benson, 2002), NDVI (Tucker, 1979), visible bands sum (sum of ETM+ bands 1,2,3,4,5,7), ETM+ bands 1+2+3, ETM+ bands 4+5, ETM+ bands 4+5+7, Tasseled Cap (TC) Brightness, TC Greenness, and TC Wetness (Huang et al., 2002).

For use in the proposed algorithm, a signal must be stable in all baseline observations, and not exhibit a strong seasonal green-up. Sampling only from within a village's extent minimizes seasonal green-up, as well as only recording the village's lowest 20% of pixels (Fig. 3-12). Additionally images from the months of June, July, August and September were not used because they correspond to the region's wet season (Huffman et al., 2009). Although these measures were taken, there is some evidence of village's producing lower reflectance scores following the wet season in October (Fig. 3-8 and 3-9) indicating that a seasonal green-up is minimized, but not fully negated.

A one-way ANOVA F-test statistic evaluated the relative stability of each band/index (Table 3-2) by measuring the between-group variability over within-group variability (Weisstein, 2003). In this algorithm, the variability between the 179 villages is divided by the variability within a single village (over up to 17 dates) so the larger the F-statistic, the more stable the signal is in comparison to observations across all villages.

Table 3-2: The stability of Landsat-based metrics in the algorithm was tested through an F-test statistic over baseline years. The variability between the 179 villages was divided by the variability within a single village so the larger the F-statistic the more stable the signal is in comparison to observations across all villages. ETM+ bands 4 and 5, and their sum, produced the most stable observations in the algorithm.

Band 1	5.32	NDVI	4.32
Band 2	11.91	1+2+3+4+5+7	23.68
Band 3	16.73	1+2+3	12.26
Band 4	34.62	4+5	37.19
Band 5	36.15	4+5+7	32.6
Band 6	0.29	TC Brightness	23.91
Band 7	21.44	TC Greenness	6.66
NBR	7.64	TC Wetness	28.35

The combination of NIR and SWIR1 (Landsat band 5 ~1.5µm) produced the least amount of variability within a village compared to between villages. SWIR1 was the most stable single band followed by NIR. SWIR1, and to a lesser degree Wetness, produced high F-statistics because they are sensitive to moisture content of soil and vegetation. Because all observations were taken in the dry season, there was little change in moisture content within a village over time resulting in a stable signal (Fig. 3-8 and 3-9).

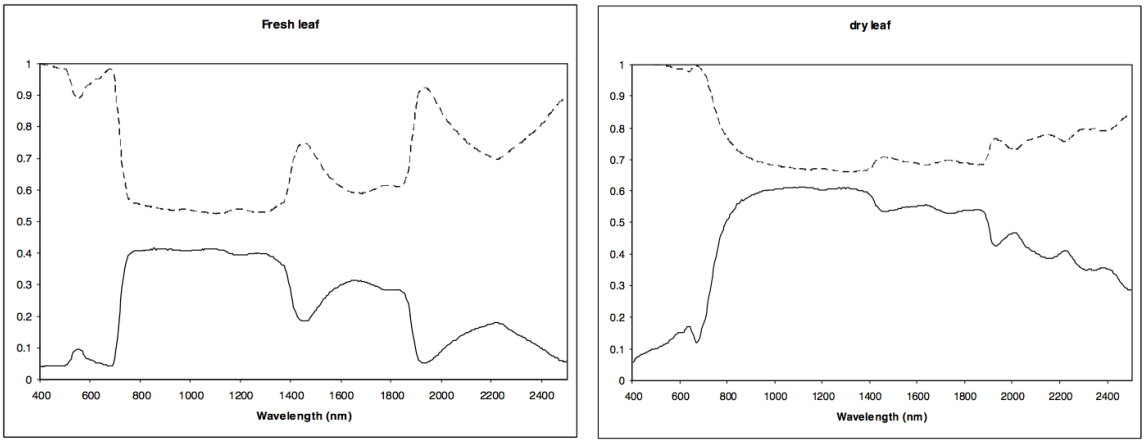

Figure 3-7: Reflectance (solid line) and transmittance (dashed line) of (left) fresh leaf and (right) dry leaf of a semiarid species, Quercus pubescens (Ustin, 2005).

NIR, which is sensitive to changes in biomass, both green vegetation (GV) and non-photosynthetically active vegetation (NPV) (Numata et al., 2007; Ustin et al., 2009) (Fig. 3-7), produced a stable population of baseline

observations because these arid villages are composed of dry plant material and bare, unvegetated ground. Additionally, because only dry-season images were used, seasonal green-up within these villages is minimized (Fig. 3-8 and 3-9). While NBR is based on bands that were stable in this evaluation (NIR and SWIR1), NBR produced a very low F-statistic because it is a ratio designed to amplify differences in the signals (Table 3-2).

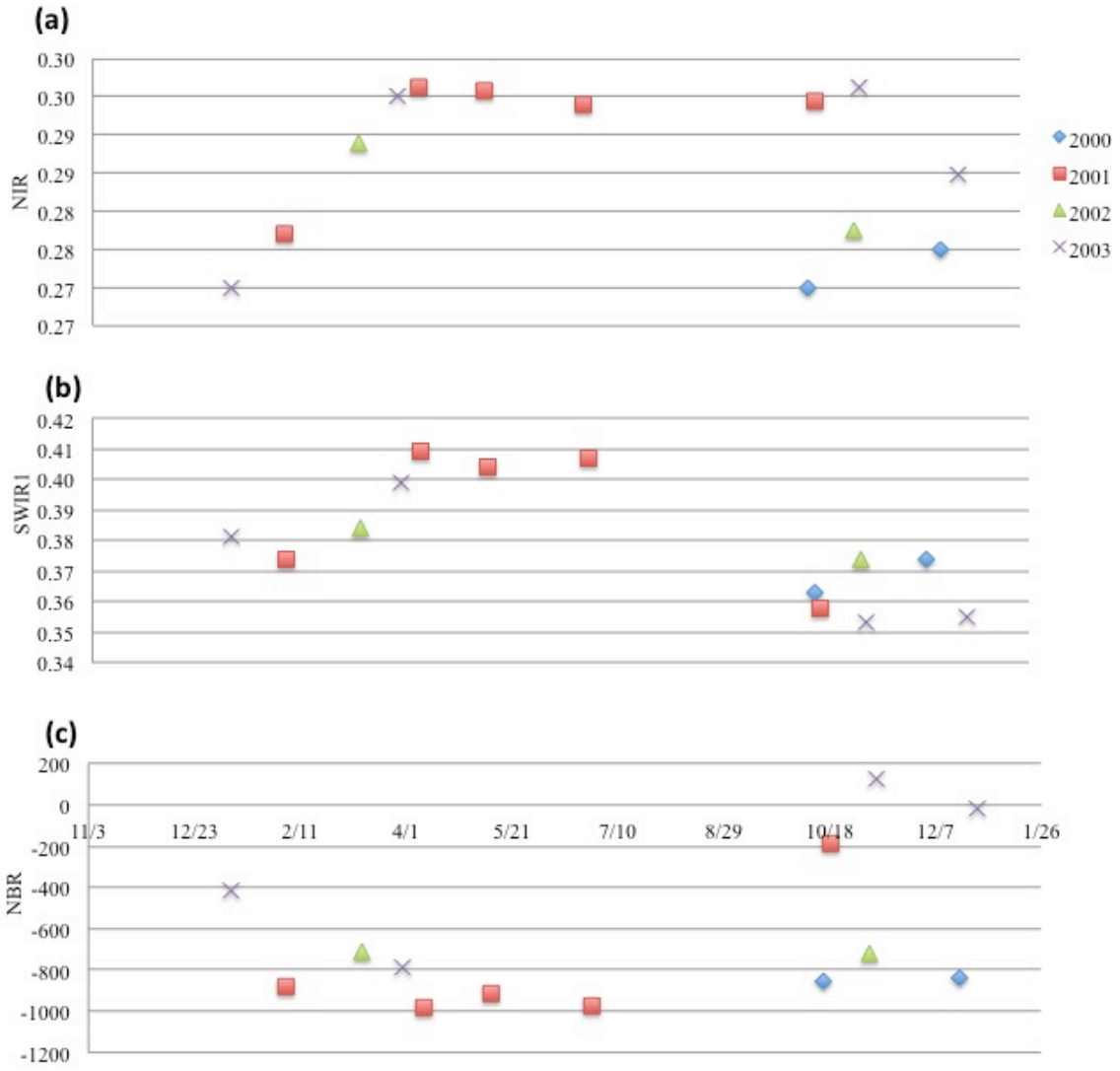

Figure 3-8: Baseline observations in the algorithm for NIR (a), SWIR1 (b), and NBR (c) for test village #5. SWIR1 and NIR provided the most stable population of observations in baseline years as measured by their F-statistic (Table 3-2). Observations were not used from 1 July to 30 September due to cloud cover and green-up during the wet season and because fighting took place during the dry season.

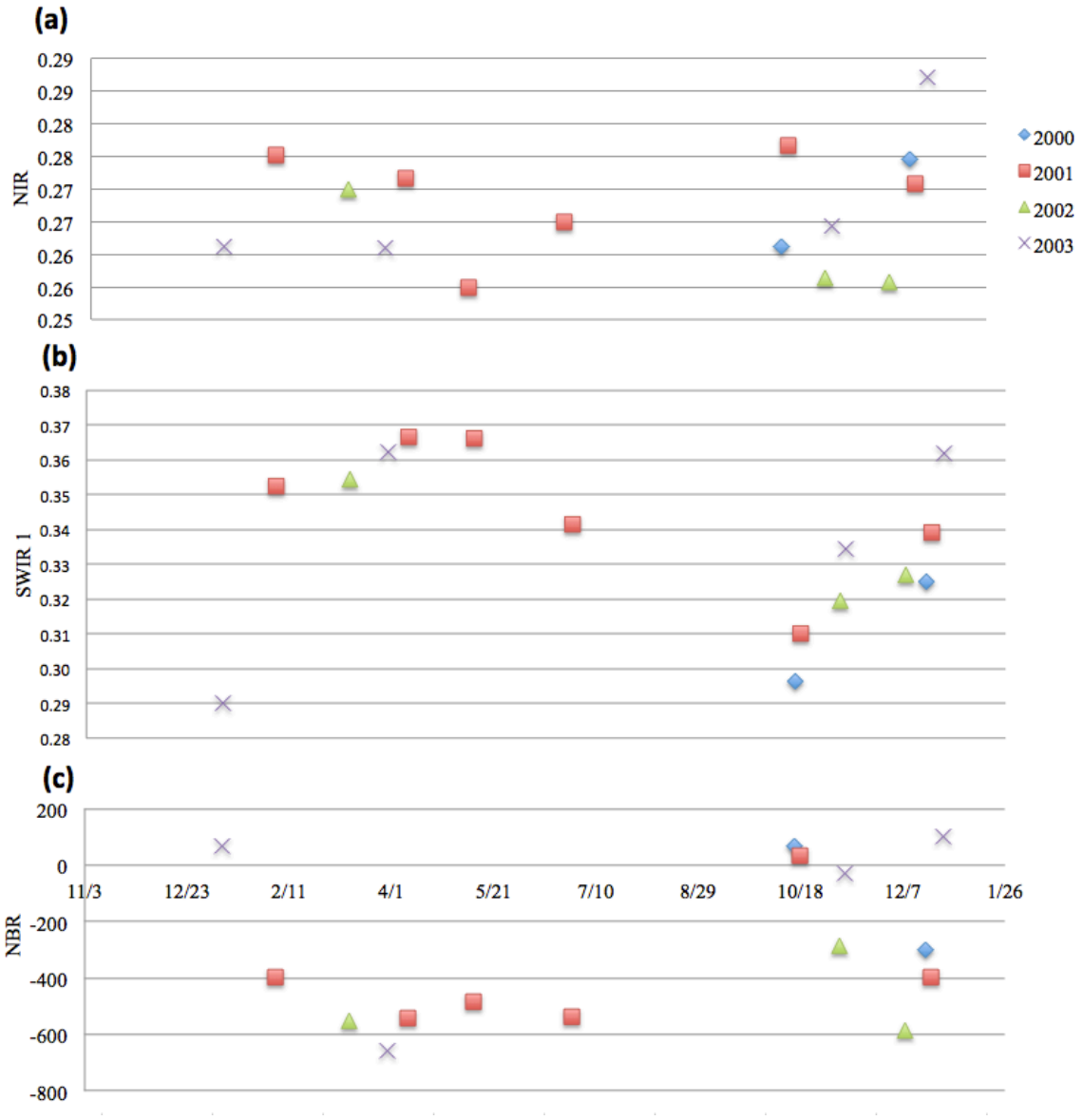

Figure 3-9: Baseline observations in the algorithm for NIR (a), SWIR1 (b), and NBR (c) for test village #67. SWIR1 and NIR provided the most stable population of observations in baseline years as measured by their F-statistic (Table 3-2). Observations were not used from 1 July to 30 September due to cloud cover and green-up during the wet season and because fighting took place during the dry season.

Figure 3-10. Um Zaifa, South Darfur, Sudan, burned on 10 December 2004. This village is not in the extent of the study area (lat: 24.667, lon: 11.067) (Petersen & Tullin, 2006). Photo: Brian Steidle © Courtesy of United States Holocaust Memorial Museum.

3.4.2. Sensitivity

16 different metrics derived from ETM+ were evaluated in their ability to detect the destruction of a village during the test year. These metrics were chosen because they are the bands and indices most commonly researched in burn scar detection. For the 92 villages listed as destroyed for the test year of 2004 (HIU, 2010), each metric should produce at least one observation that is separated from the body of baseline observations, which

is estimated as the detection of the village now destroyed (Fig. 3-11). Additionally for the 87 villages confirmed as not destroyed for 2004, there should be no observations that separate from the body of baseline observations.

The test year consisted of 11 ETM+ images in 2004 for the 179 villages. A one-tailed, student's t-test was used to determine if a village's observation during the test year was significantly lower than all observations during the baseline years (Weisstein, 2003). If the p value was less than a significance value of 0.0001, the village was considered destroyed (Table 3-3). There was assumed to be no variability in any single test observation, permitting a very low significance value of 0.0001.

Table 3-3: Landsat-based metrics were tested in the algorithm against the reference database. A one-tailed, student's t-test was used to determine if any single, test year observation was lower than that village's baseline observations. There was assumed to be no variability in the single test observation, permitting an α of 0.0001.

	Omission Error	Commission Error	Accuracy
Band 1	88.0%	16.1%	46.9%
Band 2	90.2%	3.4%	52.0%
Band 3	92.4%	5.7%	49.7%
Band 4	17.4%	13.8%	84.4%
Band 5	65.2%	14.9%	59.2%
Band 6	57.6%	77.0%	33.0%
Band 7	82.6%	4.6%	55.3%
NBR	16.3%	47.1%	68.7%
NDVI	17.4%	72.4%	55.9%
1+2+3+4+5+7	84.8%	10.3%	51.4%
1+2+3	89.1%	9.2%	49.7%
4+5	42.4%	12.6%	72.1%
4+5+7	73.9%	10.3%	57.0%
TC Brightness	79.3%	9.2%	54.7%
TC Greenness	19.6%	77.0%	52.5%
TC Wetness	72.8%	26.4%	49.7%

L7 ETM+ visible bands and indices that use a combination of these bands, such as 1+2+3+4+5+7 and Red+Green+Blue, performed poorly with very high omission rates and very low commission rates (Table 3-4). These metrics were not able to detect the signal for a village's destruction from the signal's noise, primarily because these metrics were not stable during the baseline years. SWIR2 (Landsat band 7 ~2.1 μm), Brightness, and Wetness

performed better than the visible bands, but were also unable to separate the signal indicating a village's destruction from the metric's noise.

By contrast, NBR, NDVI, and Greenness all produced very strong signals representing the destruction of a village, but because of the high variability of these indices (as indicated in their low F-statistics) (Table 3-2), they have very large commission error rates on control villages (Table 3-3). While SWIR1 and NIR + SWIR1 produced very stable populations of baseline observations, the signals produced for destroyed villages were insufficient for detection of destroyed villages as seen in their high omission rates.

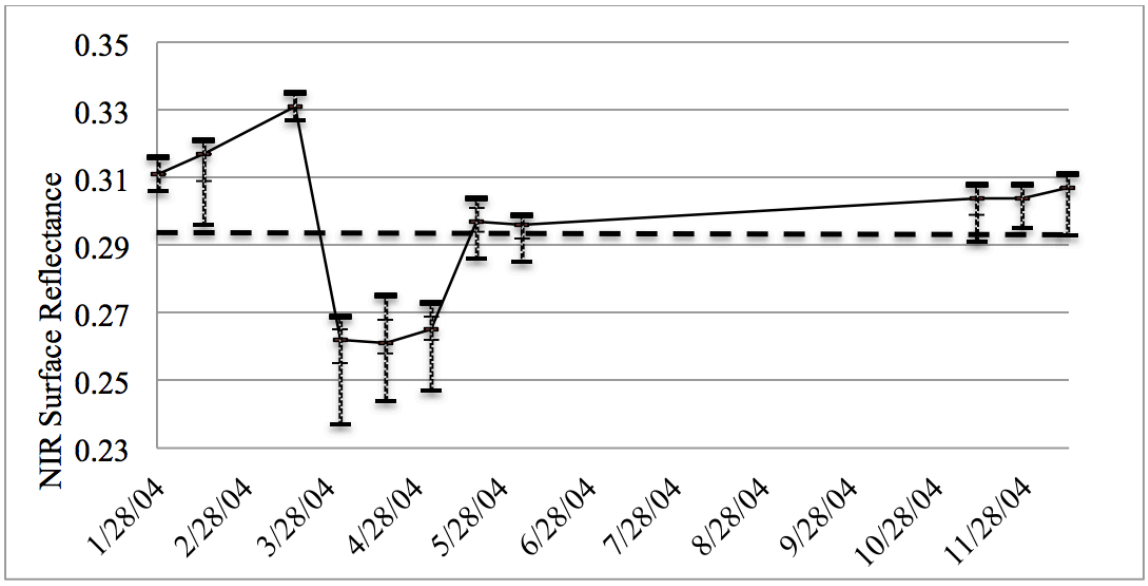

Figure 3-11: Year 2004 observations for test village #5 show the sensitivity of NIR in the algorithm to detect a possible destruction; between the third and fourth observations in this case. The village's average for baseline observations (0.294) is shown as a dashed line.

ETM+ band 4 or NIR was the most effective metric tested for the algorithm. NIR produced a stable population of observations in the baseline years, as evidenced in a high F-statistic. This stability is also seen in the low commission rate for control villages in the test year. Additionally, the signal correctly representing the detection of a destroyed a village was strong enough for detection from the signal's noise, as evidenced by the low omission error rate (Table 3-4).

NIR likely performs well because villages in the study area are primarily constructed with deadwood and straw (Fig. 3-10) (Steidle, 2004). When a village is destroyed there is a significant and persistent drop in biomass that is detectable in Landsat's NIR band. NIR is sensitive to changes in biomass, both in green vegetation and non-photosynthetically active vegetation (Fig. 3-7) (Numata et al., 2007; Ustin et al., 2009). The change in NIR reflectance represents the transition in the village's structures from dead plant material to char and ash (Fig. 1-5) (U.S. Geological Society, 2011).

3.5. Algorithm Flow

Two satellite images from two dates, spaced one year apart (or annual multiples), are most often used in change detection because they minimize

discrepancies in reflectance caused by seasonal vegetation fluxes and sun angle differences (Coppin et al., 2004). This has been shown to be very effective in detecting forest disturbance using Landsat TM and ETM+ (Huang et al., 2008; Kennedy et al., 2007). Temporal trajectory analysis is less accurate, attempting to identify changes within a calendar year by building seasonal development curves or profiles of the study area. Changes are detected when the study area departs from the baseline curve (Kasischke & French, 1995).

This algorithm proposes new methodology by detecting if a village's observation at each new pass of the sensor during the test year is significantly lower than the body of observations from baseline years (Fig. 3-12). To identify when structures within the village transition from dry plant material to charwood and charred soil, observations are calculated averaging the lowest 20% of the village's pixels.

$$T\_Test = \frac{Mean - Observation}{Stdev/\sqrt{df}}$$

During the test year, a one-tailed, student's t-test (p=0.0001) is used to determine if village's observation is significantly lower than the historical body of its observations (Weisstein, 2003), where "mean" is the mean of all baseline observations, "observation" is the value for the test observation,

"Stdev" is the standard deviation of all baseline observations, and "df" is degrees of freedom, or the count of all baseline observations. This T-Test is assumes there is no variability in the observations, resulting in very low probability values.

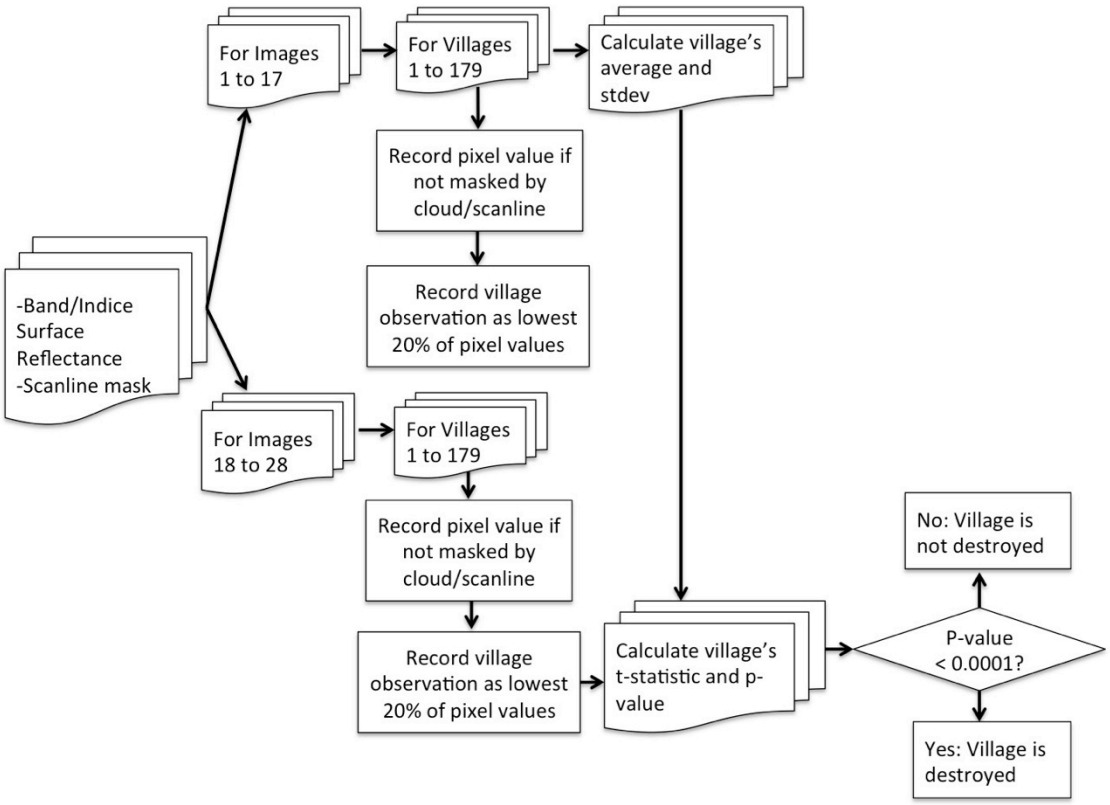

Figure 3-12. Landsat ETM+ destroyed village detection algorithm process stages.

This methodology is possible in part because LEDAPS is effective at reducing differences in the images caused by atmospheric effects (Masek et al., 2006). The method of comparing a village's observation to a stack of its

previous observations increases the sensitivity of the algorithm by eliminating differences between villages such as local land cover and the density of build structures. This is similar to Loboda, et al. (2007), increasing the sensitivity of fire detection methods by modifying the algorithm based on the local environment.

3.6. Validation dataset and methodology

The validation reference base used to test the algorithm's performance on these 197 villages is the U.S. Department of State's Office of the Geographer and Global Issues' HIU database (HIU, 2010). This database lists the location of villages in Darfur, Sudan and their annual status as either damaged, destroyed, or no damage. A destroyed village is defined as confirmed evidence of complete destruction of the village. Villages where the date of damage could not be determined (those listed in the database as "damaged at any time") were not included in this study. A confusion matrix was calculated with commission and omission errors and the overall accuracy (Table 3-4).

3.7. Results

The use of ETM+ band 4 in the algorithm correctly detected 82% of the villages identified as destroyed by the HIU database in 2004. The algorithm incorrectly detected 14% of the control villages as being destroyed. Increasing the significance level to 0.0005 reduces the omission rate, but it also significantly increases the number of villages incorrectly detected as destroyed. While there is limited fine or very fine resolution imagery of this area in 2004 and subsequent years, a survey of available fine or very fine resolution imagery from 2005 to 2007 confirmed that at least six of the eight control villages identified as destroyed in 2004 were in fact identified incorrectly.

There is not a single identified factor for why twelve of the 87 control villages had an observation in the test year that was significantly lower than its body of baseline observations. These villages had a slightly higher baseline average and standard deviation (0.34 and 0.024, respectively) than all control villages (0.32 and 0.022, respectively). While small control villages (less than 50 pixels) were more likely to have commission errors, large control villages (at least 180 pixels) had few commission errors (Table 3-4). These large villages tend to have lower NIR averages and less NIR

variability throughout the year, likely because they are more densely built and reflect seasonal green-ups less than small villages. There was no temporal correlation, such as the first image after the wet season, for when a control village registered a commission error. It is most likely that these few control villages which were detected by the algorithm as being possibly destroyed in the test year was because of anthropological reasons such as the burning of agricultural plots very close or within the village's border, or because fences or other structures were destroyed on a limited basis in the village.

Table 3-4: Omission and Commission Errors by village size. The control village data set had a larger number of smaller villages and a higher percentage of commission errors. Large villages (over 179 pixels) had few errors. While control villages were selected randomly, they tended to be smaller on average than destroyed villages that have more eyewitnesses reporting attacks and are easier to identify through imagery.

	Destroyed Villages		Not Destroyed Villages	
Pixels	Total	Omission Error	Total	Commission Error
20-49	9	1	26	7
50-99	28	6	33	4
100-179	41	8	22	0
180-285	14	1	6	1

16 of 92 villages listed as destroyed in 2004 (HIU, 2010) were not detected as destroyed using our approach. Similar to the villages that had commission errors, villages with omission errors had higher baseline reflectances and standard deviations (0.28 and 0.016, respectively) than those where a burn was detected (0.29 and 0.017, respectively), indicating villages with more seasonal plant growth. A survey of available VHR imagery confirmed that 13 of these 16 villages were destroyed sometime before 2007. One of the villages was identified as intact in the VHR imagery, indicating shortcomings in the reference database. Further visual inspection of Landsat ETM+ imagery indicates that three of these villages were destroyed in the end of 2003, effectively reducing omission error to 12 of 92, or 13%.

During the wet season, there is a five-month gap in satellite coverage from 4 June to 11 November 2004 due to cloud cover. Although village destruction declines during this time due to impassable roads (Petersen & Tullin, 2006), other omission errors may be because villages were destroyed during this time period. While the HIU database was used because it contained the largest collection of villages identified as destroyed, the few errors in the database reveal that a study of its accuracy using smaller databases compiled from eyewitness reporting (Petersen & Tullin, 2006; Raleigh et al., 2010) would be valuable for future studies that cover the entire Darfur conflict.

3.8. Conclusion

Currently few organizations are able to conduct human rights monitoring campaigns because existing methods are prohibitively costly and labor-intensive. The presented algorithm provides an approach that reduces the cost of human rights monitoring campaigns in arid regions by focusing the purchase of VHR imagery and analysis to areas that have been alerted by MODRES sensors. This does not eliminate the costs however. While the MODRES imagery and imagery pre-processing software (LEDAPS) is available online at no cost to users, the software used to run the algorithm,

VHR imagery purchases to confirm village destruction, and trained analysts to interpret the results still make this a costly monitoring program to implement.

Our results show that the approach provides a reliable detection of village destruction in 84% of the cases with very few false alarms. As a warning mechanism, the demonstrated approach provides a worst-case lag of 16 days (assuming no cloud cover), the revisit rate of ETM+. The Landsat Data Continuity Mission (LDCM), launched in 2013, in combination with ETM+, would reduce the warning lag by up to eight days. Additionally, other MODRES sensors, such as India's ResourceSat-1 Advanced Wide Field Sensor (AWiFS), have been shown to be interchangeable with Landsat in earth-observing applications (Goward et al., 2012). The inclusion of other MODRES sensors to this algorithm could also be used to improve accuracy by modifying the algorithm to detect when two sequential observations are significantly different from baseline observations.

The threshold, developed within this algorithm, is aimed at monitoring villages in Darfur, Sudan in 2004, and is specific to this region's building materials as well as the methods of the perpetrators (e.g. the burning of villages). The expansion of this approach necessitates the identification of an observable signal in the region of interest that indicates a

possible international humanitarian law violation. We plan to expand the algorithm to other regions following the overall framework presented in this paper. In the future, data from a constellation of MODRES sensors could provide a low-cost and continual monitoring of regions at-risk of international humanitarian law violations.

Chapter 4. Analysis of the Darfur Conflict, 2002 to 2008

4.1. Introduction

Since the late 1980s there have been minor clashes in the Sudanese state of Darfur due to inter-tribal conflicts and rebel-armed insurrection. The beginning of the waves of mass atrocities in Darfur, however, started in April 2003 with the government's response to the successful 25 February 2003 rebel attack against an army garrison in the Marrah Mountains (Power, 2004). At this time, government-supported militia groups, known as Janjaweed, and later Sudanese military forces, attacked thousands of villages, killing and raping their inhabitants. They also prevented the return of escaped villagers by slaughtering their livestock and destroying homes (Flint & De Waal, 2008). By September 2005 over 2 million people had fled the rural areas of Darfur to camps and the larger towns, and another 200,000 had sought refuge in neighboring Chad (Petersen & Tullin, 2006).

4.2. Study Area

The study area consists of West Darfur, and portions of North and South Darfur where villages were documented as destroyed from 2003 to 2008 in the HIU database (HIU, 2010). Using the U.N. Land Cover Classification System, the study area consists primarily of bare and

grassland with closed and open tree canopy in the north, increasing to rainfed croplands and mosaic vegetation/croplands in the south (Fig. 4-1) (Defourny et al., 2006). This region experiences heavy rain from the beginning of July to the end of September, with little rainfall in other months (Huffman et al., 2009). Scenes that occur during the wet season (July, August, and September) were not used to minimize seasonal green-up within these villages.

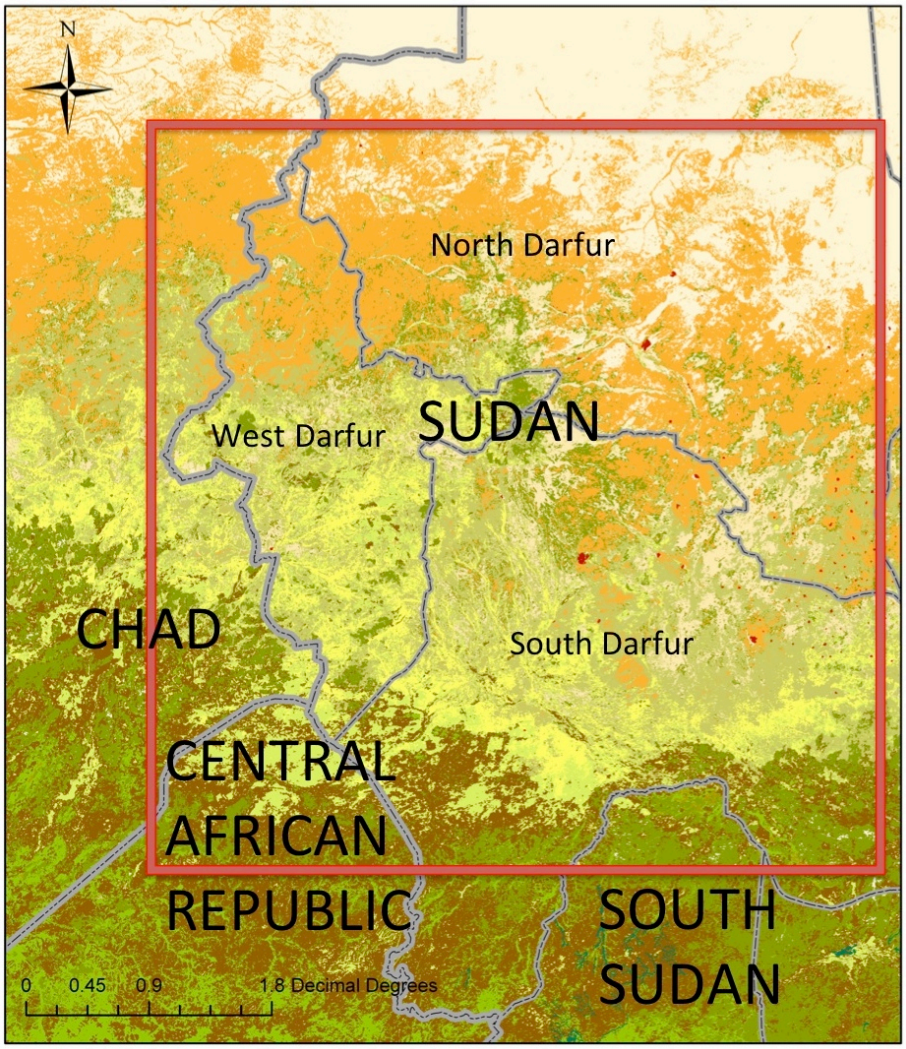

Figure 4-1: The study area (red) consists of West Darfur, and portions of North and South Darfur. The U.N. Land Cover Classification System describes the study area as consisting primarily of bare (200) and grassland (140) in the north, increasing to croplands (14) and vegetation in the south (30) (Defourny et al., 2006).

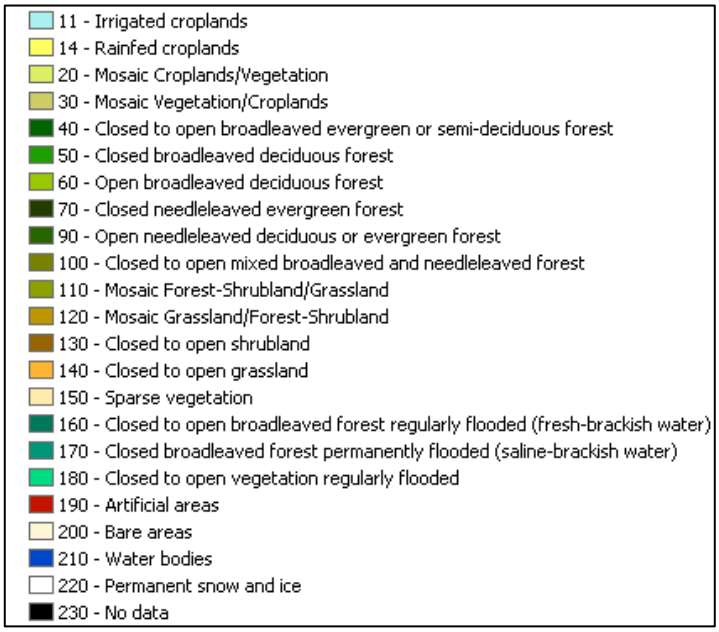

4.2.1 Reference Dataset

The reference dataset used in this study is the U.S. Department of State's Office of the Geographer and Global Issues' HIU database (HIU, 2010). This database lists the location of villages in Darfur, Sudan and their annual status as either damaged, destroyed, or no damage. A destroyed village is defined as confirmed evidence by government analysts of complete destruction of the village. Damaged villages were not used in the study. Additionally villages where the date of damage could not be determined (those listed in the database as "damaged at any time") were not included. During the study period from October 2002 to 2008, 2,668 villages were documented as destroyed in this database (Fig. 4-2).

For this study, each village was assigned a single specific satellite footprint, or path/row to prevent double counting (Table 4-1). The Worldwide Reference System-2 (WRS-2) is a notation system for Landsat data that allows users to define satellite imagery over any portion of the world by specifying a designated by path and row number. Path/rows with the largest number of available images were assigned all villages in their area to provide the largest number of observations. Two villages were contained in a twelfth path/row and were not included in this study, bringing the study total to 2,666 villages.

Table 4-1: Destroyed Villages in Study by Path / Row, Images Used, the color for Figure 4-2.

Path, Row	Villages	Images Used	Fig. 4-2 Color
177, 51	13	47	Blue
177, 52	512	52	Dark Green
178, 50	124	65	Dark Red
178, 51	534	69	Dark Purple
178, 52	362	61	Light Red
178, 53	25	54	Light Purple
179, 50	204	63	Aqua
179, 51	555	74	Magenta
179, 52	70	64	Green
180, 50	40	39	Brown
180, 51	227	75	Light Green
Total	2,666	663	

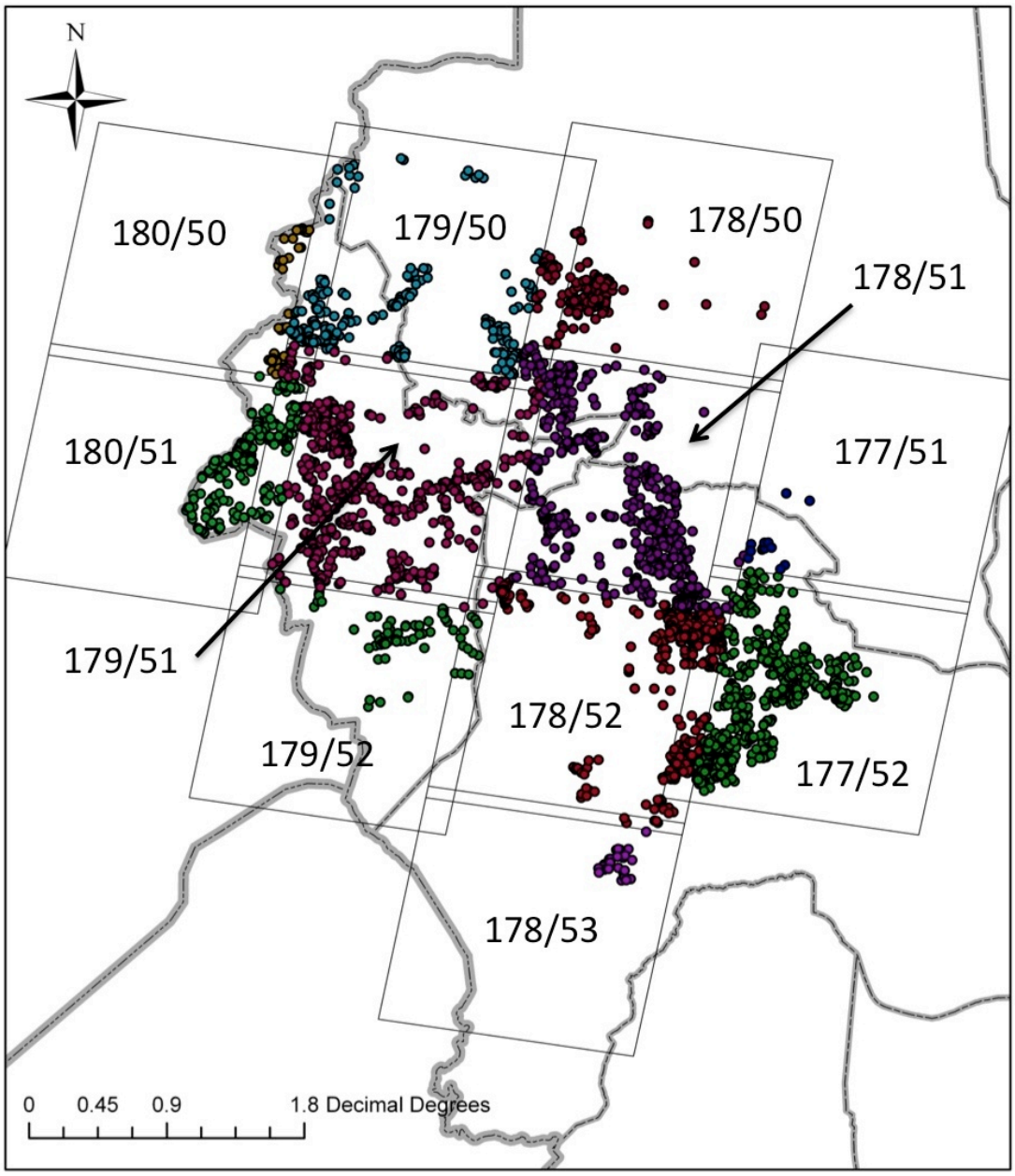

Figure 4-2: The study area consists of 2,666 destroyed villages distributed across eleven path/rows indicated in black text and by color defined on Table 4-1. Each village is assigned to a single specific path/row to prevent double counting (Table 4-1). Villages are shown in colors which reflect the different path/rows they are assigned.

4.2.2 Remote Sensing Satellite Data

All images from 1 January 2000 to 31 December 2008, excluding wet-season images from July, August, and September, were downloaded from USGS Landsat archive (http://earthexplorer.usgs.org) and included in the study (Appendix A). Landsat 4 and 5 TM imagery are not available for this location because of the 1987 failure of the Tracking and Data Relay Satellite System (TDRSS) transmitter and because this path/row is not within range of a downlink station (Goward et al., 2006). All imagery was orthorectified at USGS EROS (L1T) adjusting for any relief displacement. Images were preprocessed using the Landsat Ecosystem Disturbance Adaptive Processing System (LEDAPS) preprocessing software chain (http://ledapsweb.nascom.nasa.gov). This chain converts the L1T imagery product to surface, spectral reflectances (Wolfe et al., 2004) and also includes the Automated Cloud Cover Assessment (ACCA) algorithm, which generates a cloud mask based on Landsat bands 2 through 6 (Irish et al., 2006).

Wet-season images from July, August, and September were not used because violence in the region corresponds to the dry season when roads permit the movement of rebel, militia, and military forces (Flint & De Waal,

2008). Additionally not including the wet-season produces a more stable baseline of observations by minimizing village reflectance changes due to the annual seasonal green-up cycle (Huffman et al., 2009).

The study area consists of eleven Landsat ETM+ path/rows in western Darfur, Sudan (Fig. 4-3). Although Landsat-7 passes over nearly 850 scenes in a 24 hour period, technical satellite and sensor limitation as well as ground processing limitations (Wulder et al., 2008) reduce the acquisitions to ~ 250 scenes per day, which are determined by the long-term acquisition plan, which uses cloud cover and other priority factors to prioritize scene selection (Arvidson et al., 2006). Goward (2006) notes that discrepancies in scene collection by path/row is magnified by the fact that not all Landsat observations are held in the National Satellite Land Remote Sensing Data Archive (NSLRSDA). Those acquired at the International Ground station reside at those ground stations. The collection of images used in this study is available at USGS indicating that they were acquired using the L7 LTAP approach (http://landsat.usgs.gov/tools_pend_acq_l7.php).

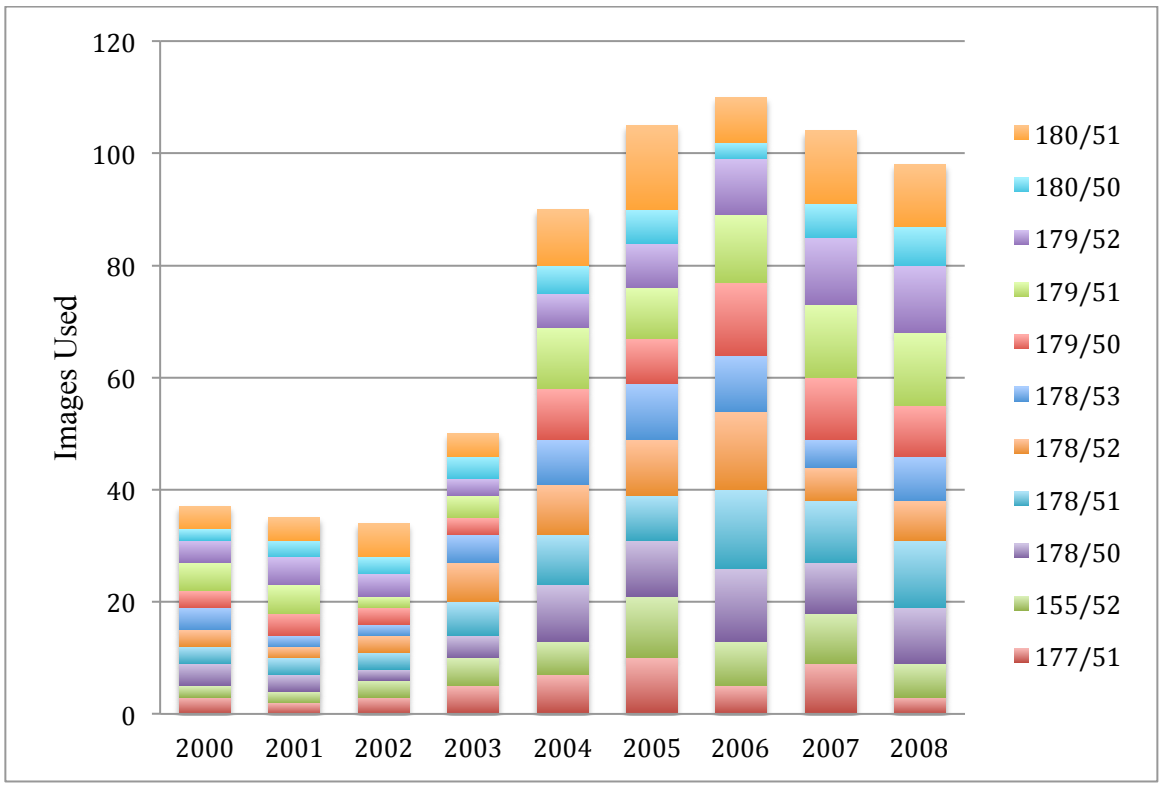

Figure 4-3: Images used in the study demonstrate the greater number of images available starting in 2004.

For the study area, there are more images available per year for the study area starting in 2004 (Fig. 4-3). This is due to the increase in daily scene collection from 250 to 300 starting on 11 May 2004 (Arvidson et al., 2006). Arvidson (2006) notes the significant increase in desert scene acquisition starting in 2004 (Table 4-2).

Table 4-2: Acquisitions of desert scenes increased significantly starting in 2004 as produced by Arvidson (2006).

Boreal	2001	2002	2003	2004	2005
Avg. acquisitions/scene	5.6	5.3	3.7	4.8	6.1
% clear images	26.2	28.4	33.6	27.3	27.7
Desert	2001	2002	2003	2004	2005
Avg. acquisitions/scene	7.4	7.7	7.9	12.1	12.4
% clear images	71	70.6	67.6	73.3	70.6

4.3. Methodology

The methodology used in this study builds on results from Chapter 3. Specifically it detects a drop in the village's surface reflectance when a village is burned. This drop shows the transition of the village from pre-burn materials (soil, deadwood, dead twigs and dead litter) to post-burn materials (soil, charwood, charred soil and ash) (Fig. 1-4). Previous analysis (Chap. 3) demonstrated that Landsat ETM' near-infrared band was most sensitive to this change. This prior approach was limited to the year 2004 and to the areas of WRS-2 path 179 row 51 that were not affected by scanline errors. ETM+ band 4 showed a high degree of accuracy in the approach, with an omission error of 17% and commission error of 14% (Table 3-3).

Due to the expansion of this approach to all of Darfur, from October 2002 to 2008, there were two significant modifications to the approach

developed in Chapter 3. These included a change to how villages delineated and changes to the algorithm.

4.3.1 Village Buffer

In Chapter 3, the buffer of each of the 198 villages was delineated manually using very fine resolution imagery (Google Earth). Because this study looks at 2,666 villages, a village's extent was instead estimated with a 200-meter buffer around the center point of each village's location. Based on visual analysis of Landsat ETM+ imagery, a 200-meter buffer was the largest a buffer possible before including adjacent rivers for some villages. This 200 m buffer, or 4,380 square meters was converted into a 146 pixels mask on the Landsat ETM+ imagery.

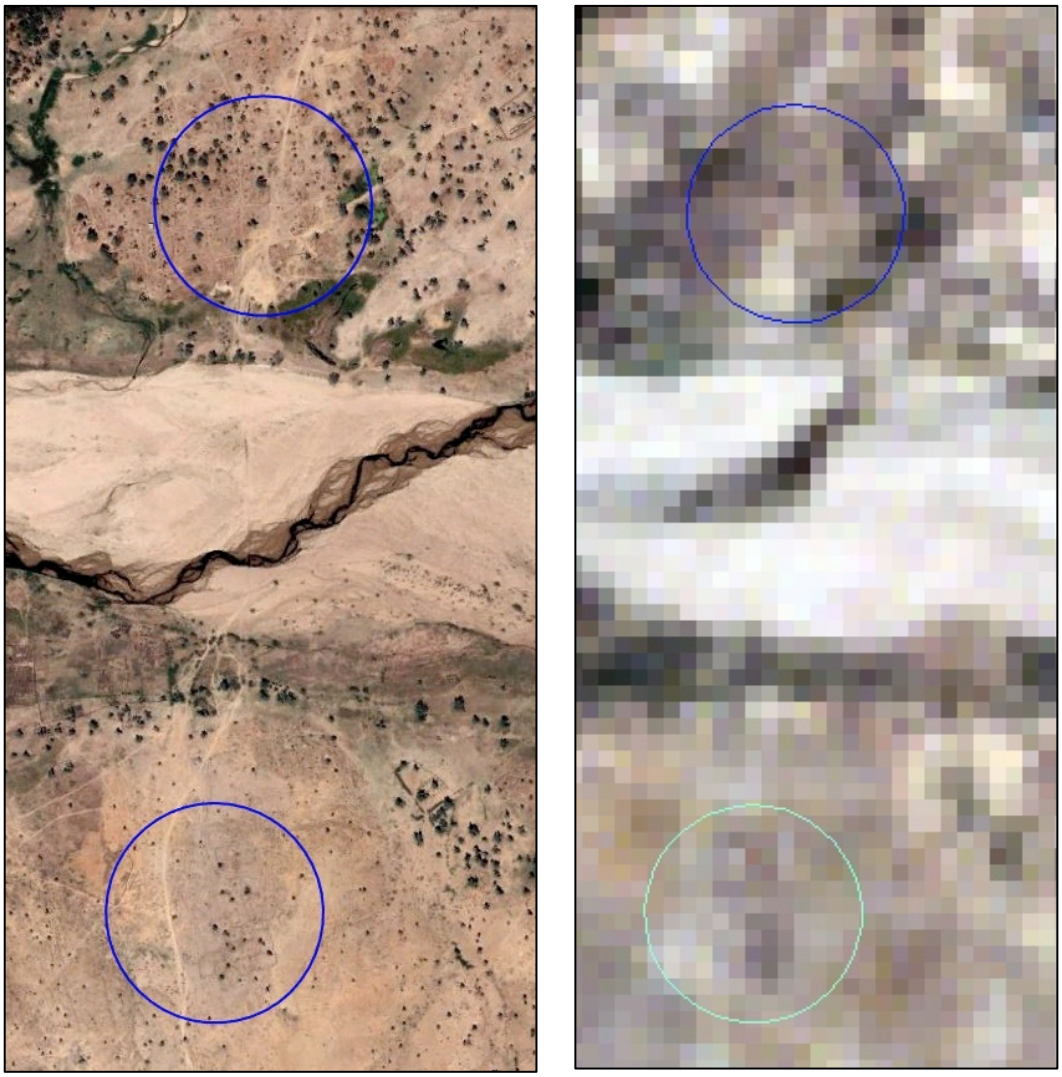

Figure 4-4: 200 meter buffer extent for two villages in path/row 179/51. Left panel: DigitalGlobe, 2005. Right panel: Landsat ETM+, 5 March, 2000 (ture color). Both villages were detected as destroyed in 2003.

4.3.2 Algorithm

Each village's observation, from all scenes from October of 2002 to 31 December 2008, was evaluated if it was destroyed. Unlike the approach used in Chapter 3, this analysis compares each new observation to all

observations before it, called a rolling algorithm. This approach provides for more baseline observations and greater accuracy. Although violence in the region significantly increased following the 25 February 2003 successful rebel attack, the algorithm starts in October 2002 to capture the limited village destruction which occurred in the Fall of 2002 in West Darfur (Flint & De Waal, 2008; Petersen & Tullin, 2006).

With each new pass of the sensor, each village's observation was compared to a baseline of all previous observations starting in 2000. A more restrictive T-Test was used in this study in comparison to Chapter 3 because villages had a greater number of baseline observations. A one-tailed, student's T-Test is used to determine if village's observation is significantly lower than all previous observations (Weisstein, 2003), where "mean" is the mean of all previous observations, "observation" is the value for the test observation, "Stdev" is the standard deviation of all previous observations, and "df" is degrees of freedom, or the count of all previous observation.

$$\text{T\_Test} = \frac{\text{Mean} - \text{Observation}}{\text{Stdev}\sqrt{(1/\text{df})} + 1}$$

This T-Test assumes some variability in the observations, resulting in higher probability, or p-values, than those used in Chapter 3. This algorithm uses two confidence levels for the detection village destruction. A p-value

under 0.005 alerts as high confidence of a recent fire in the village's perimeter and a p-value of 0.05 alerts as medium confidence.

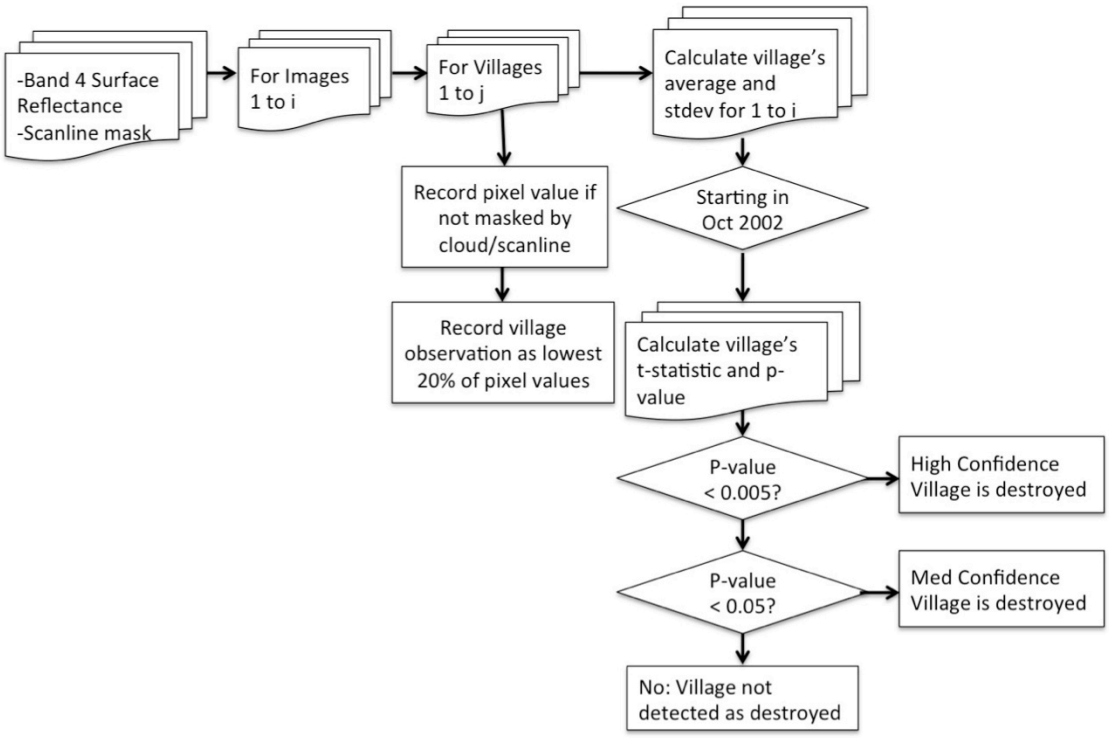

Figure 4-5: Landsat ETM+ destroyed village detection algorithm process stages. Version 2.

Starting in October 2002, all villages were then analyzed for the date they are first detected as destroyed. The buffered area of a village may have been burned several times over the six year study period, so only the first observation where a village alerts is recorded. Large-scale fires were observed in many areas of Darfur in 2006 and 2007, and covered many villages that were already detected as destroyed earlier in the conflict. Because there is no evidence of village rebuilding in Darfur in this time

period (Flint & De Waal, 2008), only the first time a village is detected as destroyed is recorded. The last date a village is observed as intact is also recorded. The period between last detected intact, and first detected destroyed, may range from 16 days, the repeat cycle of the sensor, to several months if the village is detected as destroyed just after the wet season, or is in an area significantly impacted by scan line errors.

4.4. Results

4.4.1 Summary

There were a total of 2,666 villages in the study that were reported as destroyed. Of these 66% alerted as being destroyed; 1,106 (41%) at a high confidence level and 651 (24%) at a medium confidence level. 909 (34%) were not detected as destroyed. The average time between when a village alerted as destroyed and when a village was last detected as not destroyed was 73 days. High confidence level alerts had a slightly longer lag time than medium confidence alerts (76 and 69 days, respectively) (Fig. 4-6). 39% of all detections occurred after one pass of the sensor (16 days), and 64% of detections were after three passes of the sensor (48 days).

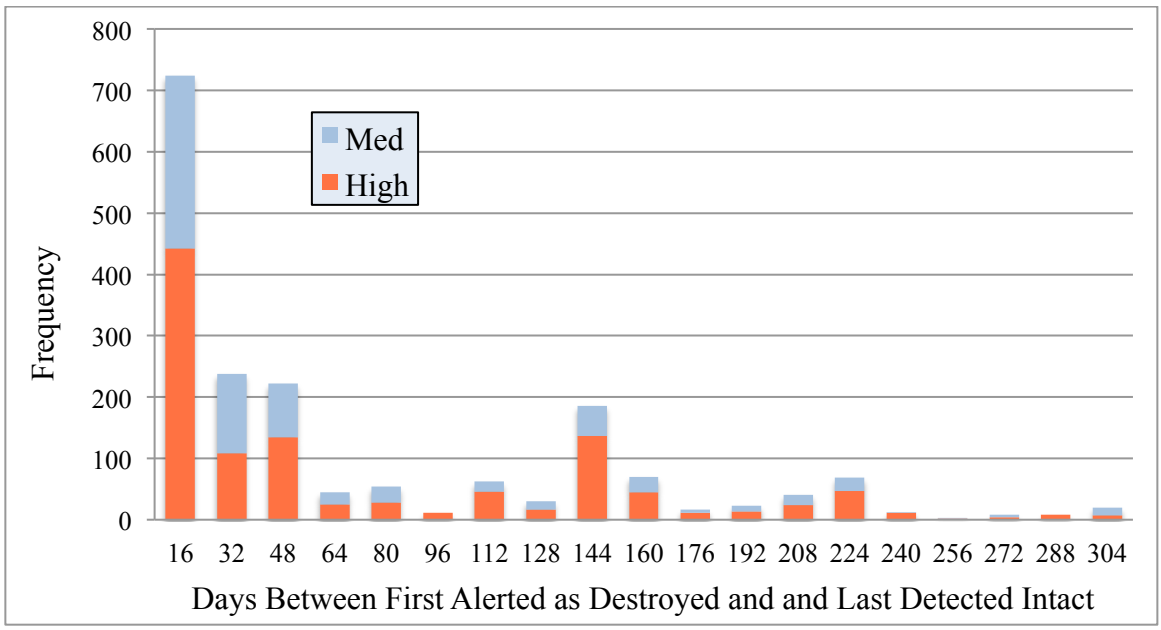

Figure 4-6: Lag between when villages are last detected as intact, and first detected as destroyed by confidence level of the destroyed alert.

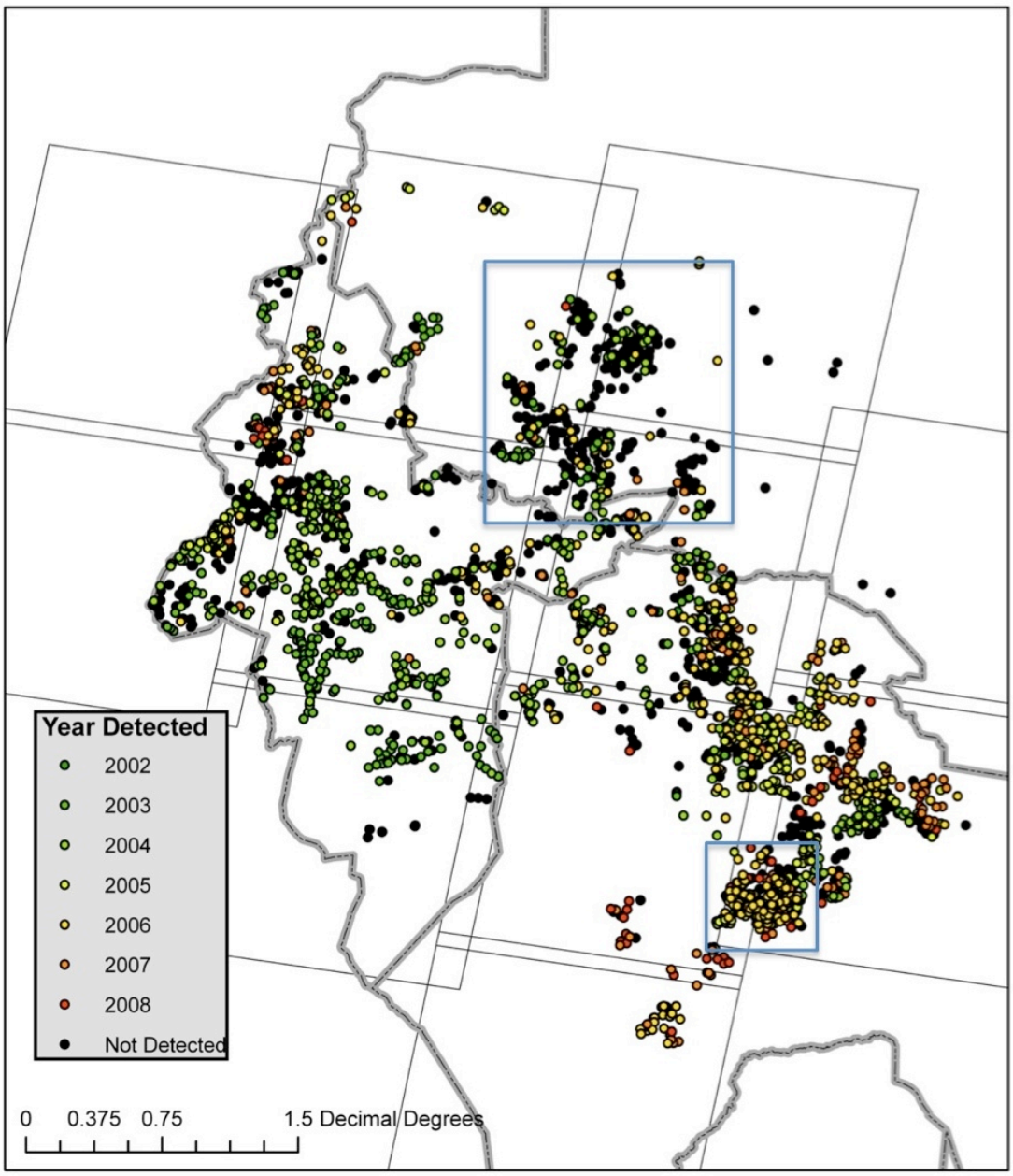

Figure 4-7: Villages detected as destroyed by year. Focus areas near Kutum, North Darfur, and Donkey, South Darfur are outlined in blue.

4.4.2 Accuracy Assessment

4.4.2.1 Inter-comparison with Chapter 3 Results

There were 90 common destroyed villages between those used in Chapter 3 and Chapter 4 (although the Chapter 3 study consisted of 92 control villages, two villages were covered by a different path/row in the Chapter 4 study). The methodology differed for these 90 villages due to Chapter 4 methodology using an automated buffer instead of manually delineating a village's extent, and using a more restrictive test for the detection of village destruction. The omission rate for these villages was 14 of 90 (15%) in the Chapter 3 study and 26 of 90 (29%) for the Chapter 4 study.

The reason for the significantly higher omission rate is due to the more restrictive test in Chapter 4, not the less precise buffer. When the Chapter 4 villages with buffered extents were put into the less restrictive approach, their omission rate fell 17 of 90 (19%). Additionally when the more precisely delineated villages were put into the more restrictive version of the algorithm the omission rate increased to 25 of 90 (28%). The more restrictive approach was chosen because all dates after Oct 2003 are tested and only the first date a village is detected is destroyed is recorded. A more

restrictive approach minimizes the occurrences of false alarms although it significantly increases the omission rate.

4.4.2.2 Comparison with Bloodhound Database

Bloodhound in a Danish non-governmental organization founded in early 2004 to document atrocities perpetrated by the Government of Sudan (www.bloodhound.dk). Their report, authored by Petersen and Tullin (2006), "The Scorched Earth of Darfur: Patterns in Death and Destruction Reported by the People of Darfur" is a collection of detailed witness testimonies and reports on village attacks in Darfur from January 2001 to September 2005. There are 178 accounts of attacks collected from media, human rights, and United Nations sources. Although the violence in Darfur affected an estimated 2 million people during this time, all access to the area was denied to journalists and human rights groups until March 2004, with only limited access allowed subsequent to that date. This resulted in the small number of reports as well as making it impossible to conduct a detailed on-site verification of the scale and nature of these attacks.

Of the 178 accounts of attacks, only 16 accounts were of a village destruction including a date and specific location that corresponded to a destroyed village in this study. Eight of the 16 eyewitness accounts were

detected with the algorithm within the same period as the Bloodhound Database. Three villages were not detected destroyed at any time and five were detected at different times. In one of the cases where the approach did not match the time of the eyewitness report, village destruction was detected just one sensor pass after the eyewitness-reported destruction date. In many cases the date of the village destruction is approximate, as villagers may not know exactly what date it was when they were attacked, and refugees report that villages often experienced multiple attacks over a prolonged period before they are destroyed by burning or bombing (U.S. Department of State, 2004). Of the 13 villages that were detected as destroyed by the algorithm, 9 (69%) were within 16 days of the eyewitness account.

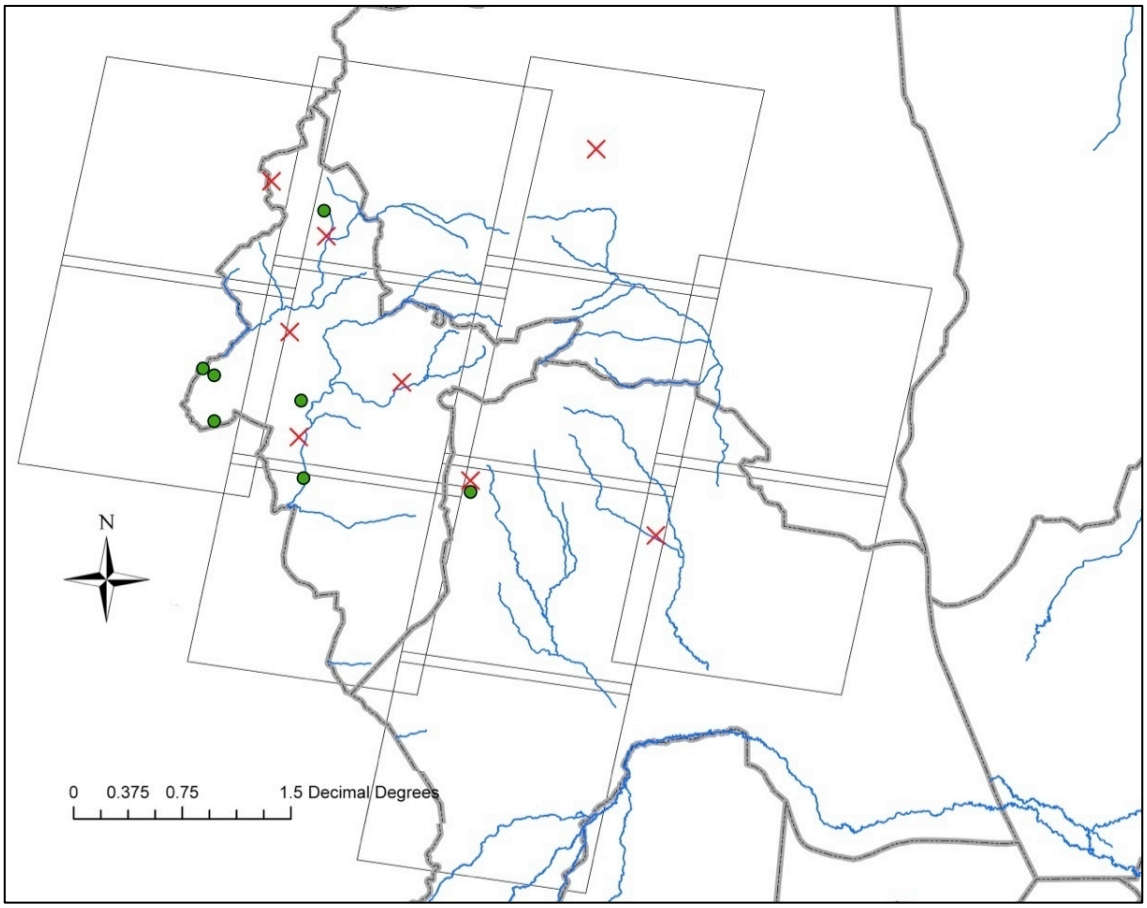

Figure 4-8: Location of 16 villages used to compare village destruction dates with algorithm results. The algorithm detected 8 villages (circle) as destroyed in the same time period and 8 were not detected or detected at a different time period (X).

Table 4-3: Eight of the 16 villages with eyewitness reporting of the attack were detected with the algorithm. Three villages were not detected as destroyed and five were detected as destroyed on different dates.

Reported Destroyed	Last Detected Intact	First Detected Destroyed	Name	Path Row	Result
29-Aug-03	21-Apr-03	15-Nov-03	Beida	180 51	Y
30-Aug-03	8-Nov-03	26-Dec-03	Mororo	179 51	N
Oct-03	29-Mar-03	8-Nov-03	Habila	179 50	Y
3-Nov-03	21-Apr-03	15-Nov-03	Beida	180 51	Y
3-Nov-03	21-Apr-03	15-Nov-03	Shushtah	180 51	Y
Dec-03	8-Nov-03	26-Dec-03	Kenyo	179 52	Y
20-Dec-03		not detected	Habila Kanari	179 51	N
5-Jan-04	8-Nov-03	26-Dec-03	Korare	179 51	N
Feb-04	5-Dec-04	21-Dec-04	Kaileck	178 52	N
Feb-04	20-Jan-04	21-Feb-04	Shattai	178 52	Y
7-Feb-04	28-Jan-04	13-Feb-04	Tongfuka	179 51	Y
15-Feb-04	4-Feb-04	7-Mar-04	Terbiba	180 51	Y
18-Feb-04	23-Dec-05	24-Jan-06	Anka	178 50	N
15-Mar-04		not detected	Haish Bara	180 50	N
9-Aug-04		not detected	Diiba	179 50	N
15-Dec-04	20-Oct-05	5-Nov-05	Marla	178 52	N

4.4.3 Sources of Error

4.4.3.1 Nature of Village Destruction

The largest contributor to omissions by the algorithm was the nature of village destruction. The HIU dataset does not discriminate between a burned village and an otherwise destroyed village, therefore selecting only burned villages for the algorithm is not possible. Although there is some variation, eyewitness accounts indicate that the perpetrators of attacks tended to use the same tactics in a region, during a specific time period. For

example in western Darfur, near the border with Chad, eyewitnesses report that in 2003 Sudanese military forces and militias systematically burned and looted towns and villages that are supporting the rebels (Fig. 4-9) (U.S. Department of State, 2004).

Figure 4-9: Burned shops in a village between Al Junaynah and Sisi, Western Darfur, Sudan (U.S. Department of State, 2004).

An example of the link between methods of the perpetrators and algorithm detection of village destruction can be seen in North Darfur, where a large concentration of villages were destroyed in 2003 and early

2004, just west of Kutum. There are four eyewitness accounts of the villages of Orschi, Miski, Disa and Kutum being attacked in that region from the New York Times, and Amnesty International compiled in the Bloodhound report (Petersen & Tullin, 2006). All four of these eyewitness accounts report the village being attacked by Janjaweed and Sudanese soldiers, but not being burned. The eyewitness report for Orshci describes "government planes circled overhead before the Janjaweed stormed their villages. The village trashed, animals were stolen" (Petersen & Tullin, 2006). Of the 324 villages identified as destroyed in this area in 2003 and 2004, only 104, or 32%, were detected as destroyed.

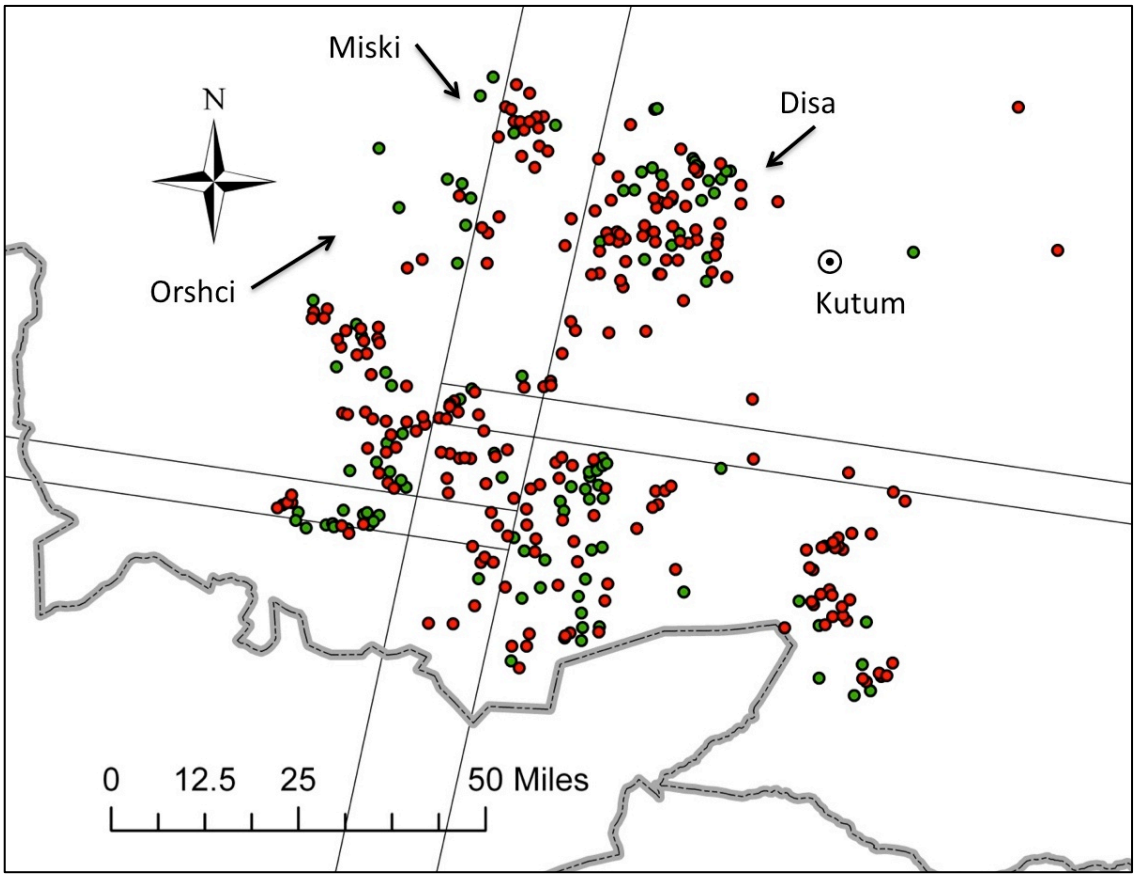

Figure 4-10: Eyewitnesses from villages attacked west of Kutum in 2003 and 2004 reported that villages were destroyed, but not burned (Petersen & Tullin, 2006). The algorithm was unable to detect many of the destroyed villages because fire was not used in the perpertrator's methods (villages detected in green; villages not detected in red).

In contrast to attacks west of Kutum in 2003 and 2004, a grouping of attacks in South Darfur, near Donkey, had a very high rate of detection of village destruction. In 2006, 240 villages in this cluster were destroyed (Fig 4-10). One eyewitness reported "An attack by more than 400 armed horsemen on the village of Donki Dereisa on July 12. The attack, which was supported by a fixed-wing aircraft that bombed the village and by several

military vehicles filled with Sudanese foot soldiers, resulted in the death of as many as 150 villagers, including six young children" (Petersen & Tullin, 2006). The village was reported as burned in the summary of the attack. Reports from the Eyes on Darfur project, which uses DigitalGlobe imagery to track the destruction of villages, also show the burning of villages Donki Dereisa during this time (Fig. 4-11).

Figure 4-11: Donkey Dereisa destroyed by burning between 1 November, 2004 (left) and 20 October, 2006 (right) (Amnesty International, 2007). The village is identified as burned because there are no fence lines and there are dark areas where structures once stood. © DigitalGlobe Inc.

In this concentration of villages in 2006, which were identified as burned as part of the attacks, only 20 of 240 (8.3%) were not detected by the algorithm as destroyed (Fig. 4-12). Imagery coverage for this path/row did

improve after 2003, but was not greater than other path/rows in 200,6 so imagery availability was likely not responsible for the high detection rate.

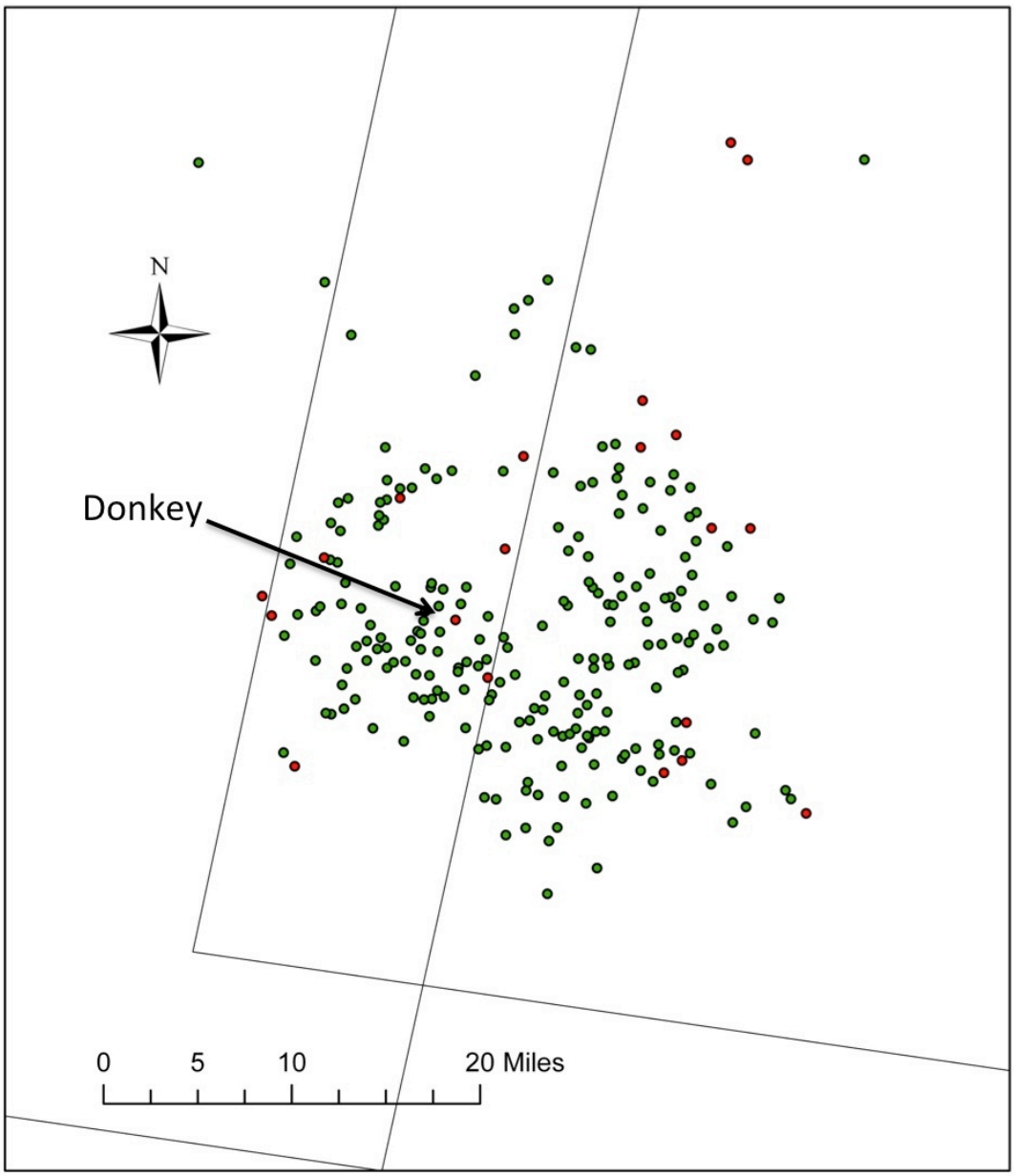

Figure 4-12: Eyewitnesses from Donkey in 2006 report the burning of the village as part of the attack (Petersen & Tullin, 2006). The algorithm performed well in this region and time period because fire was used in the prepertrator's methods (villages detected in green; villages not detected in red).

4.4.3.2 Scene Availability

The number of scenes for a path/row during the study was not correlated with that path/row's omission rate (Table 4-4). Path/row 178/50, which mostly consists of villages near Kutum that were identified as destroyed but not burned, had a very low detection rate, but only slightly fewer scenes than the average (56 scenes). While path/rows 177/52, identified as consisting of villages that were often burned as part of the attack, had a much higher detection rate, and also slightly fewer images than average.

Poor image availability in 2003 was likely a factor in the approach's low detection rate. While there were many reported incidents of village's burning in the middle of 2003 (Flint & De Waal, 2008), scene availability remained poor until 11 May 2004 when daily scene collection from 250 to 300. Greater scene availability was also not tied to a decreased lag between last time a village was detected as intact and first time a village is detected as destroyed. Factors such as if a village was attacked just after the wet season (causing at least a three month lag) was more significant than scene availability.

Table 4-4: Detection Rate by Path/Row.

Path/Row	Images	Detected	Total	% Detected	Average Lag
177/51	47	9	13	69.2%	108.4
177/52	52	402	512	78.5%	93.3
178/50	46	31	124	25.0%	22.7
178/51	57	319	534	59.7%	50.3
178/52	61	280	362	77.3%	79.1
178/53	54	24	25	96.0%	53.3
179/50	63	134	204	65.7%	98.3
179/51	61	374	555	67.4%	56.7
179/52	64	53	70	75.7%	144.7
180/50	39	24	40	60.0%	124.1
180/51	75	107	227	47.1%	50.0
	619	1,757	2,666	65.9%	

4.4.3.3 Village Size

1,308 villages of the 2,666 villages in the study have a value in the field "structures" for the HIU database. This value describes approximately how many destroyed structures were identified along with the total structures in the village (e.g. "~700 of ~1000"). There however was little correlation between the number of structures identified as destroyed and the omission rate (Table 4-5). Villages with more destroyed structures (76 or greater) had slightly lower omission rates than villages with fewer structures.

Table 4-5: There is little correlation between number of destroyed structures and the omission rate. Villages with more destroyed structures (76 or greater) had slightly lower omission rates.

Structures Destroyed	Detected Destroyed?		
	Yes	% Yes	Total
< 25	249	68%	364
26 to 50	152	64%	238
50 to 75	205	63%	323
76 to 150	142	72%	198
150 <	124	67%	185
	872	67%	1308

4.4.3.4 Scan line Gaps

Areas significantly impacted by scanline errors did not affect whether a village was detected as destroyed or not. There were 738 villages in high scanline gap areas, identified as the area where one path covers the neighboring path to the east or the west (Fig. 4-13). Eliminating those villages leaves 2,195 villages of which 1,457 (66.4%) were detected destroyed after the 11 May 2004 scanline corrector error. For all villages the detection rate was slightly lower (65.9%).

Eliminating those villages from the study does reduce the lag between last intact and first detected destroyed (from 73 days to 70 days), showing that scanline gaps did affect the temporal precision of the study. This temporal precision would likely be much greater if villages were manually

delineated. Villages smaller than the 200-meter buffer would likely have a significant drop in number of observations.

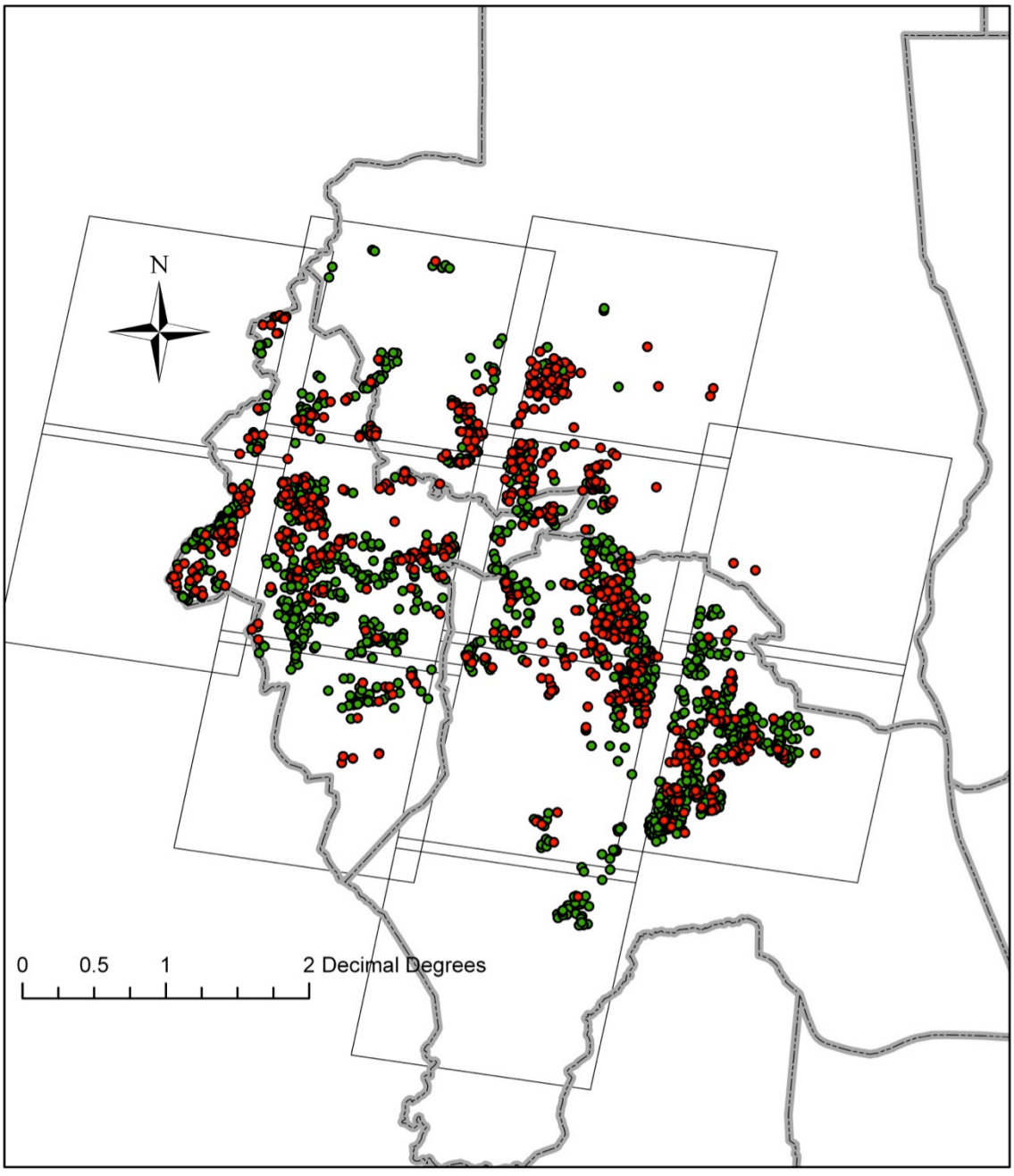

Figure 4-13: Eliminating villages from areas with high scanline error gaps only slightly improves the detection rate (from 65.9% to 66.4%). Detected villages are shown in green and villages not detected in the approach are shown in red.

4.4.4. Exploratory Analysis of Conflict

The conflict in Darfur from 2002 to 2008 was a series of government and government backed-militia responses to three major rebel groups who operated in different areas and engaged in conflict at different times (Hudson, 2013). The Sudan Liberation Movement or Army (SLA) consisted of rebels of the Zaghawa ethnicity, led by Minni Minnawi (SLA-Minnawi) and operating generally in North Darfur, and rebels of the Fur ethnicity, led by Abdul Wahid al-Nur (SLA-al-Nur) who operated generally in West Darfur. In 2006 SLA-al-Nur formed as a splinter faction of the SLA following Minnawi's signature of the Darfur Peace Agreement. Finally the Justice and Equality Movement (JEM), led by Khalil Ibrahim operates mainly in Kurdufan and the eastern part of Darfur (Flint & De Waal, 2008).

4.4.4.1 Spatial and Temporal Patterns

The beginning of the 2003 to 2008 waves of mass atrocities in Darfur began with the government's response to scattered rebel attacks in the early months of 2003. Starting in March, fighting across Darfur broke out between government troops and black African rebels with the SLA and JEM (Totten & Markusen, 2006). This first wave of violence was encouraged from a leading Janjaweed militia leader, Hilal (Power, 2004), who

repeatedly made public speeches on his intent to eliminate Black Africans from Darfur and personally led attacks on settlements in Darfur (Hagan & Kaiser, 2011). This initial wave of violence continued until the 4 September 2003 negotiated ceasefire between the government and the SLA.

The fighting, from the middle of 2003 until September 2003, is not observed in the study because scenes from the wet season (July, August and September) were not used in the study. Only 48 villages were observed destroyed during this time. However during the subsequent ceasefire (4 September to early December) there were an additional 129 villages detected as destroyed. 106 of these likely reflect the early 2003 violence because their last intact dates are from before the wet season. However twenty-three of these detections represent villages destroyed during the ceasefire. These detections are all in WRS-2 path 178 row 51 and were detected as intact and then destroyed during the ceasefire.

There are no eyewitness reports or fine resolution (under 10m spatial resolution) imagery available to confirm the destruction of these villages during this time period (Fig. 4-14). While both the government and the rebels accuse the other of breaking the ceasefire soon after it is implemented (Totten & Markusen, 2006), these attacks most likely represent the continued government responses against the JEM, who operate in this area

of Darfur and did not sign the ceasefire. In early 2003 the JEM claimed responsibility for attacks in Golo and Al Fashir and continued to operate in this area in 2003 (Tanner et al., 2007).

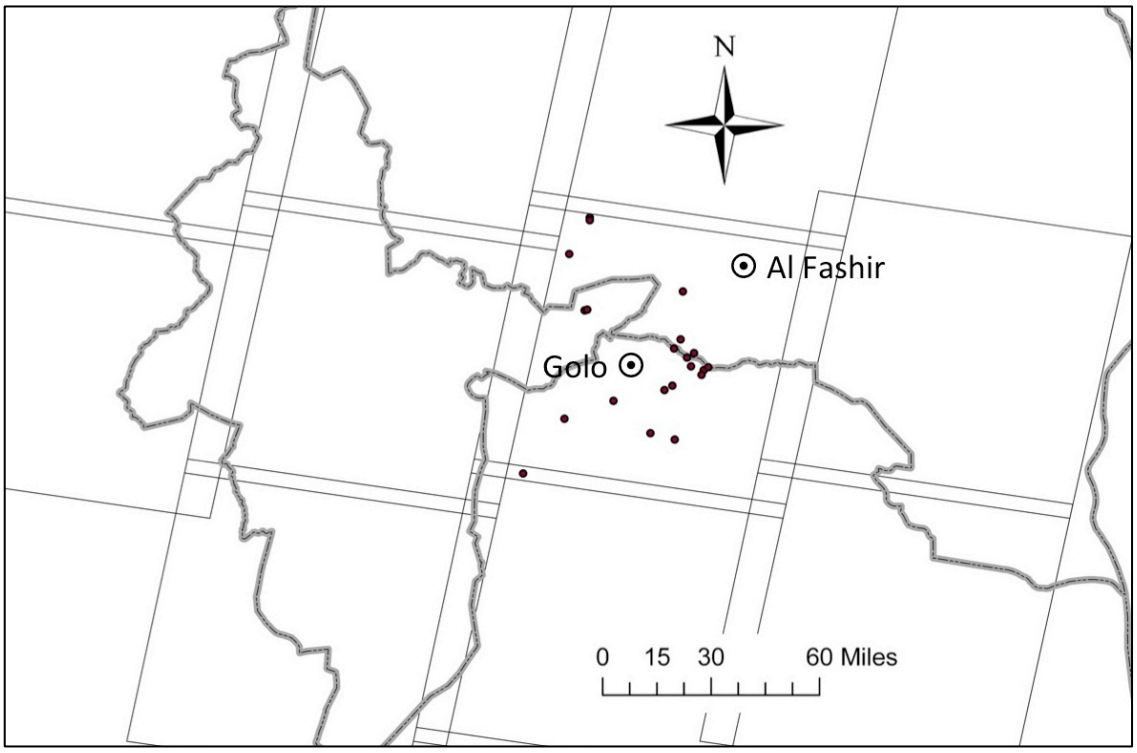

Figure 4-14: Villages detected as destroyed during the first ceasefire (September to early December 2003) only occurred in one path/row. These detections may not be violations to the ceasefire, but government operations against the JEM who were not signatories to the ceasefire and operated in this area.

A second interval of fighting began in December 2003 which coincided with a vow by Sudanese President Al-Bashir to 'annihilate' Darfurian rebels (Hagan & Kaiser, 2011). In one week, 18,000 refugees entered Chad to escape Janjaweed attacks in Darfur (Totten & Markusen,

2006). Results from the study strongly support the reported rise in attacks from December 2003 to 11 April 2004. During this time 315 villages were detected as destroyed between 3 December 2003 and 11 April 2004 (Fig. 4-15).

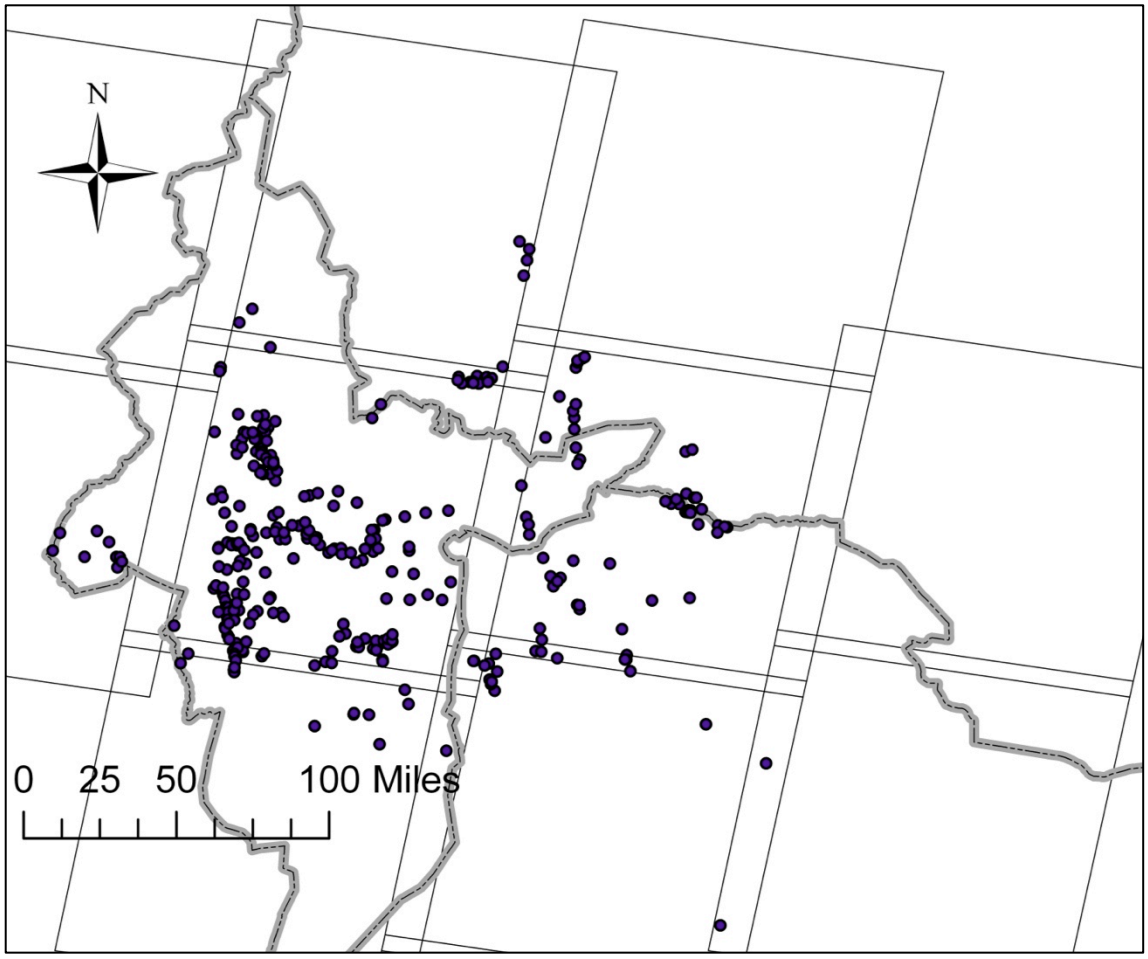

Figure 4-15: 315 villages were detected as destroyed following the first ceasefire (3 December 2003 to 11 April, 2004); an average of 2.6 per day.

This wave of violence reportedly ended in late March / early April with the remarks on 22nd March 2004 by Mukesh Kapila, the U.N.

Humanitarian coordinator for Sudan, stating that "the only difference between Rwanda and Darfur is now the numbers involved" (Petersen & Tullin, 2006). These statements were very effective at increasing press coverage of the conflict and helped bring about the 8 April 2004 "Humanitarian Ceasefire Agreement" between the government and rebel leaders (Hudson, 2013).

The 45-day "Humanitarian Ceasefire Agreement" agreement began on 11 April 2004, allowing for the deployment of observers from the African Union and for humanitarian assistance to be provided to internally displaced persons in Darfur. This ceasefire was signed between the Sudanese government, the JEM, and the SLA. A faction splintered from the JEM, the National Movement for Reform and Development (NMRD), who did not agree with the ceasefire agreement and continued operation in West Darfur.

During this ceasefire 42 villages were detected as destroyed, primarily in West Darfur. There was no eyewitness reporting or fine resolution imagery that could confirm the destruction of any of these villages during this narrow time period (Fig. 4-16). Because the NMRD did not sign the ceasefire, and operated in West Darfur during this time, these detections may not represent violations to the ceasefire, but continued government operations against the NMRD.

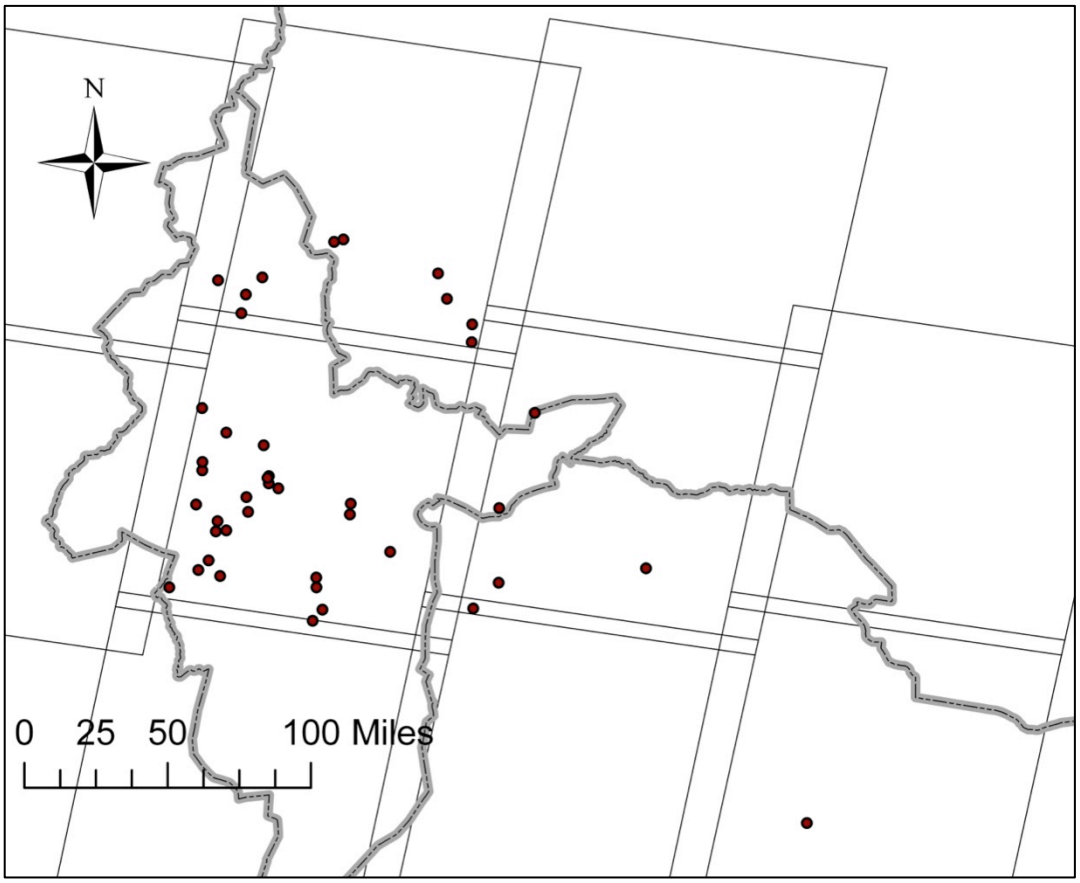

Figure 4-16: 42 villages detected were detected as destroyed during the second ceasefire (11 April to 26 May 2004). These detections may not represent violations to the ceasefire, but continued operations against the NMRD who did not sign the agreement and operated in West Darfur.

The following two dry seasons (October 2004 through June 2005; and October 2005 through June 2006) show a decreased level of village destruction (Appendix C). These dry seasons had an average of 1.0 and 1.2 villages detected as destroyed per day respectively, much lower than the preceding or following dry seasons (Table 4-6).

Table 4-6: Dry Season Detection Rates.

	Oct 2003 to Jun 2004	Oct 2004 to Jun 2005	Oct 2005 to Jun 2006	Oct 2006 to Jun 2007	Oct 2007 to Jun 2008
Detected	482	261	326	440	154
Detected/Day	1.8	1.0	1.2	1.6	0.6

On 5 May 2006, the Minni Minnawi led rebel group (SLA-Minnawi) signed the Darfur Peace Agreement with the government. The approach did not detect the destruction of any villages from this date until the start of the wet season at the end of June. The peace agreement is widely regarded a failure in stopping the violence, which is supported with findings from this study. At the start of the next dry season in October, there is a large increase in violence with 358 villages detected as destroyed within the first three months.

October through December 2006 is the most destructive three-month period in the study with 4.0 villages detected as destroyed per day (Table 4-6). The majority of these detections occurred southeast of Nyala, near Donkey, although village destruction is detected across Darfur (Fig. 4-17). These detections are consistent with press reporting of increased government attacks against rebel groups that did not sign the Darfur Peace Agreement,

and of inter-tribal conflict between Zaghawa and Nur (Flint & De Waal, 2008).

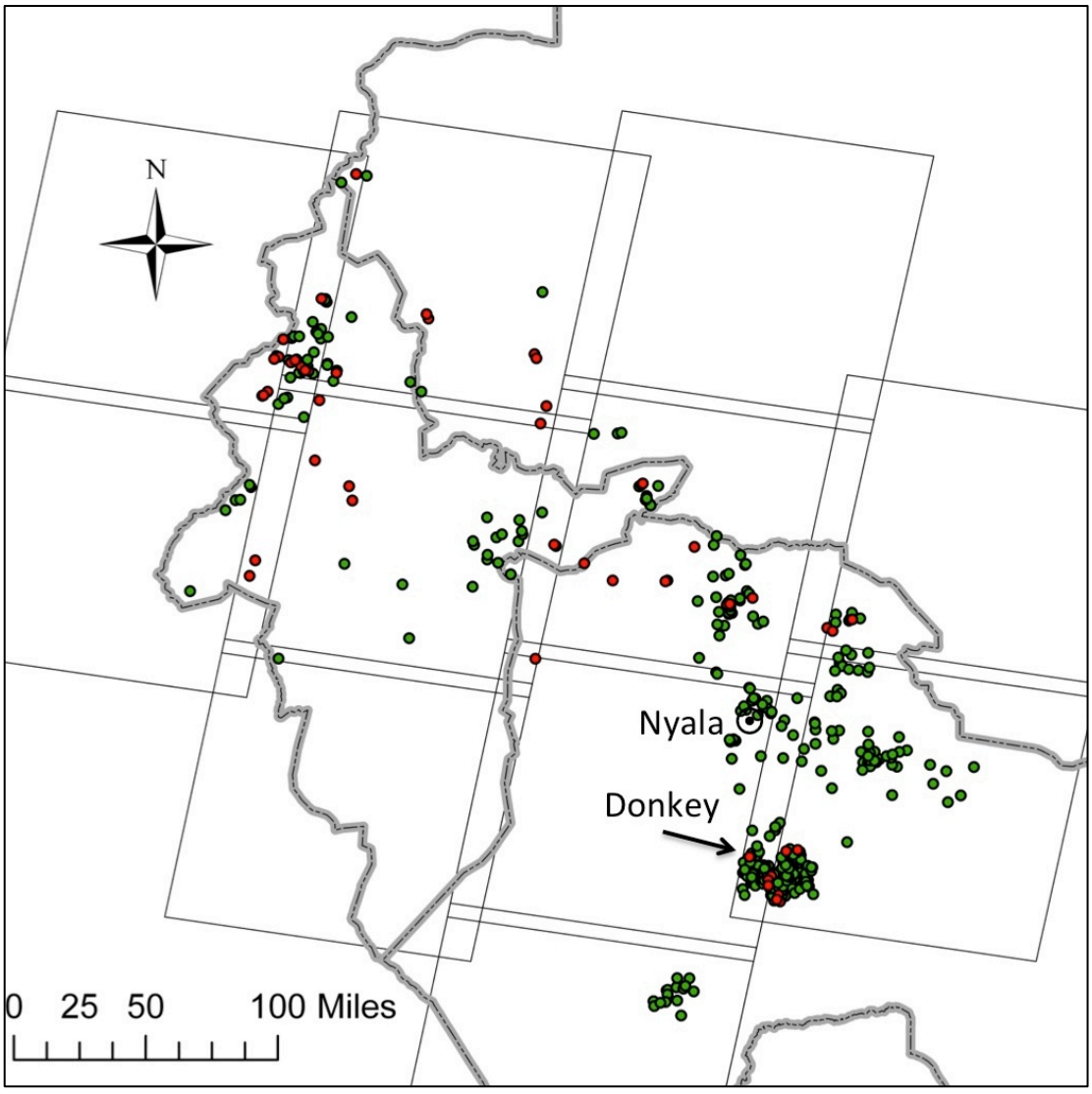

Figure 4-17: The highest rate of detections, 4.0 per day, occurred from October to December 2006 (green). The rest of the dry season (January to June 2007) only had 0.3 detections per day (red).

Violence decreases after December 2006, with an additional 81 villages detected as destroyed the rest of the dry season. The decrease coincides with the 12 January 2007 60-day ceasefire brokered by New Mexico Governor Bill Richardson between the government of Sudan and several rebel factions in Darfur. The following dry season (October 2007 to June 2008) maintains this low rate of detected village destructions, with an average of only 0.6 villages detected as destroyed during this time period (Table 4-6).

4.5. Conclusion

This chapter builds on the approach developed in Chapter 3, and was expanded to study all of Darfur from 2002 to 2008. The approach was modified in two important ways; manual village delineation using fine resolution imagery was replaced by less accurate automated village buffers, and a more rigorous rolling detection algorithm was used to compare a village's observation to all observations previously recorded. Analysis of the changes in approach demonstrated that the more stringent algorithm was responsible for the higher omission rate in Chapter 4 (66%) than Chapter 3 (84%).

The Bloodhound database (Petersen & Tullin, 2006), a collection of eyewitness accounts of attacks collected from media, human rights and United Nations sources, was used to compare results with the approach. Because access to the area was denied to journalists and human rights groups until March 2004, with only limited access after that, there were only 16 accounts of a destroyed village in the Bloodhound database that corresponded to this study. Of those three were not detected by the study and 9 of the 16 (69%) were detected within 16 days of the eyewitness account (Table 4-3).

The largest contributor to the omission rate was the nature of the village's destruction. Because the HIU dataset does not indicate if burning is part of a village's destruction, and because the approach is designed to detect the drop of a village's surface reflectance when a village is burned, the approach performed well in at specific times and locations in the conflict when the perpetrators use arson. Near Donkey, an area where eyewitness' report that villages were burned as part of their destruction, the omission rate was 8.3% (Fig. 4-12), but around Kutum, an area where burnings were not consistently part of the village's destruction, the omission rate was 68% (Fig. 4-10).

In addition to the method of the village destruction, several other sources of error were evaluated in their contribution to the omission rate. The lack of scene availability in the 2003 likely significantly reduced the number of villages successfully destructed as destroyed in this year. Additionally while a path/row with more scenes available during the study period did not improve the omission rate, it did decrease the time between when a village was last detected as intact and first detected as destroyed (Table 4-4). Villages with large numbers of destroyed structures showed slightly lower omission rates (Table 4-5) as well as villages not in areas significantly impacted by scanline errors (Fig. 4-13).

Results from this expanded study in Chapter 4 reveal new understandings about the conflict in Darfur from 2002 to 2008. While rebels from the SLA and the government claim that either side violated the first ceasefire (September 2003 to early December 2003), the study did not confirm this. Detected village destructions during this time occurred in areas where the JEM operated in 2003 and may represent operations against that JEM who did not sign the ceasefire (Fig. 4-14). The study also detected violations to the second ceasefire (11 April to 26 May 2004), with the destruction of 42 villages across Darfur (Fig. 4-16). These detections however may also not represent violations to the ceasefire, but continued

operations against the NMRD who did not sign the agreement and operated in West Darfur. Finally this study revealed that following a period of decreased village destruction (January 2005 to October 2006) there was an intense three month period of violence where an average of four villages were detected as destroyed daily (Fig. 4-17).

While this study does not provide a complete documentation of all village destruction, it does significantly improve understanding of when and where villages were destroyed in this widespread and long-lasting conflict. Further research could significantly improve this study by modifying the approach to function during the wet season (July, August, and September) and to perform better on villages that were destroyed but not burned. Additionally geospatial research could be conducted to determine the impact of other variables to the conflict such as if the presence of African Union observers was correlated to village destruction or preservation and if any of the villages destroyed during ceasefires represent violations to those ceasefires by signatories.

Chapter 5. Summary and Conclusions

5.1. Introduction

The objective of this study is to improve the practice of remote sensing in human rights by demonstrating how moderate resolution sensors can provide accurate and timely complementary data to monitoring efforts. Organizations concerned with human rights continue to rely on the same sensor types and methods of analysis since the 1990s and have struggled to find ways to introduce the increasingly powerful, and publically available data from a growing constellation of moderate resolution sensors. Research in remote sensing has also not addressed how data from these sensors can be used in operation human rights monitoring campaigns. This study demonstrates how moderate resolution sensors can provide accurate data (69% omission rate at a 95% confidence level) in a much more timely manner than eyewitness reporting to operational human rights monitoring campaigns. By doing so it intends to provide a way forward for the research and practice of using these sensors in such campaigns.

Although remotely sensed imagery has been used for decades to document specific human rights events, such as the 1995 massacre in Srebrenica, Bosnia (Figure 2-1) (New York Times, 1995), there are only a

few examples of these methods evolving since then (Sulik & Edwards, 2010; Wolfinbarger & Drake, 2012). Organizations continue to use analyst-intensive approaches to mostly visual interpretation of fine resolution imagery, which has made the monitoring of large areas cost-prohibitive to all but the most well-funded organizations (Pisano, 2011).

Although previous research using moderate resolution imagery in human rights has shown promising results, these methods are more suitable to scientific research than operational monitoring (Prins, 2008; Witmer, 2008). This is due to the considerable lag in time between the impact of the armed conflict on population and its identification in satellite imagery. These studies conducted change-detection on an annual basis, which reduced the number of scenes required for purchase, minimized changes due to the annual phenological cycles, and simplified the analysis.

The free availability of Landsat's archives has addressed the cost constraint of employing this sensor in large-scale human rights monitoring campaigns (Woodcock et al., 2008). In addition, advancements by the North American Forest Dynamics (NAFD) program has developed methods to successfully use this data in time-series analysis (Goward et al., 2008). This study built on NAFD-validated methods of working with Landsat data and

applied them to a human rights application; specifically the detection of burnt of villages in Darfur, Sudan.

5.2. Summary of Research

This study consisted of three research phases, each producing a unique contribution to the understanding the role of remote sensing in detecting human rights violations. The initial research phase produced academia's first manuscript that comprehensively addresses the concepts and methods of remote sensing in the detection of human rights violations. Findings from this work included:

- Although research has shown that moderate resolution satellites can directly or indirectly detect phenomena associated with human rights violations (Table 1-2), the vast majority of detections rely on directly sensing phenomena with fine or very-fine resolution sensors (Table 1-3).
- The reliance on visual analysis of fine resolution imagery in human rights monitoring campaigns makes these campaigns cost-prohibitive to all but the most well-funded monitoring efforts. The inclusion of data derived from moderate resolution sensors makes monitoring

efforts significantly more cost-effective, especially when conducted over large areas.

- Research into applications from moderate resolution imagery has provided promising results, though no operational methods to employ these sensors have yet been developed.
- Previous studies are more suitable to scientific research than operational monitoring due to the considerable lag in time between the impact of the armed conflict on population and its identification in satellite imagery.

Results from this research were published in the American Geographical Society's journal, the *Geographical Review* (Marx & Goward, 2013).

The second research phase was to develop an approach to employ moderate resolution sensor data for operational human rights monitoring scenario. This study showed that Landsat ETM+ could provide accurate and complementary data as part of a system to monitor the burning of villages in arid environments. Such a monitoring system depends upon on Landsat's strategic data acquisition plan which acquires systematic observations with Landsat 7 (Goward et al., 2006).

The Landsat observatory provided an economically viable combination of frequent observations of the affected area, and the appropriate spatial resolution and spectral range for detecting the footprint of the phenomena associated with the burning of villages. Findings from this work included:

- An approach can be developed to provide accurate and timely data from a moderate resolution sensor to an operational, human rights monitoring campaign.
- The inclusion of data from a moderate resolution sensor to a monitoring campaign depends on the identification of a signal associated with a violation that is observable to a sensor's spatial, spectral, and temporal characteristics.
- A single band, Landsat ETM+'s band 4, near-infrared, is the most accurate in the designed approach to detect the burning of a village with each new scene collected.
- ETM+'s band 4 is most accurate due to a combination of NIR measurement observation stability and NIR sensitivity to detect the transition of a village from pre- to post-burn materials.

Results from this research have been summarized in a manuscript that is accepted for publication by *Remote Sensing of Environment* (Marx & Loboda, 2013).

While the second phase's approach is designed to provide complementary data to campaigns already using fine resolution sensors, it was applied without these sensors in the third research phase to the entire conflict in Darfur to illustrate the benefits and shortfalls in an actual conflict. This study also produced new data for analysis of the Darfur conflict, whose research has suffered from limited, and often inaccurate, data. Findings from the chapter include:

- The study's low detection rate (66%) is partially due to the algorithm's inability to detect villages that are destroyed not using fire, indicating that the methods of the perpetrators, not scanline error gaps, or number of destroyed structures is the limiting factor for this data source.
- The study's low detection rate is also was the result of limited scene availability for the region during the first wave of violence in 2003. The May2004 increase in Landsat ETM+ daily scene collection, to compensate for the lose of the scan-line corrector mirror, significantly increased scene availability for the study (Fig. 4-4).

- 69% of village destructions that corresponded to eyewitness accounts were within 16 days of the approach's detection indicating high temporal accuracy for villages detected as destroyed (Table 4-3).
- Results indicate village destruction during both the first ceasefire (September 2003 to early December 2003) and the second ceasefire (11 April to 26 May 2004), although in both cases there were rebel groups who did not sign the ceasefires operating in areas with detected destructions.
- Results reveal an intense three-month period (October 2006 through December 2006) of violence in South Darfur State (Fig. 4-17) following a period of decreased village destruction. This represents both increased government attacks on rebels not signing the Darfur Peace Agreement, and an inter-tribal conflict between the Nur and Zaghawa.

Results from this study will be published as part of the mapping initiatives program by the Center for the Prevention of Genocide at the U.S. Holocaust Memorial Museum (http://www.ushmm.org/maps).

5.3. Future Applications

This study demonstrates that moderate resolution sensors can be used to provide complementary data to operational human rights monitoring campaigns. While the approach is validated for a specific region, conflict, sensor, and phenomenon that is linked to a violation, advancements in moderate resolution imagery and its analysis make this a data source that is increasingly applicable to a variety of human rights monitoring efforts.

The growing constellation of moderate resolution sensors provide more data and a better revisit rate than years past. For example, the Disaster Monitoring Constellation (DMC) (https://earth.esa.int) provides a daily equatorial repeat at 30m spatial resolution in four spectral bands. This imagery is significantly less expensive than commercial fine resolution imagery and other moderate resolution imagery, such as Landsat, is free to users.

The public and no-charge release of Landsat imagery has spurred research into intra-annual, time-series analysis of moderate resolution imagery. When coupled with advancements in computing processing and storage, pixel-based analysis of stacks of tens or hundreds of Landsat images is reduced to hours. Because images directly downloaded by the Earth Resources Observation Systems (EROS) Data Center Land Ground Station

from Landsat are available within 6 to 24 hours, these scenes can be quickly analyzed and included in operational human right monitoring efforts. While no special arrangement for data access is required, one could be made to speed up the analysis and processing of the scenes.

5.3.1 Generalization of Approach

The inclusion of this growing wealth of moderate resolution imagery to human rights monitoring campaigns depends first on an understanding of the conflict that is monitored. In a specified conflict, individual human rights violations and associated, detectable signals must be identified. Some violations, such as torture, will not have signals detectable by any satellite's sensor. Other violations, such as the destruction of specific houses in a neighborhood, may have a signal only detectable with fine or very fine resolution sensors. Moderate resolution sensors require a physical modification of the landscape for identification.

A single area at-risk of human rights violations could be monitored for several different signals that are associated with possible human rights violations. For example moderate resolution satellites could monitor an area for the destruction of civilian homes as well as monitoring neighboring cropland for burning. Extensive destruction of civilian infrastructure is a

violation if it is not justified by military necessity (United Nations, 1949, 1977a, b).

Once a signal is identified, the time-profile, spatial size, and spectral separability of the signal must be matched with the sensor. Some signals associated with violations, such as the burning of agricultural plots may last for several months, while others, such as a neighborhood's destruction during a foreign military's occupation may require imagery every few days. Once a detectable signal is matched with a sensor, the approach needs to be validated with ground truth data or fine resolution satellite imagery.

5.3.2 Employing Moderate Resolution Satellites in Past Cases

Table 1-15 has been amended to demonstrate how moderate resolution sensors could have been employed, or better employed, in past cases where remote sensing was used to detect human rights violations (Table 5-1). The table first lists the U.N.'s Operational Satellite Applications Programme's (UNOSAT) use of WorldView 1 (0.5m spatial resolution) to detect the artillery bombardments within a civilian safe zone in Sri Lanka in 2009 (UNOSAT, 2009). While moderate resolution sensors have not been validated in their ability to detect artillery craters, this type of sensor could be used to detect the transition of internally displaced person's

(IDP) tents as they moved from one area of the civilian safe zone to another that was not being bombarded. This situation however is most appropriate for fine resolution imagery, because the civilian safe zone was only a few square kilometers, the situation was known about by the international community in advance, and the bombardments and subsequent movement took place within seven days (UNOSAT, 2009).

Table 5-1: Revised Table (1-15) Demonstrating how Moderate Resolution Sensors could be employed

Violation (Location)	**Phenomena**	**Signal Analysis**	**Proposed Sensor / Revisit**
Artillery Targeted Near Civilians (Sri Lanka)	Relocation of IDP tents	Identification of tent relocations	DMC Constellation (30m) 4 Days
Mass Executions (Bosnia)	Creation of mass graves	Change Detection: Large plots of earth	Landsat TM (30m) 16 days
Ethnic House Destruction (Georgia)	Groups of houses destroyed	Change Detection: Destruction of groups of houses	DMC Constellation (30m) 4 Days
Targeting of Civilian Infrastructure (Georgia)	Damage to public buildings	Change Detection: Damage to large civilian buildings	Landsat ETM+ (30m) 16 days
Political Prison Camps (North Korea)	Expansions of prisons	Prison size change detection	Landsat ETM+ (30m) Monthly
Targeting of Civilian Infrastructure (Turkey)	Destroying forests, fields, and villages	Change in large infrastructure reflectance	Landsat ETM+ (30m) 16Days
Civilian Population Removed (Sudan)	Disruption of agricultural land	Identify atypical intra-annual vegetation cycle	MODIS (250m) Monthly
Civilian Population Removed (Bosnia)	Abandonment of agricultural land	Identify atypical intra-annual crops growing cycle	Landsat TM (30m) 16 Days
Attacking Village (Sudan)	Burning of arid villages	MODIS fire detection	MODIS (250m) Daily
Attacking Village (Sudan)	Burning of arid villages	Drop in village's NIR Reflectance	Landsat ETM+ (30m) 16 Days

The second listed human rights violation in Table 1-15 is the detection of recently constructed mass graves in the Bosnian town of Srebrenica (Figure 5-1), corroborating eyewitness reporting of the nearby execution of 7,000 Muslim men.

Figure 5-1: Possible mass graves in Bosnia, July 1995. The arrows indicate recently disturbed earth or vehicle revetments. Source: New York Times, 29 October 1995.

In this situation, Landsat TM could have been used to monitor areas in Bosnia that were at-risk of mass executions and burials. Upon an eyewitness report of a mass execution, change analysis could be conducted in the local area to detect if any spaces transitioned from grass to soil which could indicate a mass grave. Then fine resolution sensors could be employed to

confirm the disturbed earth. This approach would likely require relatively large mass graves due to Landsat TM's pixel size. While this is not a demonstrated capacity of Landsat, it is possible that advancements in time-series, change detection research and improvements to the bit rate of Landsat sensors (12 bit for LDCM) could successfully separate this phenomena's signal for future monitoring.

The third case in Table 5-1 is the destruction of specific homes in towns across South Ossetia, Georgia (UNOSAT, 2008). In this case, fine (DigitalGlobe) imagery was used to detect the destruction of civilian homes during a nine-day period of Russian occupation of the city. Because of the narrow time window, DMC could be used to detect groups of destroyed civilian homes although individual homes would likely be too small to identify with a 30m resolution sensor.

The fourth case in Table 5-1 detected large infrastructure destruction in Georgia with very fine (WorldView-1) imagery. Because there is no time constriction, and the civilian infrastructure is of a larger spatial extent, Landsat ETM+ could possibly have been used to monitor the area for a large change in reflectance to large industrial buildings, large apartment buildings, and bridges. Additionally the fifth case, the growth of prisons in North

Korea could be accomplished with Landsat ETM+ on a monthly revisit to monitor the prisons.

The last five cases on Table 5-1 consisted of cases where moderate resolution satellites were used on an annual basis to detect a phenomena associated with a human rights violation. These cases have been amended to include new signals and sensors that would reduce the lag between the violation and when it is detected in the remotely sensed data. This improves the operational usefulness of the remotely sensed data.

5.4. Conclusions

Remote sensing in human rights monitoring is on the cusp of a significant change. The growing constellation of moderate resolution satellites is now providing a constant stream of high-quality and, in some cases, free data. Landsat 8 (Landsat Data Continuity Mission) was launched in February 2013 with a much-improved sensor, the Operational Land Imager. This sensor will provide up to 650 scenes per day as opposed to Landsat 7's 300 scenes per day. In addition to a growing availability, research has demonstrated how data derived from moderate resolution imagery can be used in the intra-annual monitoring of landcover changes.

Finally, this study demonstrated how these methods can be applied to a landcover change which is associated with human rights violation.

Human rights monitoring thus far has largely remained reactive because it relies on eyewitness reporting to identify areas of reported violations. Practitioners then use visual analysis of fine or very fine resolution imagery to document the violation. The inclusion of data from moderate resolution sensors, can provide organizations the ability to monitor large regions without eyewitness reporting. When this analysis alerts of a possible violation, fine resolution imagery can then be purchased and analyzed with visual interpretation, significantly lowering the cost of such monitoring. The increasing potential of data derived from the constellation of moderate resolution satellites may one day provide organizations with a low-cost and continual monitoring ability of very large regions at risk of a variety of human rights violations.

Appendix A: Landsat ETM+ images used in Chapter 4 study.

177/51	177/52	178/50	178/51	178/52	178/53
4-Feb-00	24-Apr-00	26-Jan-00	26-Jan-00	14-Mar-00	14-Mar-00
24-Apr-00	17-Oct-00	15-Apr-00	1-May-00	1-May-00	1-May-00
30-Nov-00	13-Jun-01	9-Nov-00	24-Oct-00	24-Oct-00	24-Oct-00
13-Jun-01	19-Oct-01	11-Dec-00	16-Mar-01	16-Mar-01	11-Dec-00
6-Dec-01	7-Jan-02	28-Feb-01	3-May-01	3-May-01	16-Mar-01
13-Apr-02	6-Oct-02	3-May-01	11-Nov-01	14-Jan-02	3-May-01
31-May-02	22-Oct-02	11-Nov-01	14-Jan-02	20-Apr-02	14-Jan-02
22-Oct-02	10-Jan-03	15-Feb-02	15-Feb-02	14-Nov-02	14-Nov-02
11-Jan-03	31-Mar-03	14-Nov-02	14-Nov-02	17-Jan-03	18-Feb-03
15-Mar-03	2-May-03	17-Jan-03	17-Jan-03	18-Feb-03	22-Mar-03
2-May-03	10-Nov-03	6-Mar-03	18-Feb-03	22-Mar-03	30-Sep-03
10-Nov-03	12-Dec-03	1-Nov-03	22-Mar-03	7-Apr-03	17-Nov-03
12-Dec-03	1-Mar-04	3-Dec-03	30-Sep-03	30-Sep-03	3-Dec-03
2-Mar-04	18-Apr-04	8-Mar-04	1-Nov-03	1-Nov-03	20-Jan-04
3-Apr-04	4-May-04	9-Apr-04	3-Dec-03	3-Dec-03	21-Feb-04
12-Oct-04	28-Nov-04	11-May-04	21-Feb-04	20-Jan-04	24-Mar-04
13-Nov-04	14-Dec-04	27-May-04	24-Mar-04	21-Feb-04	11-May-04
29-Nov-04	30-Dec-04	28-Jun-04	9-Apr-04	24-Mar-04	2-Oct-04
15-Dec-04	14-Jan-05	18-Oct-04	11-May-04	11-May-04	18-Oct-04
31-Dec-04	15-Feb-05	3-Nov-04	18-Oct-04	18-Oct-04	5-Dec-04
16-Jan-05	3-Mar-05	19-Nov-04	3-Nov-04	3-Nov-04	21-Dec-04
4-Mar-05	19-Mar-05	5-Dec-04	19-Nov-04	19-Nov-04	5-Jan-05
20-Mar-05	4-Apr-05	21-Dec-04	5-Dec-04	5-Dec-04	6-Feb-05
5-Apr-05	6-May-05	6-Feb-05	21-Dec-04	21-Dec-04	22-Feb-05
7-May-05	13-Oct-05	22-Feb-05	6-Feb-05	21-Jan-05	11-Apr-05
14-Oct-05	29-Oct-05	26-Mar-05	22-Feb-05	6-Feb-05	13-May-05
30-Oct-05	14-Nov-05	11-Apr-05	11-Apr-05	22-Feb-05	29-May-05
15-Nov-05	30-Nov-05	27-Apr-05	13-May-05	11-Apr-05	5-Nov-05
1-Dec-05	16-Dec-05	13-May-05	20-Oct-05	13-May-05	21-Nov-05
17-Dec-05	1-Jan-06	20-Oct-05	5-Nov-05	29-May-05	7-Dec-05
26-May-06	17-Jan-06	5-Nov-05	7-Dec-05	20-Oct-05	23-Dec-05
27-Jun-06	2-Feb-06	21-Nov-05	23-Dec-05	5-Nov-05	8-Jan-06
18-Nov-06	18-Feb-06	23-Dec-05	24-Jan-06	7-Dec-05	9-Feb-06
4-Dec-06	26-Jun-06	24-Jan-06	9-Feb-06	23-Dec-05	13-Mar-06
20-Dec-06	17-Nov-06	9-Feb-06	25-Feb-06	8-Jan-06	29-Mar-06
10-Mar-07	3-Dec-06	25-Feb-06	13-Mar-06	9-Feb-06	14-Apr-06
26-Mar-07	19-Dec-06	13-Mar-06	29-Mar-06	25-Feb-06	1-Jun-06
11-Apr-07	4-Jan-07	29-Mar-06	14-Apr-06	13-Mar-06	8-Nov-06

177/51	177/52	178/50	178/51	178/52	178/53
27-Apr-07	9-Mar-07	14-Apr-06	1-Jun-06	29-Mar-06	24-Nov-06
4-Oct-07	25-Mar-07	1-Jun-06	17-Jun-06	14-Apr-06	10-Dec-06
20-Oct-07	26-Apr-07	17-Jun-06	7-Oct-06	1-Jun-06	26-Dec-06
21-Nov-07	28-May-07	23-Oct-06	23-Oct-06	17-Jun-06	16-Mar-07
7-Dec-07	3-Oct-07	8-Nov-06	8-Nov-06	7-Oct-06	1-Apr-07
23-Dec-07	20-Nov-07	24-Nov-06	24-Nov-06	23-Oct-06	3-May-07
29-Mar-08	6-Dec-07	10-Dec-06	10-Dec-06	8-Nov-06	10-Oct-07
14-Apr-08	22-Dec-07	26-Dec-06	26-Dec-06	24-Nov-06	26-Oct-07
16-May-08	7-Jan-08	2-Jan-07	27-Jan-07	10-Dec-06	30-Jan-08
	11-Mar-08	18-Jan-07	12-Feb-07	26-Dec-06	15-Feb-08
	27-Mar-08	3-Feb-07	28-Feb-07	27-Jan-07	2-Mar-08
	6-Nov-08	19-Feb-07	16-Mar-07	28-Feb-07	18-Mar-08
	22-Nov-08	23-Mar-07	1-Apr-07	16-Mar-07	19-Apr-08
	8-Dec-08	8-Apr-07	17-Apr-07	1-Apr-07	28-Oct-08
		15-Sep-07	3-May-07	10-Oct-07	13-Nov-08
		1-Oct-07	19-May-07	26-Oct-07	15-Dec-08
		17-Oct-07	10-Oct-07	14-Jan-08	
		5-Jan-08	26-Oct-07	30-Jan-08	
		21-Jan-08	11-Nov-07	15-Feb-08	
		6-Feb-08	16-Jan-08	2-Mar-08	
		22-Feb-08	1-Feb-08	28-Oct-08	
		12-May-08	17-Feb-08	13-Nov-08	
		28-May-08	4-Mar-08	15-Dec-08	

Appendix B: Landsat ETM+ images used (continued).

179/50	179/51	179/52	180/50	180/51
5-Mar-00	5-Mar-00	5-Mar-00	31-May-00	29-Apr-00
6-Apr-00	6-Apr-00	6-Apr-00	22-Oct-00	31-May-00
15-Oct-00	24-May-00	15-Oct-00	14-Mar-01	22-Oct-00
4-Feb-01	15-Oct-00	18-Dec-00	17-May-01	25-Dec-00
10-May-01	18-Dec-00	4-Feb-01	24-Oct-01	27-Feb-01
27-Jun-01	4-Feb-01	8-Apr-01	17-Mar-02	17-May-01
17-Oct-01	8-Apr-01	27-Jun-01	4-May-02	24-Oct-01
10-Mar-02	10-May-01	17-Oct-01	21-Jun-02	11-Dec-01
14-Jun-02	27-Jun-01	20-Dec-01	4-Mar-03	14-Feb-02
20-Oct-02	17-Oct-01	10-Mar-02	21-Apr-03	4-May-02
9-Jan-03	10-Mar-02	14-Jun-02	7-May-03	21-Jun-02
29-Mar-03	5-Nov-02	5-Nov-02	15-Nov-03	11-Oct-02
8-Nov-03	9-Jan-03	7-Dec-02	7-Mar-04	12-Nov-02
13-Feb-04	29-Mar-03	9-Jan-03	10-May-04	30-Dec-02
16-Mar-04	8-Nov-03	8-Nov-03	26-May-04	4-Mar-03
1-Apr-04	26-Dec-03	26-Dec-03	17-Oct-04	21-Apr-03
17-Apr-04	28-Jan-04	16-Mar-04	2-Nov-04	15-Nov-03
3-May-04	13-Feb-04	1-Apr-04	25-Mar-05	1-Dec-03
19-May-04	16-Mar-04	17-Apr-04	10-Apr-05	4-Jan-04
4-Jun-04	1-Apr-04	3-May-04	26-Apr-05	4-Feb-04
10-Oct-04	17-Apr-04	11-Nov-04	12-May-05	7-Mar-04
11-Nov-04	3-May-04	27-Nov-04	3-Oct-05	10-May-04
14-Jan-05	19-May-04	14-Jan-05	19-Oct-05	26-May-04
15-Feb-05	4-Jun-04	15-Feb-05	28-Mar-06	17-Oct-04
2-Mar-05	11-Nov-04	18-Mar-05	13-Apr-06	2-Nov-04
18-Mar-05	27-Nov-04	3-Apr-05	6-Oct-06	18-Nov-04
3-Apr-05	13-Dec-04	19-Apr-05	15-Mar-07	4-Dec-04
19-Apr-05	14-Jan-05	13-Nov-05	31-Mar-07	20-Dec-04
12-Oct-05	15-Feb-05	29-Nov-05	16-Apr-07	5-Jan-05
28-Oct-05	2-Mar-05	15-Dec-05	19-Jun-07	21-Jan-05
1-Jan-06	18-Mar-05	1-Jan-06	9-Oct-07	6-Feb-05
17-Jan-06	3-Apr-05	17-Jan-06	25-Oct-07	22-Feb-05
18-Feb-06	19-Apr-05	18-Feb-06	2-Mar-08	25-Mar-05
5-Mar-06	12-Oct-05	5-Mar-06	18-Mar-08	10-Apr-05
21-Mar-06	28-Oct-05	21-Mar-06	19-Apr-08	12-May-05
22-Apr-06	13-Nov-05	22-Apr-06	21-May-08	13-Jun-05
8-May-06	1-Jan-06	8-May-06	6-Jun-08	29-Jun-05
24-May-06	17-Jan-06	31-Oct-06	12-Oct-08	3-Oct-05

179/50	179/51	179/52	180/50	180/51
9-Jun-06	18-Feb-06	16-Nov-06	28-Oct-08	19-Oct-05
25-Jun-06	5-Mar-06	18-Dec-06		4-Nov-05
15-Oct-06	21-Mar-06	4-Jan-07		20-Nov-05
31-Oct-06	22-Apr-06	20-Jan-07		6-Dec-05
16-Nov-06	8-May-06	21-Feb-07		22-Dec-05
4-Jan-07	15-Oct-06	8-Mar-07		24-Jan-06
20-Jan-07	31-Oct-06	24-Mar-07		9-Feb-06
21-Feb-07	16-Nov-06	9-Apr-07		25-Feb-06
8-Mar-07	2-Dec-06	25-Apr-07		12-Mar-06
24-Mar-07	18-Dec-06	18-Oct-07		13-Apr-06
9-Apr-07	4-Jan-07	3-Nov-07		5-Oct-06
25-Apr-07	20-Jan-07	19-Nov-07		8-Dec-06
27-May-07	21-Feb-07	5-Dec-07		24-Dec-06
28-Jun-07	8-Mar-07	21-Dec-07		9-Jan-07
19-Nov-07	24-Mar-07	7-Jan-00		25-Jan-07
5-Dec-07	9-Apr-07	23-Jan-00		26-Feb-07
7-Jan-08	25-Apr-07	24-Feb-00		14-Mar-07
24-Feb-08	28-Jun-07	27-Mar-00		30-Mar-07
27-Mar-08	18-Oct-07	12-Apr-00		15-Apr-07
12-Apr-08	3-Nov-07	14-May-00		18-Jun-07
14-May-08	19-Nov-07	30-May-00		8-Oct-07
30-May-08	5-Dec-07	5-Oct-00		24-Oct-07
5-Oct-08	21-Dec-07	21-Oct-00		9-Nov-07
21-Oct-08	7-Jan-08	22-Nov-00		25-Nov-07
6-Nov-08	24-Feb-08	8-Dec-00		11-Dec-07
	27-Mar-08	24-Dec-00		27-Dec-07
	12-Apr-08			12-Jan-08
	14-May-08			28-Jan-08
	30-May-08			13-Feb-08
	15-Jun-08			29-Feb-08
	5-Oct-08			16-Mar-08
	21-Oct-08			17-Apr-08
	6-Nov-08			19-May-08
	22-Nov-08			4-Jun-08
	8-Dec-08			26-Oct-08
	24-Dec-08			11-Nov-08
				27-Nov-08

Appendix C: Cumulative villages detected as destroyed.

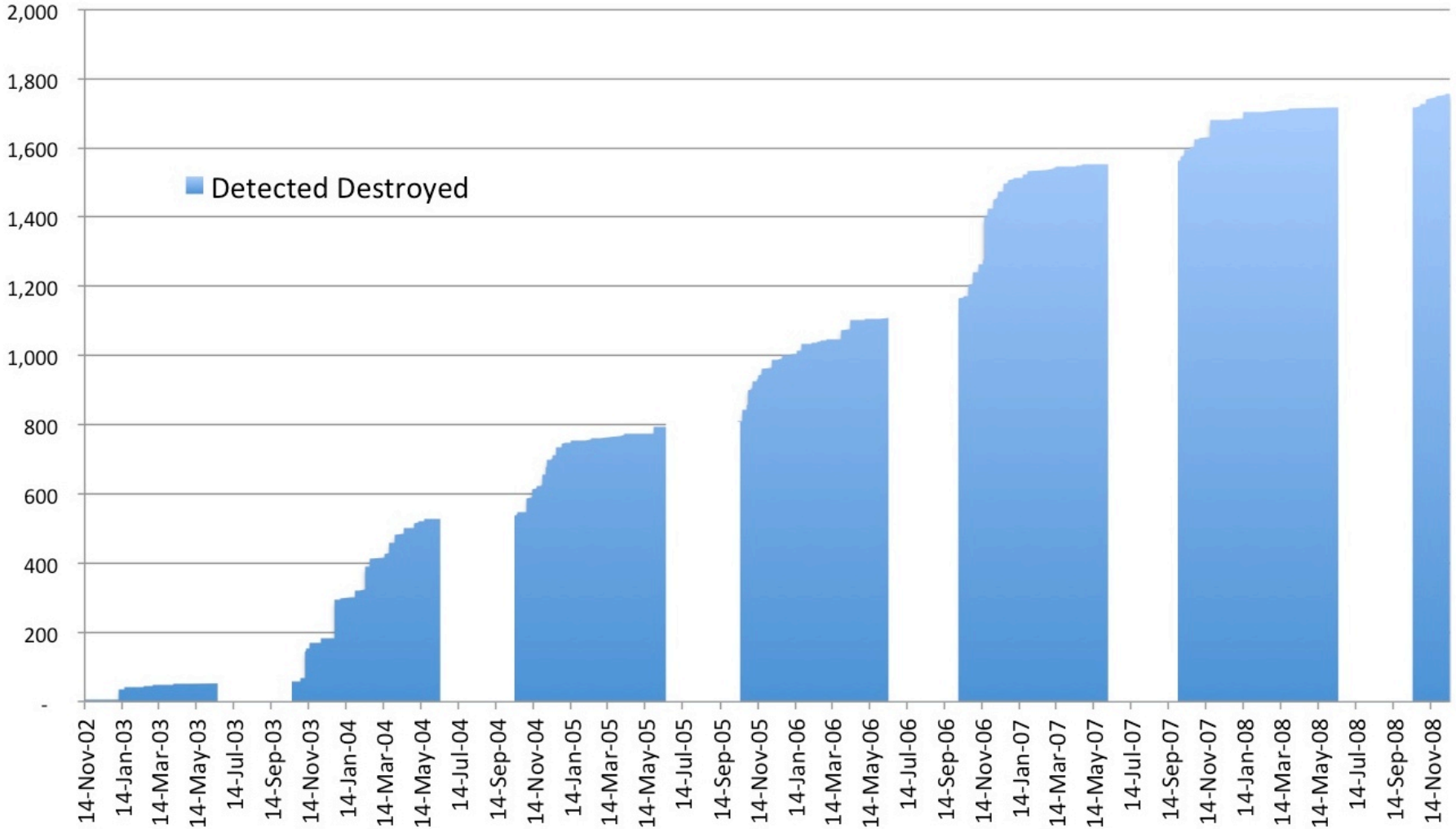

References

AAAS (2008). High-Resolution Satellite Imagery and the Conflict in South Ossetia (available at http://shr.aaas.org, retrieved April 15, 2013).

AAAS (2011). AAAS Science and Human Rights Program (available at http://shr.aaas.org/geotech, retrieved May 9, 2011).

Albright, M.K., & Cohen, W.S. (2008). *Preventing Genocide: A Blueprint for US Policymakers*. Washington, DC: Holocaust Museum.

Amnesty International (2007). Eyes on Darfur (available at http://www.eyesondarfur.org, retrieved 6 April 2013).

Amnesty International (2008). Civilians in the Line of Fire: The Georgia-Russia Conflict (available at http://www.amnesty.org/en/library/asset/EUR04/005/2008/en/d9908665-ab55-11dd-a4cd-bfa0fdea9647/eur040052008eng.pdf, retrieved 2013).

Amnesty International (2011). Images Reveal Scale of North Korean Political Prison Camps (available at http://amnesty.org/en/news-and-updates/images-reveal-scale-north-korean-political-prison-camps-2011-05-03, retrieved 30 Jul 2011).

Arvidson, T., Goward, S., Gasch, J., & Williams, D. (2006). Landsat-7 long-term acquisition plan: Development and validation. *Photogrammetric Engineering and Remote Sensing, 72*, 1137.

Bjørn, W. (2000). Eyes in the Sky - In Service of Humanity?, *Imaging Notes*. Greeley, CO: Earthwide Communications.

British Broadcasting Corporation (2009). Sri Lanka: Satellite imagery of safe zone (available at http://news.bbc.co.uk/2/hi/south_asia/8016965.stm, retrieved 18 September 2011).

Bromley, L. (2010). Relating violence to MODIS fire detections in Darfur, Sudan. *International Journal of Remote Sensing, 31*, 2277-2292.

Brown, T. (2011). Satellites for Human Rights, *Imaging Notes* (pp. 9-12). Denver, CO: Blueline Publishing LLC.

Chavez, P.S. (1996). Image-based atmospheric corrections-revisited and improved. *Photogrammetric Engineering and Remote Sensing, 62*, 1025-1035.

Coppin, P., Jonckheere, I., Nackaerts, K., Muys, B., & Lambin, E. (2004). Digital change detection methods in ecosystem monitoring: a review. *International Journal of Remote Sensing, 25*, 1565-1596.

De Vos, H., Jongerden, J., & Van Etten, J. (2008). Images of war: Using satellite images for human rights monitoring in Turkish Kurdistan. *Disasters, 32*, 449-466.

Defourny, P., Vancutsem, C., Bicheron, P., Brockmann, C., Nino, F., Schouten, L., & Leroy, M. (2006). GLOBCOVER: a 300 m global land cover product for 2005 using Envisat MERIS time series, *Proceedings of the ISPRS Commission VII mid-term symposium, Remote sensing: from pixels to processes* (pp. 8-11): Enschede, Netherlands.

Edwards, S., & Koettl, C. (2011). Looking to the Sky: Monitoring Human Rights through Remote Sensing (available at http://hir.harvard.edu/india-in-transition/looking-to-the-sky, retrieved May 9, 2011).

Flint, J., & De Waal, A. (2008). *Darfur: a new history of a long war*. New York: Zed Books.

Garcia, M.J.L., & Caselles, V. (1991). Mapping burns and natural reforestation using Thematic Mapper data. *Geocarto International, 6*, 31-37.

Goward, S., Arvidson, T., Williams, D., Faundeen, J., Irons, J., & Franks, S. (2006). Historical record of Landsat global coverage: Mission operations, NSLRSDA, and international cooperator stations. *Photogrammetric Engineering and Remote Sensing, 72*, 1155-1169.

Goward, S., Chander, G., Pagnutti, M., Marx, A., Ryan, R., Thomas, N., & Tetrault, R. (2012). Complementarity of ResourceSat-1 AWiFS and Landsat TM/ETM+ sensors. *Remote Sensing of Environment, 123*, 41-56.

Goward, S., Masek, J., Cohen, W., Moisen, G., Collatz, G., Healey, S., Houghton, R., Huang, C., Kennedy, R., & Law, B. (2008). Forest disturbance and North American carbon flux. *EOS Transactions, 89*, 105-116.

Goward, S., Williams, D., Arvidson, T., & Irons, J. (2011). The Future of Landsat-Class Remote Sensing. *Land Remote Sensing and Global Environmental Change*, 807-834.

Goward, S.N., Arvidson, T., Williams, D.L., Irish, R., & Irons, J.R. (2009). *Moderate spatial resolution optical sensors*. London, UK: SAGE Publications Ltd.

Hagan, J., & Kaiser, J. (2011). The displaced and dispossessed of Darfur: explaining the sources of a continuing state-led genocide. *The British journal of sociology, 62*, 1-25.

HIU (2004). Sudan (Darfur)-Chad Border Region Confirmed Damaged and Destroyed Villages. (available at https://hiu.state.gov/Pages/Africa.aspx, retrieved May 9 2013).

HIU (2010). Darfur, Sudan: Confirmed Damaged and Destroyed Villages, February 2003 - December 2009 (available at http://hiu.state.gov, retrieved 9 May 2011).

Huang, C., Goward, S.N., Masek, J.G., Thomas, N., Zhu, Z., & Vogelmann, J.E. (2010). An automated approach for reconstructing recent forest disturbance history using dense Landsat time series stacks. *Remote Sensing of Environment, 114*, 183-198.

Huang, C., Goward, S.N., Schleeweis, K., Thomas, N., Masek, J.G., & Zhu, Z. (2009). Dynamics of national forests assessed using the Landsat record: Case studies in eastern United States. *Remote Sensing of Environment, 113*, 1430-1442.

Huang, C., Song, K., Kim, S., Townshend, J.R., Davis, P., Masek, J.G., & Goward, S.N. (2008). Use of a dark object concept and support vector machines to automate forest cover change analysis. *Remote Sensing of Environment, 112*, 970-985.

Huang, C., Wylie, B., Yang, L., Homer, C., & Zylstra, G. (2002). Derivation of a tasselled cap transformation based on Landsat 7 at-satellite reflectance. *International Journal of Remote Sensing, 23*, 1741-1748.

Hudak, A., & Brockett, B. (2004). Mapping fire scars in a southern African savannah using Landsat imagery. *International Journal of Remote Sensing, 25*, 3231-3243.

Hudson, C. (2013). Senior Advisor, U.S. Holocaust Memorial Museum. Interview with author. Washington, DC. March 19, 2013.

Huffman, G.J., Adler, R.F., Bolvin, D.T., & Gu, G. (2009). Improving the global precipitation record: GPCP Version 2.1. *Geophysical Research Letters, 36*, 1-5.

Irish, R.R., Barker, J.L., Goward, S.N., & Arvidson, T. (2006). Characterization of the Landsat-7 ETM automated cloud-cover assessment (ACCA) algorithm. *Photogrammetric Engineering and Remote Sensing, 72*, 1179-1188.

Jia, G.J., Burke, I.C., Goetz, A.F.H., Kaufmann, M.R., & Kindel, B.C. (2006). Assessing spatial patterns of forest fuel using AVIRIS data. *Remote Sensing of Environment, 102*, 318-327.

Jin, S., & Sader, S.A. (2005). MODIS time-series imagery for forest disturbance detection and quantification of patch size effects. *Remote Sensing of Environment, 99*, 462-470.

Kasischke, E.S., & French, N.H.F. (1995). Locating and estimating the areal extent of wildfires in Alaskan boreal forests using multiple-season AVHRR NDVI composite data. *Remote Sensing of Environment, 51*, 263-275.

Kaufman, Y.J., Wald, A.E., Remer, L.A., Gao, B.C., Li, R.R., & Flynn, L. (1997). The MODIS 2.1- m channel-correlation with visible reflectance for use in remote sensing of aerosol. *IEEE Transactions on Geoscience and Remote Sensing, 35*, 1286-1298.

Keeley, J.F., & Huebert, R.N. (2004). *Commercial satellite imagery, and United Nations peacekeeping: a view from above*. Ashgate Pub Ltd.

Kennedy, R.E., Cohen, W.B., & Schroeder, T.A. (2007). Trajectory-based change detection for automated characterization of forest disturbance dynamics. *Remote Sensing of Environment, 110*, 370-386.

Key, C., & Benson, N. (2002). Measuring and remote sensing of burn severity. K.C.R. L. F. Neuenschwander, & G. E. Goldberg (Ed.), *Proceedings of the Joint Fire Science Conference* (pp. 02-11). Boise, Idaho 15–17 June, 1999: University of Idaho and the International Association of Wildland Fire, vol. II (p. 284).

Koutsias, N., & Karteris, M. (2000). Burned area mapping using logistic regression modeling of a single post-fire Landsat-5 Thematic Mapper image. *International Journal of Remote Sensing, 21*, 673-687.

Landsberg, F., Vanhuysse, S., & Wolff, E. (2006). Fuzzy multi-temporal land-use analysis and mine clearance application. *Photogrammetric Engineering and Remote Sensing, 72*, 1245-1253.

Leimgruber, P., Christen, C.A., & Laborderie, A. (2005). The impact of Landsat satellite monitoring on conservation biology. *Environmental Monitoring and Assessment, 106*, 81-101.

Levinger, M. (2009). Geographical Information Systems Technology as a Tool for Genocide Prevention: The Case of Darfur. *Space and Polity, 13*, 69-76.

Loboda, T., O'Neal, K., & Csiszar, I. (2007). Regionally adaptable dNBR-based algorithm for burned area mapping from MODIS data. *Remote Sensing of Environment, 109*, 429-442.

Lu, D., Mausel, P., Batistella, M., & Moran, E. (2005). Land-cover binary change detection methods for use in the moist tropical region of the Amazon: a comparative study. *International Journal of Remote Sensing, 26*, 101-114.

Lunetta, R.S., Knight, J.F., Ediriwickrema, J., Lyon, J.G., & Worthy, L.D. (2006). Land-cover change detection using multi-temporal MODIS NDVI data. *Remote Sensing of Environment, 105*, 142-154.

Lyon, J.G., Yuan, D., Lunetta, R.S., & Elvidge, C.D. (1998). A change detection experiment using vegetation indices. *Photogrammetric Engineering and Remote Sensing, 64*, 143-150.

Marburger, J.H., III, (2005). Landsat Data Continuity Strategy Adjustment, Memorandum from the Office of Science and Technology Policy: Executive Office of the President, Office of Science and Technology Policy, 23 December.

Markham, B.L., Thome, K.J., Barsi, J.A., Kaita, E., Helder, D.L., Barker, J.L., & Scaramuzza, P.L. (2004). Landsat-7 ETM+ on-orbit reflective-band radiometric stability and absolute calibration. *Geoscience and Remote Sensing, IEEE Transactions on, 42*, 2810-2820.

Marx, A., & Goward, S. (2013). Remote Sensing in Human Rights and International Humanitarian Law Monitoring. *Geographical Review, 103*, 100-111.

Marx, A., & Loboda, T. (2013). Landsat-based early warning system to detect the destruction of villages in Darfur, Sudan. *Remote Sensing of Environment,* accepted for publication 1 May 2013.

Masek, J.G., Vermote, E.F., Saleous, N.E., Wolfe, R., Hall, F.G., Huemmrich, K.F., Gao, F., Kutler, J., & Lim, T.-K. (2006). A Landsat surface reflectance dataset for North America, 1990-2000. *Geoscience and Remote Sensing Letters, IEEE, 3*, 68-72.

Moran, M.S., Jackson, R.D., Slater, P.N., & Teillet, P.M. (1992). Evaluation of simplified procedures for retrieval of land surface reflectance factors from satellite sensor output. *Remote Sensing of Environment, 41*, 169-184.

National Research Council (1969). *Useful Applications of Earth-Oriented Satellites*. Washington, DC: National Academy of Sciences.

New York Times (1995). Massacre in Bosnia; Srebrenica: The Days of Slaughter (available at http://www.nytimes.com/1995/10/29/world/massacre-in-bosnia-srebrenica-the-days-of-slaughter.html, retrieved August 8, 2011).

Nicholson, S., & Farrar, T. (1994). The influence of soil type on the relationships between NDVI, rainfall, and soil moisture in semiarid Botswana. NDVI response to rainfall. *Remote Sensing of Environment, 50*, 107-120.

Numata, I., Roberts, D.A., Chadwick, O.A., Schimel, J., Sampaio, F.R., Leonidas, F.C., & Soares, J.V. (2007). Characterization of pasture biophysical properties and the impact of grazing intensity using remotely sensed data. *Remote Sensing of Environment, 109*, 314-327.

Office of the High Commissioner for Human Rights (2001). Training Manual on Human Rights Monitoring. New York and Geneva: United Nations.

Petersen, A., & Tullin, L. (2006). *The Scorched Earth of Darfur: Patterns in death and destruction reported by the people of Darfur. January 2001-September 2005*. Copenhagen: Bloodhound.

Pisano, F. (2011). Director, UNITAR'S Operational Satellite Applications Programme. Interview with author. Washington, DC. April 29, 2011.

Power, S. (2004). Dying in Darfur. *New Yorker, 80*, 56-73.

Prins, E. (2008). Use of low cost Landsat ETM+ to spot burnt villages in Darfur, Sudan. *International Journal of Remote Sensing, 29*, 1207-1214.

Raleigh, C., Linke, A., Hegre, H., & Karlsen, J. (2010). Introducing ACLED: An Armed Conflict Location and Event Dataset Special Data Feature. *Journal of peace Research, 47*, 651-660.

Roy, D.P., Boschetti, L., & Trigg, S.N. (2006). Remote sensing of fire severity: assessing the performance of the normalized burn ratio. *Geoscience and Remote Sensing Letters, IEEE, 3*, 112-116.

Roy, D.P., Ju, J., Mbow, C., Frost, P., & Loveland, T. (2010). Accessing free Landsat data via the Internet: Africa's challenge. *Remote Sensing Letters, 1*, 111-117.

SatSentinel (2011). The world is watching because you are watching. (available at http://www.satsentinel.org/, retrieved 9 May 2011).

Schimmer, R. (2008). Tracking the Genocide in Darfur: Population Displacement as Recorded by Remote Sensing: *Working Paper*. *36* (Yale Genocide Studies Program).

Singh, A. (1989). Review Article Digital change detection techniques using remotely-sensed data. *International Journal of Remote Sensing, 10*, 989-1003.

Steidle, B. (2004). Um Zaifa, Darfur (available at http://hmd.org.uk/resources/image-library/darfur, retrieved April, 15 2013).

Sulik, J., & Edwards, S. (2010). Feature extraction for Darfur: geospatial applications in the documentation of human rights abuses. *International Journal of Remote Sensing, 31*, 2521-2533.

Tanner, V., Tubiana, J., & Griffin, M. (2007). *Divided they fall: The fragmentation of Darfur's rebel groups*. Small Arms Survey Geneva, Switzerland.

Terres, J., Biard, F., & Darras, G. (1999). *Kosovo: assessment of changes of agricultural land use areas for the 1999 crop campaign using satellite data*. Ispra, Italy: Joint Research Centre (Space Applications Institute Report).

Totten, S., & Markusen, E. (2006). *Genocide in Darfur: Investigating the atrocities in the Sudan*. New York: CRC Press.

Townshend, J., & Justice, C. (1988). Selecting the spatial resolution of satellite sensors required for global monitoring of land transformations. *International Journal of Remote Sensing, 9*, 187-236.

Tucker, C.J. (1979). Red and photographic infrared linear combinations for monitoring vegetation. *Remote Sensing of Environment, 8*, 127-150.

U.S. Congress (1992). *Public Law 102-555: Land Remote-Sensing Policy Act of 1992*. 102nd Congress, 28 October. Washington, DC: U.S. Government Printing Office.

U.S. Department of State (2004). Documenting Atrocities in Darfur, State Publication 11182 (available at http://2001-2009.state.gov/g/drl/rls/36028.htm, retrieved April, 15 2013).

U.S. Geological Society (2011). Spectral Library: Western Montana (available at http://frames.nbii.gov/portal/server.pt/community/spectral_library/500/western_montana/2271, retrieved 9 May 2011).

United Nations (1948). Universal Declaration of Human Rights (available at http://www.un.org/en/documents/udhr/index.shtml, retrieved April 15, 2013).

United Nations (1949). Convention (I) for the Amelioration of the Condition of the Wounded and Sick in Armed Forces in the Field. Geneva, 12 August 1949. Convention (II) for the Amelioration of the Condition of Wounded, Sick and Shipwrecked Members of Armed Forces at Sea. Geneva, 12 August 1949. Convention (III) relative to the Treatment of Prisoners of War. Geneva, 12 August 1949. Convention (IV) relative to the Protection of Civilian Persons in Time of War. Geneva, 12 August 1949. (available at http://www.icrc.org, retrieved May 9, 2011).

United Nations (1977a). Protocol Additional to the Geneva Conventions of 12 August 1949, and relating to the Protection of Victims of International

Armed Conflicts (Protocol I) (available at http://www.icrc.org, retrieved May 9, 2011).

United Nations (1977b). Protocol Additional to the Geneva Conventions of 12 August 1949, and relating to the Protection of Victims of Non-International Armed Conflicts (Protocol II) (available at http://www.icrc.org, retrieved May 9, 2011).

United Nations (1998). Rome Statute Of The International Criminal Court (available at http://untreaty.un.org/cod/icc/statute/romefra.htm, retrieved May 9, 2011).

UNOSAT (2008). Overview of Satellite Damage Assessment for Gori, Georgia (available at http://www.unitar.org/unosat/node/44/1257, retrieved August 12, 2011).

UNOSAT (2009). Newly Erected IDP Shelters within Civilian Safety Zone (CSZ) - Mulattivu District, Sri Lanka (available at http://www.unitar.org/unosat/node/44/1333, retrieved August 22, 2011).

UNOSAT (2011). UNITAR'S Operational Satellite Applications Programme (available at http://www.unitar.org/unosat/, retrieved May 9, 2011).

Ustin, S., Jacquemoud, S., Palacios-Orueta, A., Li, L., & Whiting, M. (2009). Remote sensing based assessment of biophysical indicators for land degradation and desertification. *Recent Advances in Remote Sensing and Geoinformation, Processing for Land Degradation Assessment. London: ISPRS Series*, 15-44.

Vermote, E.F., El Saleous, N.Z., & Justice, C.O. (2002). Atmospheric correction of MODIS data in the visible to middle infrared: first results. *Remote Sensing of Environment, 83*, 97-111.

Warner, T.A., Nellis, M.D., & Foody, G.M. (2009). *The SAGE handbook of Remote Sensing*. Thousand Oaks, California: SAGE Publications Limited.

Weisstein, E.W. (2003). *CRC concise encyclopedia of mathematics*. CRC press.

Witmer, F.D.W. (2008). Detecting war-induced abandoned agricultural land in northeast Bosnia using multispectral, multitemporal Landsat TM imagery. *International Journal of Remote Sensing, 29*, 3805-3831.

Wolfe, R., Masek, J., Saleous, N., & Hall, F. (2004). LEDAPS: Mapping North American disturbance from the Landsat record, *Geoscience and Remote Sensing Symposium, 2004. IGARSS '04. Proceedings. 2004 IEEE International*.

Wolfinbarger, S., & Drake, J. (2012). Time Series Satellite Imagery Analysis for Flare Detection in the Niger Delta. (available at http://shr.aaas.org/geotech/flaring.shtml, retrieved April 15, 2013).

Woodcock, C.E., Allen, R., Anderson, M., Belward, A., Bindschadler, R., Cohen, W., Gao, F., Goward, S.N., Helder, D., & Helmer, E. (2008). Free access to Landsat imagery. *Science, 320*, 1011-1011.

Wulder, M.A., White, J.C., Goward, S.N., Masek, J.G., Irons, J.R., Herold, M., Cohen, W.B., Loveland, T.R., & Woodcock, C.E. (2008). Landsat continuity: Issues and opportunities for land cover monitoring. *Remote Sensing of Environment, 112*, 955-969.